



## Exploration and optimisation of structure-activity relationships of new triazole-based C-terminal Hsp90 inhibitors towards *in vivo* anticancer potency

Jaka Dernovšek<sup>a</sup>, Živa Zajec<sup>a</sup>, Goran Poje<sup>b</sup>, Dunja Urbančič<sup>a</sup>, Caterina Sturtzel<sup>c</sup>, Tjaša Goričan<sup>d</sup>, Sarah Grissenberger<sup>c</sup>, Krzesimir Ciura<sup>e</sup>, Mateusz Woziński<sup>e</sup>, Marius Gedgudas<sup>f</sup>, Asta Zubrienė<sup>f</sup>, Simona Golič Grdadolnik<sup>d</sup>, Irena Mlinarič-Raščan<sup>a</sup>, Zrinka Rajić<sup>b</sup>, Andrej Emanuel Cotman<sup>a</sup>, Nace Zidar<sup>a</sup>, Martin Distel<sup>c</sup>, Tihomir Tomašič<sup>a,\*</sup>

<sup>a</sup> Faculty of Pharmacy, University of Ljubljana, Aškerčeva cesta 7, Ljubljana 1000, Slovenia

<sup>b</sup> Faculty of Pharmacy and Biochemistry, University of Zagreb, Ante Kovačića 1, Zagreb 10000, Croatia

<sup>c</sup> St. Anna Children's Cancer Research Institute, Zimmermannplatz 10, Vienna 1090, Austria

<sup>d</sup> Laboratory for Molecular Structural Dynamics, Theory Department, National Institute of Chemistry, Hajdrihova 19, Ljubljana 1001, Slovenia

<sup>e</sup> Department of Physical Chemistry, Medical University of Gdańsk, Gdańsk 80-416, Poland

<sup>f</sup> Department of Biothermodynamics and Drug Design, Institute of Biotechnology, Life Sciences Center, Vilnius University, Saulėtekio al. 7, Vilnius LT-10257, Lithuania

### ARTICLE INFO

#### Keywords:

Cancer  
Hsp90  
Inhibitor  
Ewing sarcoma  
Zebrafish

### ABSTRACT

The development of new anticancer agents is one of the most urgent topics in drug discovery. Inhibition of molecular chaperone Hsp90 stands out as an approach that affects various oncogenic proteins in different types of cancer. These proteins rely on Hsp90 to obtain their functional structure, and thus Hsp90 is indirectly involved in the pathophysiology of cancer. However, the most studied ATP-competitive inhibition of Hsp90 at the N-terminal domain has proven to be largely unsuccessful clinically. Therefore, research has shifted towards Hsp90 C-terminal domain (CTD) inhibitors, which are also the focus of this study. Our recent discovery of compound C has provided us with a starting point for exploring the structure-activity relationship and optimising this new class of triazole-based Hsp90 inhibitors. This investigation has ultimately led to a library of 33 analogues of C that have suitable physicochemical properties and several inhibit the growth of different cancer types in the low micromolar range. Inhibition of Hsp90 was confirmed by biophysical and cellular assays and the binding epitopes of selected inhibitors were studied by STD NMR. Furthermore, the most promising Hsp90 CTD inhibitor 5x was shown to induce apoptosis in breast cancer (MCF-7) and Ewing sarcoma (SK-N-MC) cells while inducing cell cycle arrest in MCF-7 cells. In MCF-7 cells, it caused a decrease in the levels of ER $\alpha$  and IGF1R, known Hsp90 client proteins. Finally, 5x was tested in zebrafish larvae xenografted with SK-N-MC tumour cells, where it limited tumour growth with no obvious adverse effects on normal zebrafish development.

### 1. Introduction

Cancer is one of the most pressing public health issues in the world and is predicted to be the leading cause of death worldwide by 2060 [1]. In the search for cures, often targeting a single oncogenic protein does not result in long-term anti-tumour efficacy, but multi-target approaches show better performance and can delay or even prevent the development of resistance. Treatment can be optimised by combining multiple single-target therapies or by using a single multi-target agent [2–4].

Interestingly, by inhibiting the function of the molecular chaperone heat shock protein 90 (Hsp90) a single-target approach can lead to widespread effects on the oncogenic proteome that halt cancer growth and disease progression [5,6].

The Hsp90 family consists of four isoforms and is mostly indirectly involved in cancer pathology [5]. Its effects are mediated by the role of Hsp90 in folding, maturation and aggregation prevention of many oncogenic proteins – so-called Hsp90 client proteins [7]. Due to its diverse oncogenic clientele, ranging from receptors (e.g. oestrogen

\* Corresponding author.

E-mail address: [tihomir.tomasich@ffa.uni-lj.si](mailto:tihomir.tomasich@ffa.uni-lj.si) (T. Tomašič).

<https://doi.org/10.1016/j.bioph.2024.116941>

Received 31 January 2024; Received in revised form 30 May 2024; Accepted 10 June 2024

Available online 17 June 2024

0753-3322/© 2024 The Author(s). Published by Elsevier Masson SAS. This is an open access article under the CC BY license (<http://creativecommons.org/licenses/by/4.0/>).

receptor  $\alpha$ , ER $\alpha$ ) to transcription factors (e.g. p53) and protein kinases (e.g. CDK-4), Hsp90 is important in many different cancer types [5–9]. Its expression levels are elevated in most cancers, and it is found in a multichaperone complex in cancer cells, making it more susceptible to ATP or inhibitor binding. Taken together, this provides a basis for the selective toxicity of Hsp90 inhibitors for malignantly transformed cells [10,11].

Since Hsp90 is an ATPase, it is not surprising that the first inhibitors such as geldanamycin and its analogue 17-DMAG (Fig. 1) interact with the ATP-binding site at the N-terminal domain (NTD). Many NTD inhibitors have been tested in clinical trials for the treatment of various types of cancer [12]. To date, only pimitespib (TAS-116, Fig. 1) has been approved in Japan for the treatment of gastrointestinal stromal tumours [13,14]. One of the main reasons for failure in clinical trials is induction of the heat shock response (HSR) because of equipotent inhibition of the ATPase activity in all four Hsp90 paralogues. The HSR, which is mediated by heat shock factor 1, causes upregulation of several heat shock proteins that can abrogate the effect of the Hsp90 inhibitor. As a consequence, the dose has to be increased, which often results in undesired side effects [5,15–17].

However, Hsp90 also allows for C-terminal allosteric modulation of its function [18]. The C-terminal domain (CTD) is connected to the Hsp90 NTD via a charged linker and the middle domain (MD), as shown in Fig. 1. The main role of the MD is to bind client proteins. The CTD, on the other hand, is required for the dimerisation of Hsp90, which can perform most of its biological functions only as a dimer [13,19]. Most importantly, CTD inhibition of Hsp90 has been shown not to induce the HSR, thus circumventing this disadvantage of ATP-competitive NTD inhibitors [15,16,18,20].

Therefore, it is not surprising that CTD has been explored for the development of Hsp90 inhibitors. In the absence of a co-crystal structure of Hsp90 with a non-covalent CTD inhibitor, the discovery of new allosteric modulators initially revolved mainly around the coumarin

antibiotic novobiocin and its analogues [18,21,22]. Over the years, a structure-activity relationship (SAR) has been established for various classes of compounds, indicating that a basic centre at a sufficient distance from an aromatic lipophilic moiety is required for potent anti-cancer activity [22–28]. This SAR is based on several structurally distinct classes of C-terminal allosteric modulators of Hsp90 that have been developed in recent years, including the triazole-based compounds A and B (Fig. 1) [22,26].

We recently identified compound C as a new type of triazole-based Hsp90 CTD inhibitors [29]. Compound C was shown to inhibit Hsp90 function in a luciferase refolding assay [30], while it hindered the growth of the breast cancer cell line SK-BR-3 *in vitro* with a relatively high IC<sub>50</sub> value of  $51 \pm 2 \mu\text{M}$  [29]. Therefore, the aim of this study was to improve the anticancer activity of compound C and develop SAR around this novel type of Hsp90 CTD inhibitors.

## 2. Results and discussion

### 2.1. Design of analogues of inhibitor C

Based on compound C (Fig. 1) [29], we explored SAR of these new 1,4-disubstituted triazole-based Hsp90 CTD inhibitors. Previously published Hsp90 CTD inhibitors, including compounds A and B (Fig. 1), indicated that the distance between the basic centre at one end and the aromatic ring at the other end is important for Hsp90 CTD inhibition and anticancer activity [22,23,26]. Therefore, we decided to keep the 1-phenyltriazole-4-yl core of C intact and vary the distance and angle between the two critical parts of the molecule. The design was aided by the molecular docking of inhibitor C to Hsp90 (Fig. 2), which guided the modifications in both the aromatic and cationic regions of the molecule. For the molecular docking studies, the binding site on the Hsp90 $\beta$  CTD dimer proposed by us and others was used [25,31,32]. The basic centre of the piperazine in compound C was predicted to form an ionic

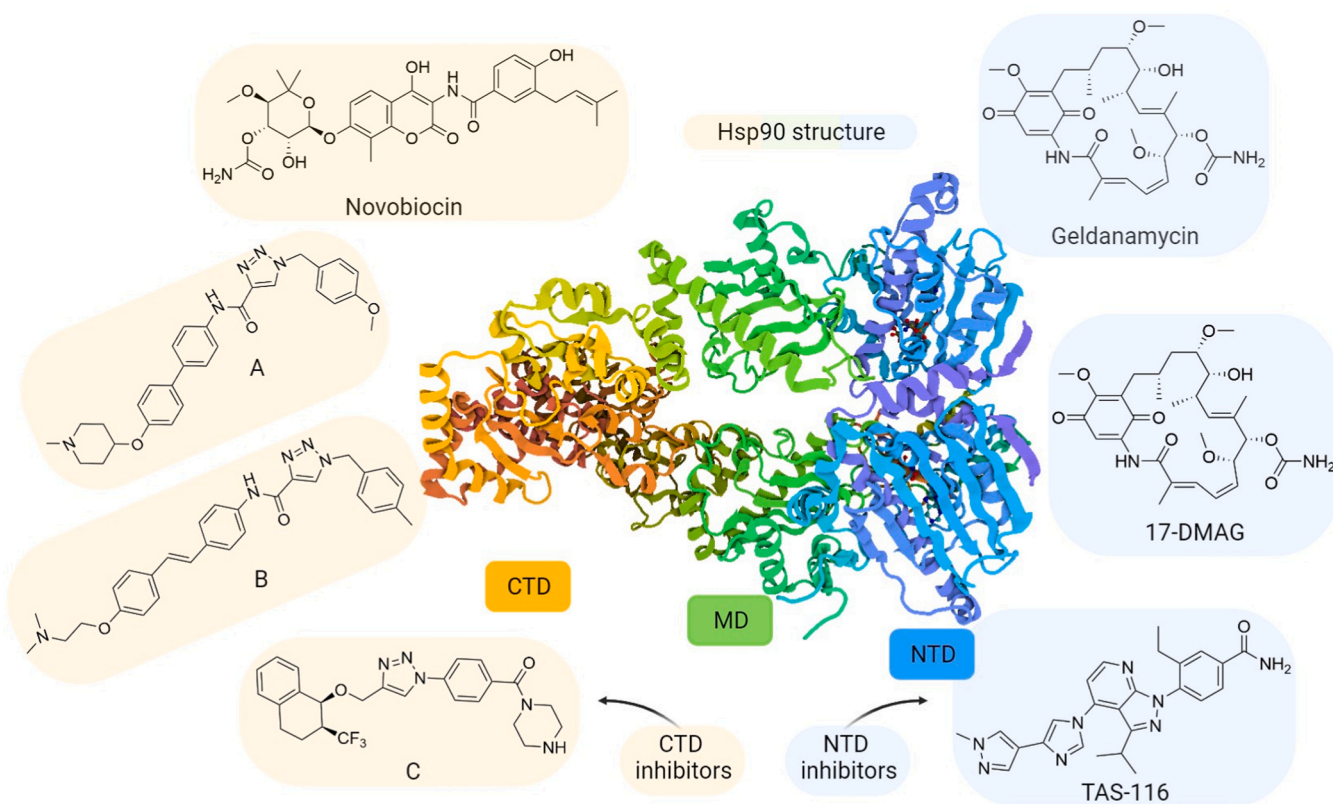


**Fig. 1.** Structure of the Hsp90 dimer (PDB ID: 7L7J), where the NTD is coloured blue, the MD green and the CTD orange. Representative N-terminal inhibitors include geldanamycin, 17-DMAG and TAS-116 – pimitespib, while C-terminal inhibitors include novobiocin and triazole-based inhibitors A, B and C.

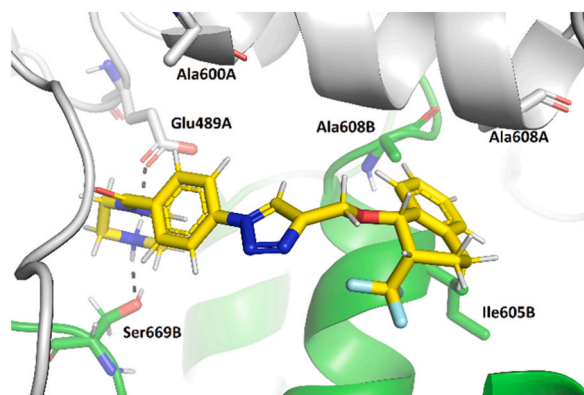


**Fig. 2.** Docking binding mode of compound C (in yellow sticks) in the Hsp90 $\beta$  dimer (PDB entry: 5FWK, protomers A and B are coloured grey and green, respectively) C-terminal domain binding site. For clarity, only the amino acids that interact with the inhibitor are shown. Hydrogen bonds are shown as black dashed lines.

interaction with the Glu489A carboxylate group and a hydrogen bond with the Ser669B hydroxyl group. In addition, hydrophobic interactions were predicted between the phenyl ring and Ala600A and between the (1*S*,2*S*)-1-(prop-2-yn-1-yloxy)-2-(trifluoromethyl)-1,2,3,4-tetrahydronaphthalene moiety and Ala608A, Ile605B and Ala608B (Fig. 2).

First, library A was outlined to study the effect of the substitution at position 4 of the triazole ring by introducing amides and ethers linking different aromatic substituents to the triazole core (Fig. 3). Based on the predicted binding mode of compound C (Fig. 2), the attachment of homochiral  $\beta$ -CF<sub>3</sub> benzyl alcohols as well as other aromatic substituents was envisaged. After optimisation of the aromatic substituent, the most promising moiety elucidated in library A was selected for further optimisation in library B (Fig. 3). In the latter, changes to the positioning of the cationic centre at the other end of the molecule were considered by incorporating different piperidines, by introducing different linkers and by changing the orientation of the amide bond. Finally, the importance of the positively ionisable amine was tested by introducing some non-ionisable functional groups.

## 2.2. Synthesis

Library A was prepared to explore the SAR of the aromatic substituents at position 4 of the core triazole ring. Firstly, the amide bond between 4-azidobenzoic acid and Boc-piperazine was formed using EDC and HOBt-facilitated amide coupling (Scheme 1). Subsequently, the amine of **1** was deprotected by acidolysis using trifluoroacetic acid in dichloromethane to obtain **2**.

Next, corresponding alkynes were prepared using propargyl bromide in reaction with an appropriate aliphatic or aromatic alcohol under basic conditions to synthesise **3a-3f** and **3m-x**, while propargylamine was

reacted with a suitable carboxylic acid to give the amides **3g-l** (Scheme 1). Building blocks **3a-l** were then reacted with **1** in a copper-catalysed click reaction to give **4a-l**. Copper(II) sulphate was used as a copper donor in combination with ascorbic acid to produce copper(I) ions *in situ*, which catalysed the Copper(I)-catalysed Azide-Alkyne Cycloaddition (CuAAC). In the following step, the amine was deprotected by acidolysis using either trifluoroacetic acid or hydrogen chloride to produce the final products **5a-l**. In the preparation of the final compounds **5m-x**, the deprotected compound **2** was used in the click reaction together with the alkynes **3m-x** to carry out the synthesis in a more convergent manner.

The alkyne **3x** was used as the aromatic moiety in the synthesis of library B and introduced at position 4 of the triazole ring (Scheme 2). To this end, **3x** was reacted in the click reaction with 4-azidobenzoic acid to produce compound **6** or 4-azidoaniline to obtain **7**. Compound **6** was then coupled with various mono-Boc-protected diamines using EDC and HOBt to form compounds **8a-e**, while morpholine and 4-aminopiperidine were used for the synthesis of **8f-g** to yield final compounds without a basic centre. On the other hand, compound **7** was coupled with four *N*-Boc-protected amino acids to obtain reversed amides **9a-d**. In the final step of the synthesis of compounds **10a-i**, the *N*-Boc-protected intermediates **8a-e** and **9a-d** were deprotected with trifluoroacetic acid in dichloromethane to obtain the respective final compounds.

## 2.3. Evaluation of physicochemical properties

To assess the suitability of the synthesised compounds for further hit-to-lead optimisation and biological evaluation, their physicochemical properties were analysed by high performance liquid chromatography (HPLC). Chromatographic approaches have been widely applied to determine preclinical drug candidates' lipophilicity and biomimetic properties in the drug discovery pipeline. Here, we measured the chromatographic hydrophobicity indices (CHI) of C<sub>18</sub> and immobilised artificial membrane (IAM), which relate to lipophilicity and binding to phospholipids, respectively, and binding to plasma albumin using methods developed by Valko and co-workers [33,34]. Chromatographically determined properties are summarised in Table 1S, and compound retention times are given in Table 2S.

When comparing libraries A and B, some differences in the chromatographically determined properties can be observed as compounds of library B have slightly higher CHI<sub>C18</sub>, CHI<sub>IAM</sub>, and %PPB values than those of library A (Supplementary information Figures 1SA-C). In general, the final compounds **5a-x**, **8f**, **8g** and **10a-i** have CHI<sub>C18</sub> values between 49.2 and 85.0 with an average value of 71.0. The most lipophilic compound with a CHI<sub>C18</sub> value of 85.0 was **8g** without the basic centre, which was also found to be inactive (see below). Other compounds in the synthesised compound library have CHI<sub>C18</sub> values in the range of the two clinical candidates 17-DMAG and PU-H71 with CHI<sub>C18</sub> indices of 80.3 and 53.7, respectively. Therefore, the new triazole-based Hsp90 CTD inhibitors have suitable lipophilic properties for further evaluation and optimisation.

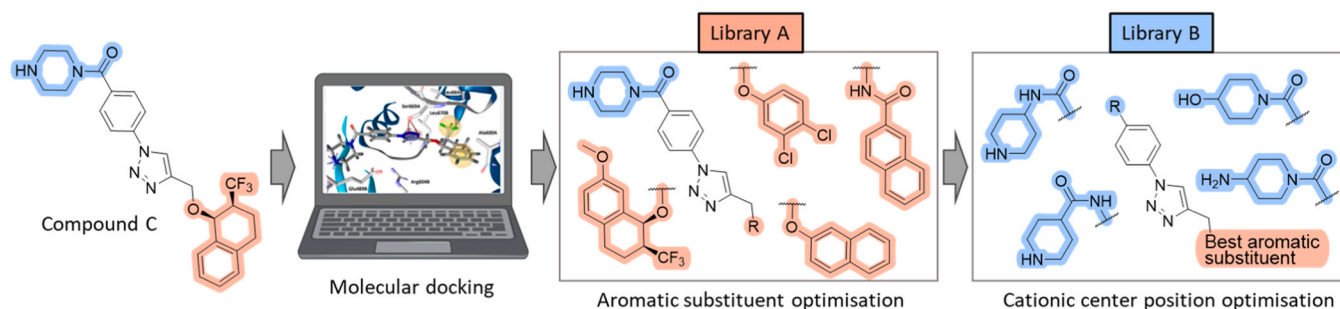
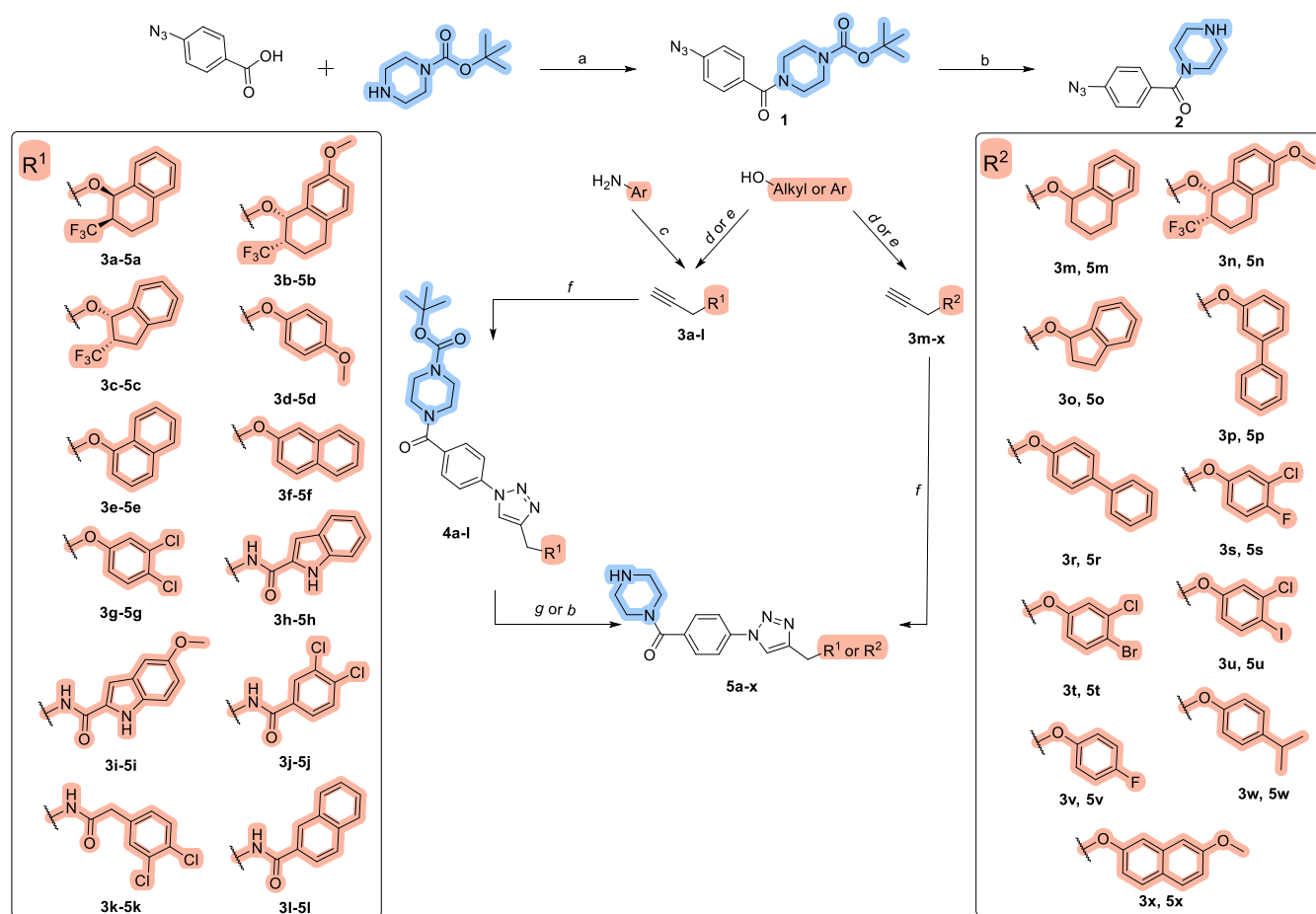


**Fig. 3.** Schematic representation of the design workflow following the discovery of compound C, the exploration of its proposed binding mode, the search for the most suitable aromatic substitution pattern and finally, the exploration of potential changes in the basic region of the inhibitor.



**Scheme 1.** Reagents and conditions for the preparation of library A: (a) (i) EDC, HOBt, NMM, DMF, 0 °C, 20 min; (ii) Boc-piperazine, r.t., overnight; (b) for the synthesis of compounds 2, 5a-5e and 5j: CF<sub>3</sub>COOH, DCM, r.t., overnight; (c) (i) respective carboxylic acid, SOCl<sub>2</sub>, dry DCM, 0 °C to r.t., overnight; (ii) propargyl amine, dry DCM, r.t., overnight; (d) for the synthesis of compounds 3a-3c and 3m-3o: (i) respective alcohol, NaH, dry THF, 0 °C, 30 min; (ii) propargyl bromide, r.t., overnight; (e) for the synthesis of compounds 3d-3g and 3p-3x: (i) respective phenol, K<sub>2</sub>CO<sub>3</sub>, DMF, r.t., 30 min; (ii) propargyl bromide, r.t., overnight; (f) azide 1 for the synthesis of compounds 4a-4l, or azide 2 for the synthesis of compounds 5m-5x, respective alkyne, CuSO<sub>4</sub>, sodium ascorbate, water:MeOH = 1:2, r.t., overnight; (g) for the synthesis of compounds 5f-5i, and 5k-5l: 4 M HCl in 1,4-dioxane, 1,4-dioxane, r.t., overnight.

To estimate the affinity of the compounds for phospholipids  $CHI_{IAM}$  values were determined, which ranged from 31.3 to 54.8 with an average value of 43.2. It has been reported that molecules with  $CHI_{IAM}$  values greater than 50 have the potential to bind promiscuously and affect phospholipidosis [35]. All compounds in library A had lower  $CHI_{IAM}$  values, while in library B about half of the molecules only slightly exceeded the  $CHI_{IAM}$  index of 50. Importantly, the  $CHI_{IAM}$  values of the most potent compounds were comparable to the  $CHI_{IAM}$  values of 17-DMAG and PU-H71.

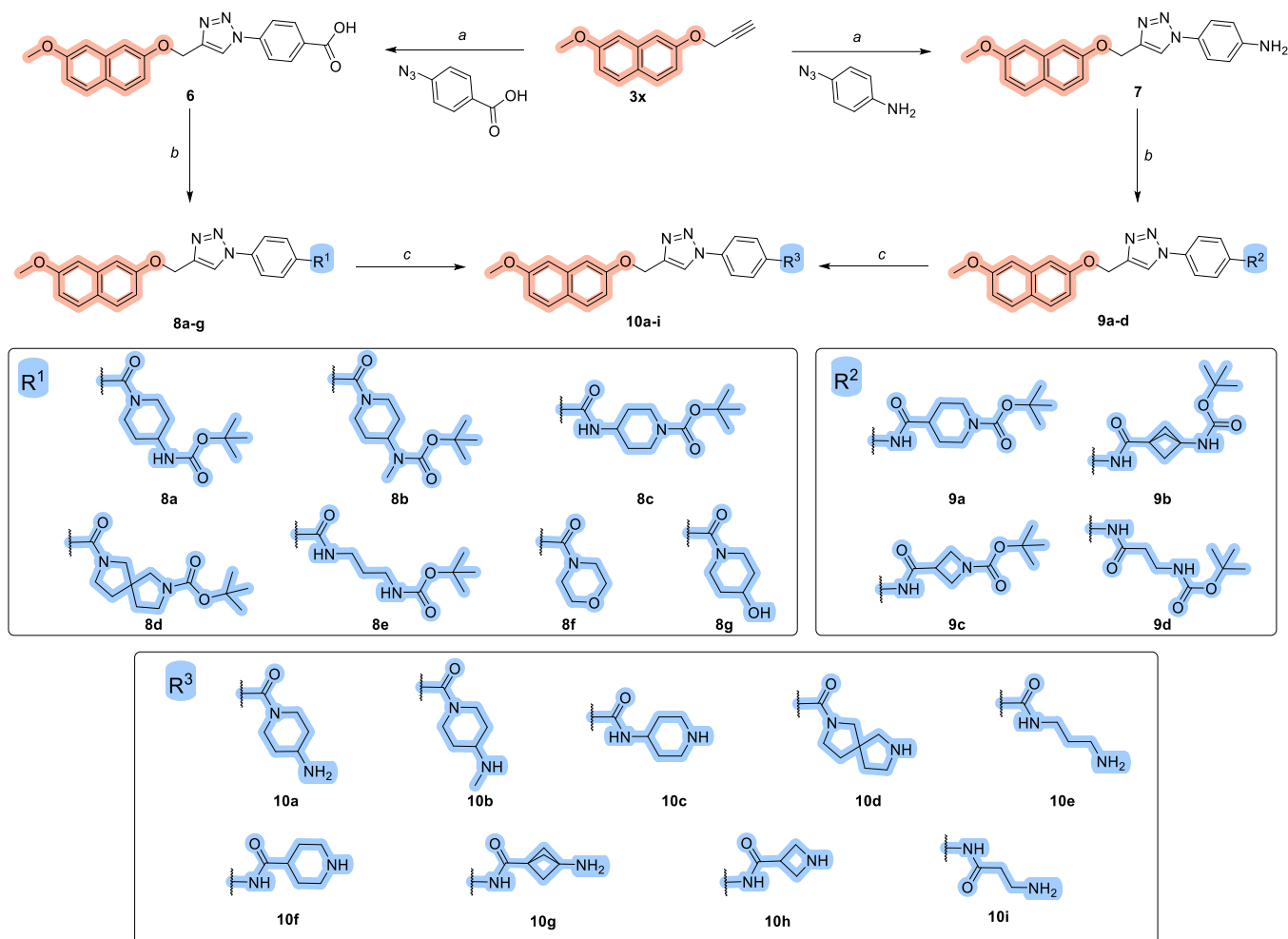
A chromatographic approach was also used to estimate the extent of binding to plasma proteins. Among the compounds tested, the bound fraction of the new triazole-based compounds was similar (96.7 % on average) to that of PU-H71 (92.5 %), but higher than that of 17-DMAG (74.7 %). The lack of significant correlation between  $CHI_{C18}$  parameters and affinity to HSA (Supplementary information Fig. 2S) suggests that the interaction between the tested compounds and plasma proteins is not driven only by lipophilicity.

#### 2.4. Structure-activity relationships of compound C analogues

After the confirmation of suitable physicochemical properties of the final compounds, 5a-x, 8f-g and 10a-i were tested for their anti-proliferative activities in various cancer cell lines (Tables 1-3). These included glioblastoma U-251, colorectal carcinoma HCT-116, hepatocellular carcinoma Hep-G2, Ewing sarcoma SK-N-MC and breast cancer

MCF-7 cell lines. Additionally, the compounds were tested for their anti-proliferative activity against the renal cell line HEK-293 T, which has limited tumorigenic properties and is sometimes considered non-carcinogenic. The effects of compounds on cell viability could potentially be influenced by various factors other than the desired on-target effects. The IC<sub>50</sub> values, determined by MTS assay, can be potentially affected by the permeability of the compound into the cells and its retention time as well as the cell line-specific sensitivity to the treatment [36-39] and potential off-target action [40]. Since the aim of this study was to optimise the *in vitro* anticancer activity of the compounds, the SARs for the triazole-based Hsp90 CTD inhibitors were determined based on their effect on cancer cell viability, as this is a common approach in the field of Hsp90 C-terminal inhibitor design and evaluation [18,22,26,27,41-44]. As described below, the SARs determined were mostly comparable for all cancer cell lines used for the evaluation.

First, the variations in the aromatic region were investigated, and the results are presented in Tables 1 and 2. The β-CF<sub>3</sub> benzyl alcohol motif from compound C (IC<sub>50</sub> (MCF-7) = 33.2 ± 0.1 μM) was retained and only slightly modified in compounds 5a-c and 5n, while compounds 5m and 5o were prepared as their counterparts without the CF<sub>3</sub> group. The results indicate that in the case of the 1,2,3,4-tetrahydronaphthalene ring, the trifluoromethyl group contributes to more potent anti-proliferative activity (5a-b vs 5m) in most cases, in spite of compound 5o displaying greater potency in MCF-7 cell line. The opposite stereochemistry of 5a with respect to compound C appears to be less



**Scheme 2.** Reagents and conditions for the preparation of library B: (a) **3x**, CuSO<sub>4</sub>, sodium ascorbate, water:MeOH = 1:2, r.t., overnight; (b) (i) respective aliphatic or aromatic carboxylic acid, EDC, HOBT, NMM, DMF, 0 °C, 20 min; (ii) respective aliphatic or aromatic amine, r.t., overnight; (c) CF<sub>3</sub>COOH, DCM, r.t., overnight.

important, as the potency in MCF-7 cancer cells is not drastically altered. Moreover, the activity was slightly increased by the introduction of a methoxy group at position 6 or 7 of the 1,2,3,4-tetrahydronaphthalene ring of compound **C**, as can be seen from the activities of **5b** and **5n** in MCF-7 cells. On the other hand, the activities of compounds **5c** and **5o** indicate that the introduction of the indanol ring is detrimental to the anticancer activity regardless of the presence of the β-CF<sub>3</sub> group.

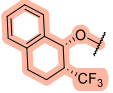
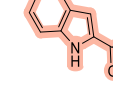
Taken together, optimisation of the fused aromatic and aliphatic bicycles did not significantly improve the activity, therefore, fully aromatic substituents were considered at this position. The introduction of 4-methoxyphenyl (**5d**) via an ether linker had lowered the potency. Fortunately, the introduction of 1- or 2-naphthyl and 3,4-dichlorophenyl at this position resulted in compounds **5e**, **5f**, and **5g** with improved growth inhibition that reached the low micromolar range in the breast cancer cell line MCF-7 and the Ewing sarcoma cell line SK-N-MC. Next, an amide was introduced in place of the ether linker, which resulted in the compounds **5h-5l** that unexpectedly showed weak or no growth inhibition in tested cancer cell lines. For this reason, the more flexible ethers were used in the design of further analogues.

Since biphenyls have previously been used as aromatic substituents in C-terminal triazole-based Hsp90 inhibitors [22,26], biphen-3-yl and -4-yl derivatives **5p** and **5r** were prepared. In agreement with previous findings, compounds **5p** and **5r** had enhanced antiproliferative activity in most cancer cell lines. Since **5r** showed slightly better activity, position 4 appeared to be more suitable for the incorporation of large lipophilic substituents than position 3. Next, because halogen bonding has

already been proposed for Hsp90 CTD inhibitors [23,24], compounds **5s-5v** were prepared to investigate possible halogen bond formation. Compound **5s** carrying a 3-chloro-4-fluorophenyl showed weaker anti-cancer activity than **5g**, **5t** and **5u**, with chloro, bromo and iodo substituents at position 4, respectively. Meanwhile, the introduction of monosubstituted 4-fluorophenyl in **5v** resulted in an almost complete loss of activity. Compound **5g** also appears to be a slightly more effective growth inhibitor in most cell lines compared to **5t** and **5u**, suggesting that the halogen bonding might not be an important contributor to binding. This was additionally confirmed by the introduction of 4-isopropylphenyl in **5w**, as this compound had similar effects as **5g** and **5r**, indicating the need for lipophilic substituents at position 4. Considering that the 3,4-disubstitution of the phenyl ring was the most explored in our study and that the limit of substituent size was not reached by any of the introduced moieties, compound **5f** was further modified by introducing a methoxy group at position 7 of the naphthalene ring to produce **5x**. The introduction of the methoxy group slightly increased the antiproliferative activity, as previously observed for compounds **5b** and **5n**. Overall, all active compounds are significantly more potent than the first described C-terminal Hsp90 inhibitor novobiocin (Table 3) [45]. Furthermore, the growth inhibition of **5x** against the MCF-7 cell line was the strongest of the series with an IC<sub>50</sub> value of 1.3 ± 0.2 μM, while the activity against the other cell lines was comparable to that of other compounds. Therefore, 7-methoxynaphthalene was selected as the optimal aromatic substituent and was further used in optimising the position of the basic centre on the other side of the

**Table 1**

Antiproliferative IC<sub>50</sub> values (mean ± SD) of the synthesised triazoles **5a-5l** in hepatocellular carcinoma HepG2, colorectal carcinoma HCT-116, glioblastoma multiforme U-251, breast cancer MCF-7, Ewing sarcoma SK-N-MC and embryonic kidney HEK-293T cell lines: establishment of the structure activity relationships of the lipophilic part of the molecule (Library A – part 1).

Cmpd. No.	Structure	IC <sub>50</sub> (μM)					
		MCF-7	SK-N-MC	U-251	HCT-116	Hep-G2	HEK-293T
							
<b>5a</b>		33.0 ± 0.4	28.8 ± 0.0	37.8 ± 1.3	39.2 ± 2.3	31.9 ± 6.8	42.2 ± 5.1
<b>5b</b>		26.6 ± 4.7	27.8 ± 2.7	32.7 ± 4.5	36.1 ± 0.9	22.2 ± 3.6	> 50
<b>5c</b>		> 50	> 50	> 50	> 50	32.9 ± 1.6	> 50
<b>5d</b>		> 50	> 50	> 50	> 50	> 50	> 50
<b>5e</b>		14.8 ± 7.3	8.9 ± 1.0	19.2 ± 1.3	16.3 ± 1.2	16.8 ± 2.2	20.2 ± 4.6
<b>5f</b>		8.0 ± 0.2	6.3 ± 0.7	18.0 ± 0.5	14.8 ± 1.5	13.6 ± 2.7	17.1 ± 0.9
<b>5g</b>		7.4 ± 0.7	6.5 ± 0.6	17.9 ± 0.9	16.4 ± 0.3	15.4 ± 3.9	17.4 ± 3.9
<b>5h</b>		> 50	> 50	> 50	> 50	> 50	> 50
<b>5i</b>		> 50	> 50	> 50	> 50	> 50	> 50
<b>5j</b>		22.9 ± 1.9	23.9 ± 1.0	> 50	> 50	36.8 ± 7.9	> 50
<b>5k</b>		> 50	> 50	> 50	> 50	43.0 ± 3.9	> 50
<b>5l</b>		17.6 ± 1.6	> 50	> 50	> 50	> 50	> 50

molecule.

The results of cation centre variations are presented in [Table 3](#). Initially, the neutral piperazine bioisosteres, morpholine and 4-hydroxypiperidine, were introduced in **8f** and **8g**, respectively. In agreement with previous results and the binding mode of compound **C**, these

variations did not improve the activity, as basic amine is important for the interaction with Glu489A in the CTD of Hsp90 [23–25]. On the contrary, the introduction of positively ionisable aliphatic rings with comparable spatial orientation to piperazine resulted in compounds **10a-10d** with slightly lower inhibitory IC<sub>50</sub> values relative to **5x** in most

**Table 2**

Antiproliferative IC<sub>50</sub> values (mean ± SD) of the synthesized triazoles **5m-5x** in hepatocellular carcinoma HepG2 colorectal carcinoma HCT-116, glioblastoma multiforme U-251, breast cancer MCF-7, Ewing sarcoma SK-N-MC and embryonic kidney HEK-293T cell lines: establishment of the structure activity relationships of the lipophilic part of the molecule (Library A – part 2).

Cmpd. No.	Structure	IC <sub>50</sub> (μM)					
		MCF-7	SK-N-MC	U-251	HCT-116	Hep-G2	HEK-293T
<b>5m</b>		21.0 ± 5.5	> 50	> 50	> 50	> 50	> 50
<b>5n</b>		14.2 ± 4.8	13.4 ± 0.4	20.7 ± 0.8	36.6 ± 0.8	10.0 ± 1.9	38.6 ± 3.4
<b>5o</b>		22.2 ± 6.1	> 50	> 50	> 50	> 50	> 50
<b>5p</b>		8.1 ± 0.2	6.9 ± 0.1	17.6 ± 0.4	17.5 ± 1.5	14.0 ± 2.3	18.2 ± 0.6
<b>5r</b>		3.4 ± 0.3	2.6 ± 0.1	9.3 ± 0.9	13.5 ± 2.8	6.0 ± 0.4	15.1 ± 2.9
<b>5s</b>		10.7 ± 0.0	10.9 ± 0.2	20.0 ± 15.6	30.9 ± 3.9	11.7 ± 2.4	33.1 ± 4.9
<b>5t</b>		7.8 ± 0.9	6.9 ± 0.0	26.0 ± 3.7	32.5 ± 3.7	12.1 ± 2.4	40.0 ± 1.2
<b>5u</b>		9.3 ± 0.7	8.7 ± 2.0	38.0 ± 0.8	46.1 ± 5.4	18.3 ± 1.9	45.6 ± 5.1
<b>5v</b>		> 50	> 50	> 50	> 50	32.3 ± 6.6	> 50
<b>5w</b>		12.8 ± 2.4	9.6 ± 0.5	20.5 ± 1.6	32.1 ± 4.6	14.2 ± 3.7	26.4 ± 2.6
<b>5x</b>		1.3 ± 0.2	6.7 ± 0.1	16.1 ± 1.3	8.3 ± 1.1	15.4 ± 2.5	15.0 ± 1.5

of the selected cancer cell lines. The efficacy of **10e** is however less pronounced in some cancer types due to a greater distance between the 7-methoxynaphthalene and the basic centre as well as the higher flexibility of the linker.

The orientation of the amide bond, through which the group containing the basic centre is attached, was reversed in compounds **10f-10i**. As a result of this change, the inhibitory effect was mostly maintained or in some cases marginally improved, as **10g** inhibits the growth of the glioblastoma cell line U-251 in a high nanomolar range (IC<sub>50</sub> = 0.6 ± 0.1 μM). In addition, this compound shows the greatest selectivity over HEK-293T (~40-fold), which is sometimes used as a non-cancerous control. The selectivity of the other compounds is comparable to that of **5x**, which has the highest selectivity for the MCF-7 cell line (~12-fold) over HEK-293T. However, when considering the results of the clinically evaluated Hsp90 NTD inhibitors 17-DMAG and PU-H71, it is

noted that selectivity to HEK-293T may not be the best safety measure, as previously reported [46]. Both reference compounds show very low inhibitory preference for any of the cancer cell lines over HEK-293T. In view of these results, along with favourable physicochemical properties and synthetic accessibility, compound **5x** was selected for further studies.

## 2.5. Investigation of the binding to the C-terminal domain of Hsp90

### 2.5.1. Hsp90 binding and inhibition assays

To confirm the mode of action of the synthesised inhibitors, a selection of compounds was tested for inhibition of the Hsp90 CTD using a commercially available TR-FRET assay kit. In this assay, the protein-protein interaction between the CTD of Hsp90β or Hsp90α and its cochaperone cyclophilin D (PP1D) can be blocked by Hsp90 CTD

**Table 3**

Antiproliferative IC<sub>50</sub> values (mean ± SD) of the synthesized triazoles **8f-8g**, **10a-10i** and control compounds 17-DMAG and PU-H71 in hepatocellular carcinoma HepG2, colorectal carcinoma HCT-116, glioblastoma multiforme U-251, breast cancer MCF-7, Ewing sarcoma SK-N-MC and embryonic kidney HEK-293T cell lines: establishment of the structure activity relationships of the heteroaliphatic ring featuring the basic centre (Library B).

Cmpd.No.	Structure	IC <sub>50</sub> (μM)					
		MCF-7	SK-N-MC	U-251	HCT-116	Hep-G2	Hek-293T
<b>8f</b>		> 50	> 50	> 50	> 50	> 50	> 50
<b>8g</b>		> 50	> 50	> 50	> 50	> 50	> 50
<b>10a</b>		2.8 ± 0.6	4.9 ± 0.8	7.8 ± 0.4	5.4 ± 0.4	7.3 ± 0.8	7.8 ± 0.1
<b>10b</b>		5.0 ± 1.5	3.0 ± 0.1	10.5 ± 0.9	5.3 ± 0.1	7.9 ± 0.5	7 ± 1.3
<b>10c</b>		3.1 ± 0.5	2.2 ± 0.0	7.3 ± 0.3	3.4 ± 0.6	3.1 ± 0.1	7.1 ± 0.9
<b>10d</b>		3.4 ± 0.2	2.3 ± 0.0	7.9 ± 0.2	3.1 ± 0.5	5.3 ± 1.1	6.5 ± 0.3
<b>10e</b>		> 50	16.0 ± 0.8	4 ± 0.1	12.5 ± 2.4	5 ± 2.2	17.9 ± 3.4
<b>10f</b>		2.4 ± 0.1	2.3 ± 0.0	3.2 ± 0.2	4.3 ± 0.8	3.5 ± 0.1	6.7 ± 1.5
<b>10g</b>		4.6 ± 1.8	4.3 ± 0.2	0.6 ± 0.1	1 ± 0.1	15.1 ± 2.3	24.5 ± 3.5
<b>10h</b>		4.4 ± 2.7	2.8 ± 0.1	2.1 ± 0.9	1.4 ± 0.2	1.3 ± 0.5	5.9 ± 0.4
<b>10i</b>		5.0 ± 0.1	6.2 ± 0.4	3.9 ± 0.3	1.4 ± 0.1	6.8 ± 0.9	5.3 ± 0.9
17-DMAG		0.9 ± 0.1	0.01 ± 0.01	0.02 ± 0.01	0.09 ± 0.01	0.03 ± 0.00	0.04 ± 0.01
PU-H71		3.0 ± 0.5	0.1 ± 0.0	0.07 ± 0.00	0.04 ± 0.00	0.03 ± 0.00	0.05 ± 0.00
Novobiocin		633 ± 33	171 ± 7	244 ± 7	277 ± 15	331 ± 29	n.d.*

\* n.d. – not determined

inhibitors. As a result, the excited donor beads attached to PPID (via GST-tag) cannot excite the acceptor beads on Hsp90 (attached via biotin) because the distance is too long for the emitted light from the donor beads to reach the acceptor. To cover the structural changes in biologically active compounds introduced during the SAR study, compounds **5a**, **5f**, **5p**, **5r**, **5s**, **5t**, **5u**, **5v**, **5w**, **5x**, **8g**, **10f**, **10g** and **10i** were selected for Hsp90β and Hsp90α CTD binding evaluation along with the starting compound **C** (Fig. 4). The compounds were tested at a concentration of 100 μM. To confirm the validity of the assay, novobiocin

(Hsp90 CTD inhibitor) at 1000 μM was tested along with the newly prepared compounds. Although the tested compounds displaying antiproliferative activity in cancer cells were shown to bind to the Hsp90α/β CTD, they may not necessarily have the same abilities to block PPID binding. The results indicate that the compounds that inhibit cell growth bind to the C-terminal domain of Hsp90. The inverse chirality of compounds **C** and **5a** does not play a decisive role in the inhibition of protein-protein interaction of Hsp90 CTD and PPID. As shown by the small differences in the antiproliferative effect on cancer cells, even the



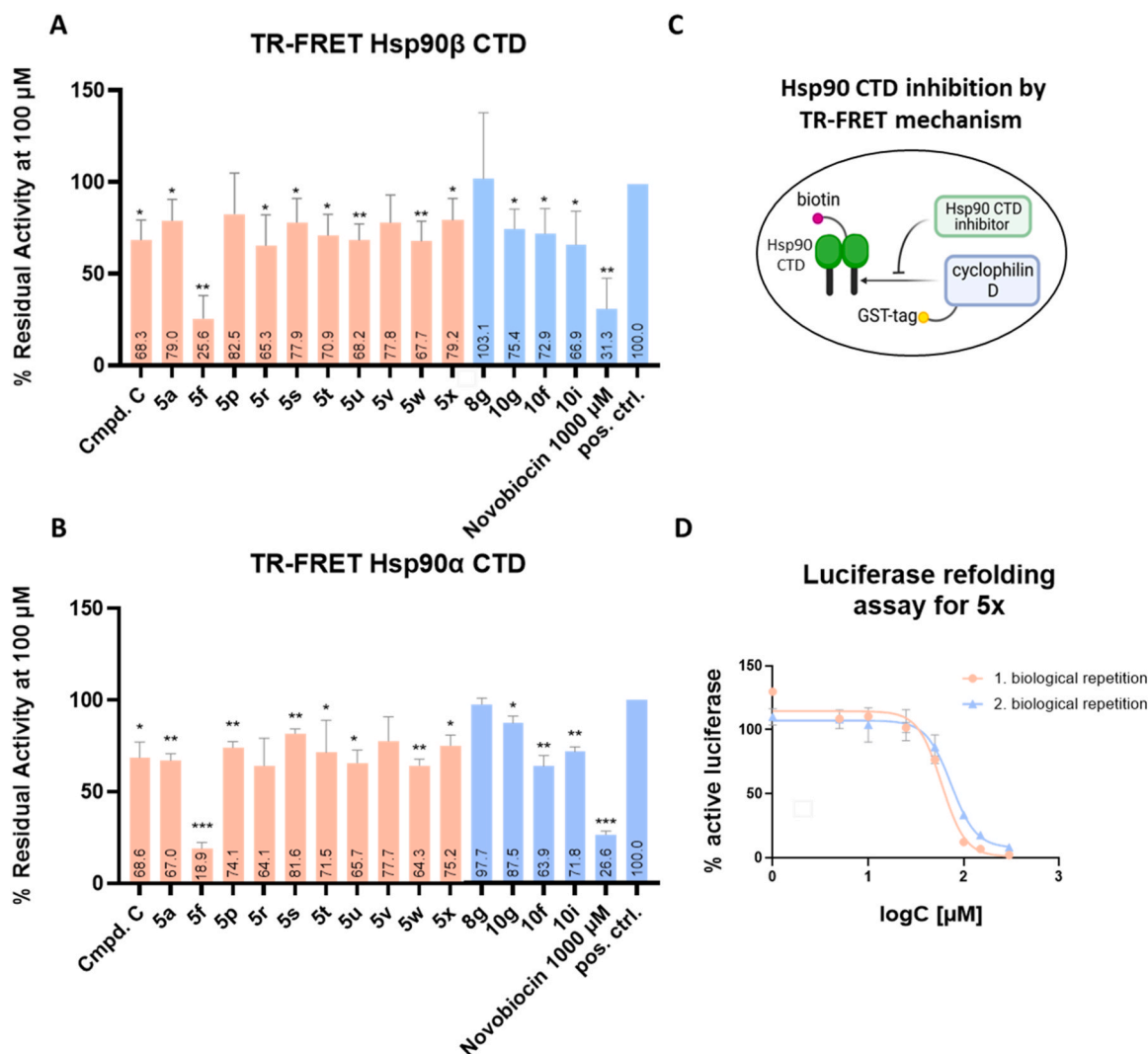


**Fig. 4.** Biochemical evaluation of Hsp90 CTD binding using TR-FRET. Residual activities of Hsp90 $\beta$  (A) and Hsp90 $\alpha$  (B) CTD when triazole-based inhibitors were applied at 100  $\mu$ M concentration: compounds C, 5a, 5f, 5p, 5r, 5s, 5t, 5u, 5v, 5w and 5x from Library A are shown in red, compounds 8g, 10g, 10f, and 10i from Library B along with novobiocin at 1000  $\mu$ M and positive control are presented in blue. The bars represent mean values with SD of at least three replicates. Statistical significance was calculated using one sample t-test (\* $p$ <0.05, \*\* $p$ <0.01, \*\*\* $p$ <0.001); C) Schematic representation of the mechanism of the TR-FRET assay in which the C-terminal Hsp90 inhibitor prevents the interaction of cyclophilin D and Hsp90 CTD; D) Dose-response curves for compound 5x in the luciferase refolding assay in two biological repetitions performed in triplicates.

residual activities of Hsp90 CTD are comparable for compounds 5f, 5p, 5r, 5s, 5t, 5u, 5v, 5w and 5x featuring aromatic variations. The superior inhibitory activity of 5f resulting from a small difference in its structure compared to 5x is not reflected in more potent antiproliferative activity in cells. Furthermore, the change in amide orientation and the modification of the linker between the amide and the basic centre in compounds 10f, 10g and 10i do not lead to a significant increase or decrease in activity at a concentration of 100  $\mu$ M. The inactivity of compound 8g also corresponds to its inactivity in all cancer cell lines.

To further confirm the binding of 5s, 5x and novobiocin to Hsp90, their  $K_d$  values with the full-length Hsp90 $\beta$  were determined using microscale thermophoresis (MST, Fig. 5–7S). The affinity of 5x ( $K_d = 204 \pm 13$   $\mu$ M) for Hsp90 $\beta$  was greater than that of 5s ( $K_d = 317 \pm 6$   $\mu$ M), while the  $K_d$  value of novobiocin was determined to be  $1089 \pm 60$   $\mu$ M. In addition, compounds 5x and novobiocin also bind to the other cytoplasmic isoform Hsp90 $\alpha$  with a similar affinity ( $K_d$  (5x) =  $193 \pm 6$   $\mu$ M,  $K_d$  (novobiocin) =  $1364 \pm 27$   $\mu$ M). Unfortunately, we could not determine the  $K_d$  values for inactive compounds in cell-based assays due to solubility issues at high concentrations.

The synergistic effect of inhibiting at least two of the four Hsp90

isoforms was also tested using a luciferase refolding assay in PC3-MM2luc cells. The genetically modified PC3-MM2 cells were heated to unfold luciferase, which is a client protein of Hsp90. When the Hsp90 function is intact, the chaperone can refold the luciferase back to its native conformation. In the presence of an Hsp90 inhibitor, however, the refolding process is incomplete [27,41,47,48]. The most promising compound 5x was tested in this assay and was shown to inhibit the function of Hsp90 in PC3-MM2 cells with an  $IC_{50}$  value of  $66.3 \pm 7.5$   $\mu$ M. The N-terminal Hsp90 inhibitor 17-DMAG at a concentration of 50  $\mu$ M was used as a positive control and showed  $57.9 \pm 6.4$  % inhibition of Hsp90 function.

To confirm that Hsp90 inhibition by the triazole-based inhibitors is mediated by binding to the C-terminal domain alone, compounds 5s, 5x and novobiocin were tested for their binding to the NTD of Hsp90 using a fluorescence-based thermal shift assay (FTSA) with 17-AAG as a positive control (Fig. 8S). No significant binding of 5s, 5x and novobiocin was detected at concentrations up to 500  $\mu$ M (Fig. 8S), which implies that the  $K_d$  values measured with MST can be attributed to binding to the C-terminal domain of Hsp90.

### 2.5.2. STD-NMR studies of 5x and 10b with full-length Hsp90 $\beta$

The binding of compounds **5x** and **10b** to Hsp90 was investigated by saturation transfer difference (STD) NMR with full-length Hsp90 $\beta$ . The 1D  $^1\text{H}$  STD experiments were performed under quantitative conditions with a ligand to protein ratio of 100:1 and the non-hydrolysable ATP analogue AMP-PCP added to the mixture. According to group epitope mapping analysis of compounds **5x** and **10b** (Figs. 5 and 6) the binding is mainly mediated by the lipophilic 7-methoxynaphthalene ring, as its protons have the highest saturation and thus the strongest interaction with Hsp90. The percent saturation of this region and the saturation transfer of 1,2,3-triazol-1-yl-benzene linker are similar for both **5x** and **10b**, indicating a similar binding position. Looking at the cationic part of the molecules, the STD amplification factors of the aliphatic regions of both **5x** and **10b** are weaker compared to the rest of the molecule. Nonetheless, the data shows that the aliphatic ring bearing the basic centre interacts with the protein. As such, piperazine in **5x** and 4-methylaminopiperidine in **10b** could ensure the proximity of the cationic amines and acidic Glu489A of Hsp90 $\beta$  CTD, which has been shown to be important for binding in previous studies [23–25].

### 2.5.3. Molecular dynamics simulations of 5x and Hsp90 CTD

To further study the binding of **5x** to Hsp90, the compound was docked to the proposed CTD binding site at the interface of the two Hsp90 monomers in a closed conformation of the dimer. The same docking protocol in Fred was used as for compound **C**. In the docking complex, **5x** was predicted to form a network of hydrophobic contacts with Ala600A, Ala608A and Ile605B as well as an ionic interaction and a hydrogen bond with the Glu489A side chain carboxylate group

(Fig. 7A). This predicted binding mode is consistent with the STD-NMR study, in which the naphthalene moiety showed higher STD amplification factors than the piperazine ring. The docking complex was subjected to two independent 500 ns MD simulations showing the stable binding mode of **5x** in the Hsp90 CTD binding site. The MD trajectories were analysed using structure-based pharmacophore modelling in LigandScout Expert 4.5. For each 500 ns MD trajectory, an ensemble of 2500 structure-based pharmacophore models (SBPM) was generated (Supplementary information Fig. 3S). The most frequently occurring SBPM appears more than 500 times and is the same as that of the docking complex. Analysis of the interactions showed that ionic interaction and hydrogen bond with the Glu489A side chain are formed 66 % and 27 % of the simulation time, respectively (Supplementary information Fig. 4S). Hydrophobic interactions with Ala600A, Ala608A, Ala608B and Ile605B account for more than 85 % of the simulation time. The phenyl and triazole moieties form cation- $\pi$  interactions with Arg604A and Arg604B side chains, however, for only around 10 % of the simulation time.

### 2.6. Phenotypic analysis of anticancer properties of compound 5x

#### 2.6.1. Oncogenic client protein degradation

The anticancer properties of Hsp90 inhibitors are primarily mediated by indirect effects on oncogenic client proteins of Hsp90 [49]. Therefore, the effects of **5x** on intracellular Hsp90 client protein levels were examined by Western blot in MCF-7 cells. This hormone-dependent breast cancer cell line overexpresses several known Hsp90 client proteins. Proteins relevant to MCF-7 oncogenesis include but are not limited

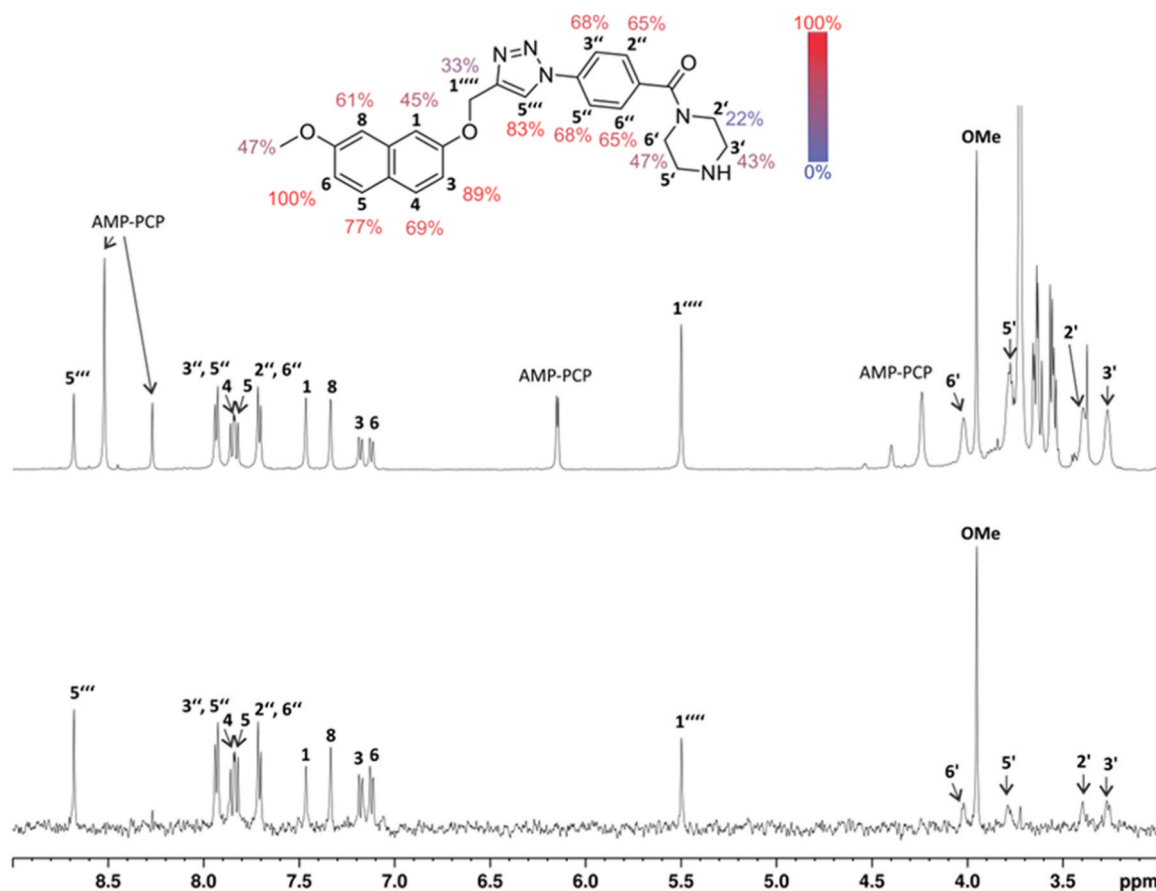
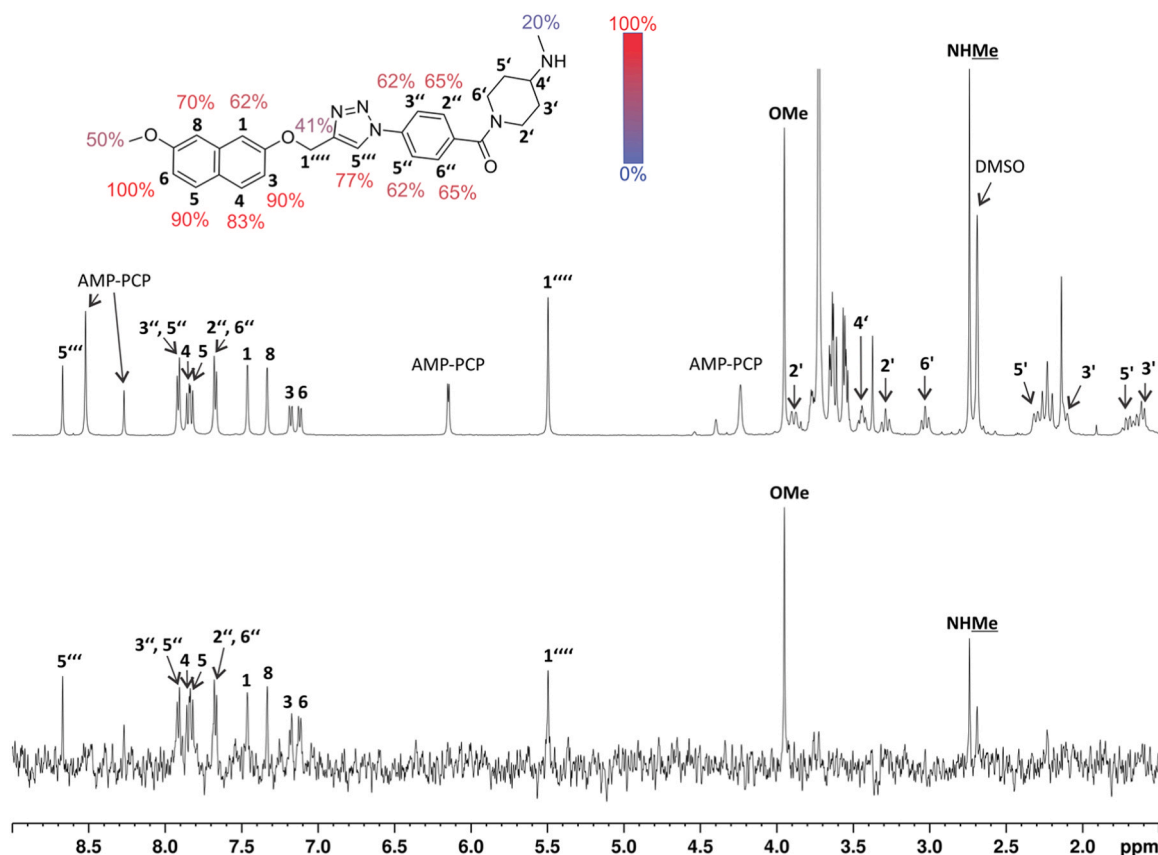
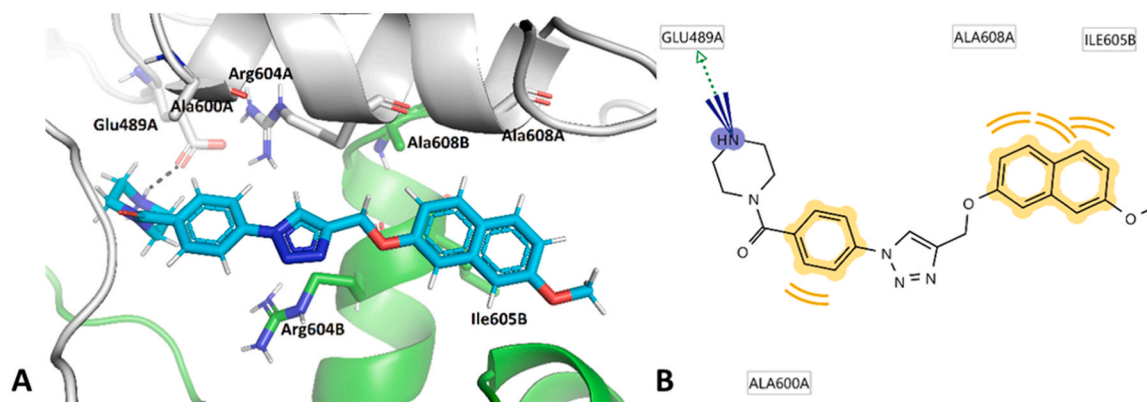


Fig. 5. 1D  $^1\text{H}$  STD NMR spectra for compound **5x** recorded at an Hsp90 $\beta$ :ligand ratio of 1:100. The molecular structure illustrates the proton nomenclature and the colour-coded relative degrees of saturation of individual non-overlapping protons. The STD amplification factors were normalised to the intensity of the signal with the largest STD effect. The reference STD spectrum (top) with proton assignment and the difference STD spectrum (bottom) are shown. The unassigned proton signals between 3.5 and 3.8 ppm belong to protein buffer with glycerol. The spectra are not to scale.



**Fig. 6.** 1D  $^1\text{H}$  STD NMR spectra for compound **10b** recorded at an Hsp90 $\beta$ :ligand ratio of 1:100. The molecular structure illustrates the proton nomenclature and the colour-coded relative degrees of saturation of the individual protons. The STD amplification factors were normalised to the intensity of the signal with the largest STD effect. The reference STD spectrum (top) with proton assignment and the difference STD spectrum (bottom) are shown. The low field signal **6'** is missing due to interference from water suppression. Signals **2'**, **3'**, **4'**, **5'**, and **6'** have insufficient signal-to-noise ratios in the difference STD spectrum. The unassigned proton signals between 3.5 and 3.8 ppm belong to the protein buffer with glycerol. The spectra are not too scale.



**Fig. 7.** A) Docking binding mode of compound **5x** (in cyan sticks) in the Hsp90 $\beta$  dimer (PDB entry: 5FWK, protomers A and B are coloured grey and green, respectively) C-terminal domain binding site. For clarity, only the amino acids that interact with the inhibitor are shown. Hydrogen bonds are shown as black dashed lines. B) Schematic representation of the most frequently occurring pharmacophore model during the MD trajectory. Hydrophobic features are shown in yellow, hydrogen bond donor feature in green and positively charged group in blue.

to oestrogen receptor  $\alpha$  (ER $\alpha$ ), insulin growth factor receptor 1 R (IGF-1R), and the protein kinases ERK 1/2 (extracellular signal-regulated kinases) and MEK (mitogen-activated protein kinase kinase) [50–52]. Therefore, these proteins were selected for the observation of the effects mediated by **5x**. As shown in Fig. 8, inhibition of Hsp90 by **5x** resulted in a statistically significant decrease in the levels of ER $\alpha$ , IGF-1R and MEK when the cells were treated with inhibitor **5x** at 25  $\mu\text{M}$  for 24 hours. Meanwhile, the effects on other proteins or at lower

concentrations were mostly not as pronounced. Nonetheless, a trend towards a reduction in MEK concentrations can also be observed. Importantly, the concentrations of the heat shock proteins Hsp70 and Hsp90 were not significantly increased at any concentration of **5x**. This is consistent with the expected mechanism of C-terminal Hsp90 inhibition, which is known not to induce the HSR. Furthermore, the first described Hsp90 C-terminal inhibitor novobiocin displayed similar effects at significantly higher concentrations of 500  $\mu\text{M}$  and 1000  $\mu\text{M}$ ,

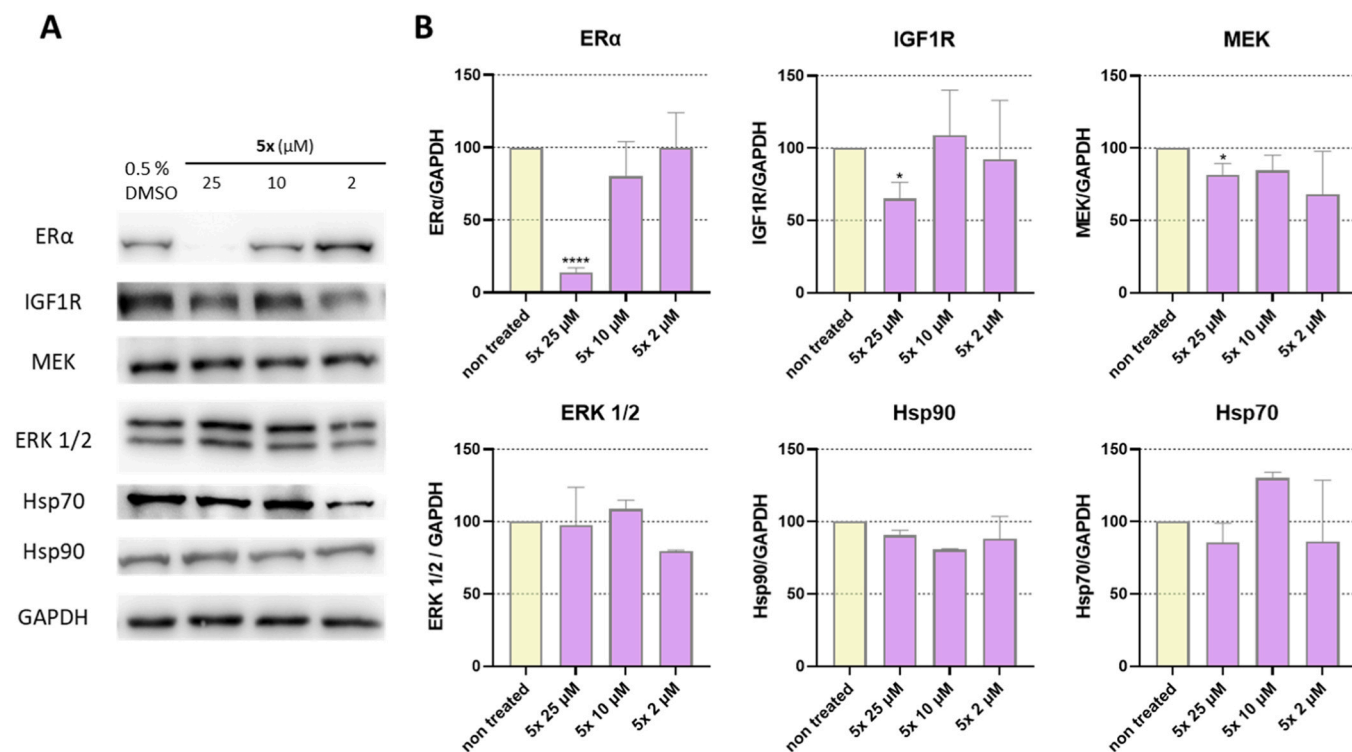


**Fig. 8.** Western blot analysis of effects of compound 5x in MCF-7 cell line on Hsp90 client protein levels (ER $\alpha$ , IGF1R, MEK, ERK 1/2) and representative heat shock proteins (Hsp70, Hsp90) after 24 hours of treatment. A) Representative Western blot images; B) Quantification results normalised on GAPDH levels. The bars represent mean values with SD and Welch's t-test was used to evaluate statistical significance (\* $p < 0.05$ , \*\* $p < 0.01$ , \*\*\* $p < 0.001$ , \*\*\*\* $p < 0.0001$ ). Full images used for quantification are shown in [Supplementary information Figures 11S-14S](#).

while the NTD inhibitor 17-DMAG decreased the client protein levels more potently but it caused a weak heat shock response induction already at 0.5  $\mu$ M after 24 hours of treatment ([Supplementary information Figures 15 S and 16 S](#)).

### 2.6.2. Apoptosis induction in breast cancer and Ewing sarcoma cells

The cytotoxic assay on MCF-7 and SK-N-MC showed extensive potency of 5x in triggering cell death. The major mode of anticancer activity of several Hsp90 inhibitors is induction of programmed cell death [53–55]. To elucidate the mechanisms through which 5x induces cell death, we investigated apoptosis and cell cycle in MCF-7 and SK-N-MC cells. We treated both types of cells with 7–70  $\mu$ M 5x for 24–72 hours and evaluated the externalisation of phosphatidylserine by Annexin V/SB assay.

We showed that inhibition of Hsp90 by 5x significantly increased exposure of phosphatidylserine on the outer plasma membrane of MCF-7 and SK-N-MC cells, measured by R-PE-Annexin V conjugate. The amount of Annexin V positive MCF-7 cells was between 3.2 % and 5.4 % in control cells at all time points and increased by 4–10 % when the cells were treated with 7  $\mu$ M 5x, with the peak effect reached at 48-hour treatment (Fig. 9A-C). The induction of apoptosis by 5x was even more pronounced in SK-NM-C cells, where 7  $\mu$ M of the compound induced an increase in Annexin V labeling from 14 % (control cells) to 38 % (treated cells) after 24-hour treatment ( $p = 0.004$ ; Fig. 9D-E). However, the proportion of apoptotic cells decreased to control levels after 48 and 72 hours of treatment with this concentration. Furthermore, the apoptosis was dose-dependent, since it was induced in 89 % and 98 % of SK-N-MC cells, when they were treated for 24 hours with 35  $\mu$ M 5x and 70  $\mu$ M 5x, respectively ( $p < 0.001$ ). Upon 5x treatment with concentrations higher than 35  $\mu$ M, all SK-N-MC cells remained apoptotic also in later time points.

### 2.6.3. Cell cycle arrest caused by 5x in MCF-7 and SK-N-MC cells

Previous studies investigating Hsp90 inhibitors have shown the influence of such compounds on cell cycle progression [56–59]. Therefore, to complement the data on apoptosis, we next examined the effects of compound 5x on the cell cycle. We treated MCF-7 and SK-N-MC cells with 7  $\mu$ M compound 5x for 24 and 48 hours. Cell cycle analysis (Fig. 9F) revealed that compound 5x significantly increased the percentage of MCF-7 cells in G2/M phase after 24 hours of treatment (from 18.1 % to 24.5 %). At this time, the proportion of living cells in the G0/G1 phase decreased slightly (from 69.39 % to 64.9 %). However, when the cells were treated for 48 hours, a statistically significant decrease in the proportion of MCF-7 cells in the S and G2/M phases was observed (from 9.9 % to 3.4 % and from 20.6 % to 11.16 %, respectively). At the same time, the proportion of living cells in the G0/G1 phase increased from 68 % to 83 %. Cell cycle analysis on SK-N-MC cells showed a similar pattern in the phase-transition when exposed to 7  $\mu$ M compound 5x for 24 hours with a 4.5 % increase in G2/M phase of cell cycle (25.4 % vs 29.9 %, control vs treated cells); however, the results were not statistically significant and showed no differences at later time points ([Supplementary information Figure 17 S](#)). This data suggests that short treatment with compound 5x induces an arrest in the G2/M phase of the cell cycle, especially in MCF-7 cells. Consistent with the information on phosphatidylserine exposure, the cells then most probably undergo apoptosis and the surviving cells remain in the G0/G1 phase.

### 2.7. In vivo inhibition of Ewing sarcoma tumour growth in zebrafish xenografts

The explored mechanism of action of compound 5x provided a starting point for its *in vivo* evaluation. Prior to treatment of zebrafish xenografts, we determined the highest no observed effect concentration (NOEC) of 5x based on overall survival and morphological abnormalities of zebrafish larvae. The larvae were monitored for two days at four

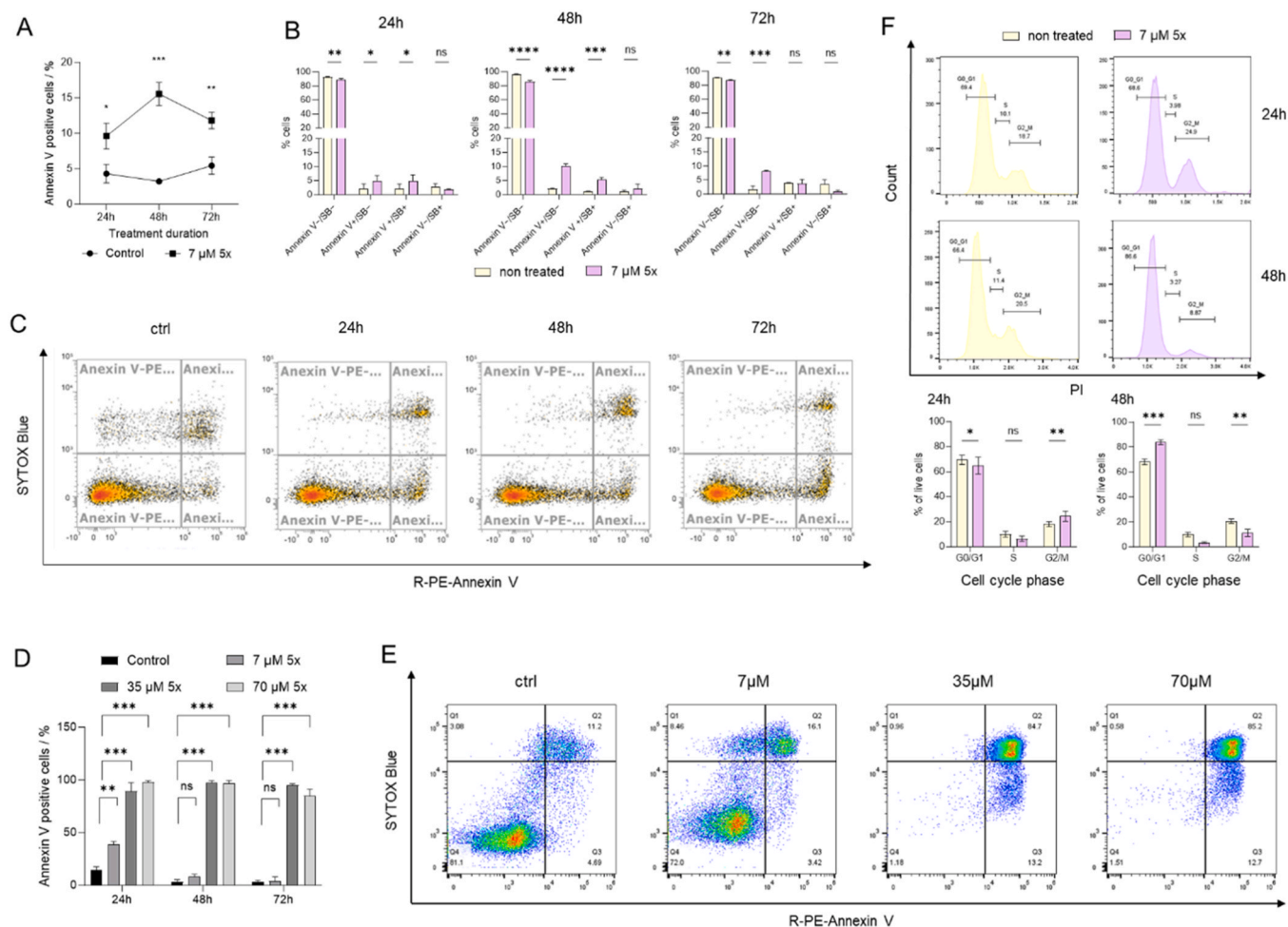


**Fig. 9.** Mechanistic insight into cytostatic behaviour of compound 5x. A) The changes in proportion of annexin V positive cells in dependence of the duration of treatment in MCF-7 cells. B) The extent of different stages of apoptosis at different time points in MCF-7 cells. C) Representative dot plot diagrams for phosphatidylserine exposure and dead cells for all time points in MCF-7 treated with 7 μM compound 5x. D) Dose and time response of phosphatidylserine detection in SK-N-MC cells exposed to 5x. E) Dot plot diagrams for analysis of apoptosis in SK-N-MC cells exposed to 5x for 24 h. F) Cell cycle analysis of MCF-7 cells (2.5 × 10<sup>5</sup> cells/mL) treated with 7 μM compound 5x for 24 h and 48 h. A representative experiment is shown. For analysis of apoptosis, MCF-7 or SK-N-MC cells were labeled with the combination of SYTOX Blue and R-PE-Annexin V conjugate and analyzed by flow cytometry. The cell histograms showing phases were created by measuring propidium iodide (PI) staining and flow cytometry. Data represents means and SD of at least three independent experiments. Multiple comparison t-tests with Bonferroni correction or Student's t-test were used (\*p<0.05, \*\*p<0.01, \*\*\*p<0.001, \*\*\*\*p<0.0001).

different concentrations of 5x (55 μM, 70 μM, 85 μM and 100 μM) and 1 % DMSO as negative control. At least 20 zebrafish larvae were used at each concentration to ensure significance of the results. As can be seen from the Kaplan-Meier curve (Supplementary information Figure 18 S) there were no obvious toxic effects visible on the larvae after the first day. The minimal loss (95 % survival) of single larvae at this developmental stage as recorded at 85 μM was not considered critical. After two days specimens treated with 55 μM and 70 μM of 5x were unaffected by the compound whereas only 85 % and 33 % survived the two-day incubation with 85 μM and 100 μM of 5x. Hence, 70 μM was selected as the NOEC and treatment concentration for zebrafish xenografts.

The larval zebrafish xenotransplantation model allows one to investigate anticancer efficacy of compounds *in vivo* and offers several advantages like comparably high throughput, excellent physiological/physicochemical properties for imaging and simplicity of compound application directly to the fish water. Therefore, a robust previously described zebrafish xenograft model for Ewing Sarcoma was selected for this study [60,61]. In principle, transparent zebrafish larvae are transplanted with fluorescently labelled cells into the perivitelline space at two days post fertilisation (2 dpf). The first image was taken one day post injection (1 dpi) to determine the initial size of the tumour as a

reference. Transplanted larvae were then incubated with either 70 μM 5x or with 1 % DMSO as a negative control. A second measurement of tumour size was performed 3 days after injection of the cancer cells (3 dpi). Comparison of the relative change in tumour area of 1 % DMSO or 70 μM 5x treated zebrafish xenografts reveals a decreased growth in compound-treated xenografts (Fig. 10 and Supplementary information Figures 19S-20S). This demonstrates that the Hsp90 CTD inhibitor 5x significantly inhibits Ewing sarcoma tumour growth *in vivo*.

### 3. Conclusions

Based on compound C and its proposed binding mode to the CTD of Hsp90, a focused library of 33 analogues was prepared. The inhibitors have suitable physicochemical properties and were shown to inhibit cancer cell growth at low micromolar concentrations by interacting with the CTD of Hsp90. In line with previous findings, the binding position of the most potent compound 5x, explored by STD-NMR and molecular dynamics simulations, suggested that the 7-methoxynaphthalene and the cationic centre are crucial for Hsp90 inhibition. Furthermore, 5x was shown to induce apoptosis in both MCF-7 and SK-N-MC cells and to cause cell cycle arrest in G2 phase and G1/G0 phase especially in MCF-7

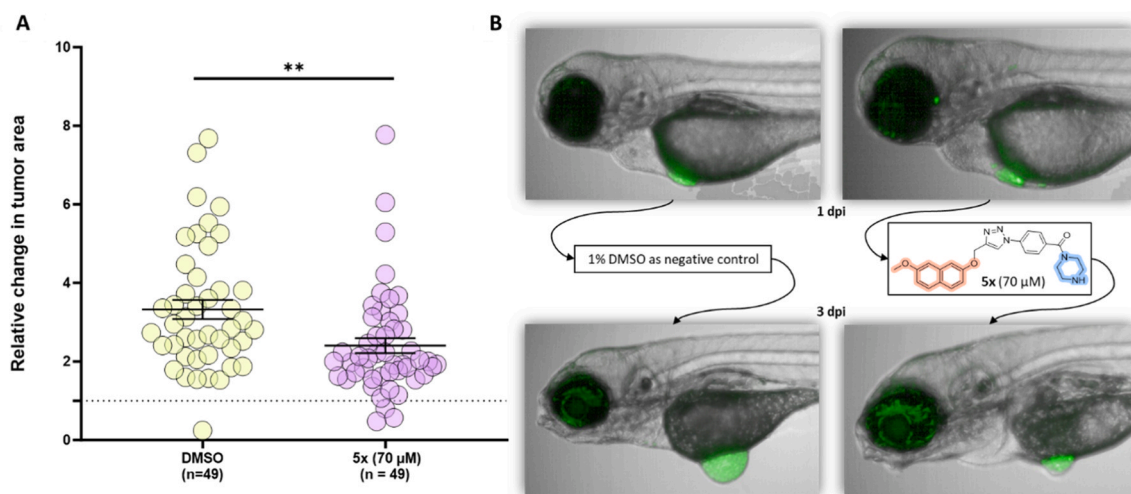


**Fig. 10.** A) Graph depicting a statistically significant difference in relative change in tumour size in larvae treated with 1 % DMSO vs. 70  $\mu\text{M}$  of **5x**; Error bars represent SEM. Statistical analysis was performed with a Kolmogorov-Smirnov test (\*\* $p < 0.01$ ) B) Comparison of representative pictures of zebrafish larvae which show an apparent increase in tumour size with 1 % DMSO (1 dpi vs. 3 dpi), while the increase in tumour volume is much smaller when treated with **5x** (70  $\mu\text{M}$ ).

cells. **5x** also inhibited the refolding of denatured luciferase in PC3-MM2luc cell line and lowered the levels of Hsp90 dependent client proteins ER $\alpha$  and IGF1R in MCF-7 cells. Finally, **5x** was proven to be an *in vivo* effective growth inhibitor of Ewing sarcoma SK-N-MC xenografted tumours in zebrafish larvae. Thus, the initial weakly biologically active CTD Hsp90 inhibitor **C** was successfully optimised to an *in vivo* active compound **5x**, which is a promising candidate for further hit-to-lead optimisation.

## 4. Experimental section

### 4.1. Chemistry

#### 4.1.1. Materials

Reagents and solvents used in the synthetic procedures were purchased from various vendors like Sigma-Aldrich (St. Louis, MO, USA), Enamine Ltd. (Kyiv, Ukraine), TCI (Tokyo, Japan), Combi-Blocks Inc. (San Diego, CA, USA), Apollo Scientific Ltd. (Stockport, UK), and Fluorochem Ltd. (Derbyshire, UK), and were used without any further purification. For analytical thin-layer chromatography silica gel aluminum sheets were used (0.20 mm; 60 F254; Merck, Darmstadt, Germany), while for column chromatography silica gel 60 (particle size, 230–400 mesh) was used as the stationary phase. To record  $^1\text{H}$ ,  $^{13}\text{C}$  and  $^{19}\text{F}$  NMR spectra in the analysis of chemical compounds a 400 MHz NMR spectrometer (Bruker Advance 3, Bruker, Billerica, MA, USA) was used. The designation of splitting patterns was done as follows: s, singlet; d, doublet; dd, double doublet; td, triple doublet; t, triplet; dt, double triplet; ddd, double of doublet of doublet; q, quartet; p, pentet; and m, multiplet. For the monitoring of purity of the final products high performance liquid chromatography (HPLC) (1260 Infinity II LC system, Agilent Technologies, Santa Clara, CA, USA) or ultra-high performance liquid chromatography (UHPLC) (Thermo Scientific Dionex UltiMate 3000 UHPLC modular system, Thermo Fischer Scientific Inc., Waltham, MA, USA) was used. Both were equipped with a wavelength detector to perform the purity determination at 254 nm. The method used on the HPLC was set up as follows: the column used was a  $\text{C}_{18}$  column (Waters xBridge BEH; 4.6 mm  $\times$  150 mm, 3.5  $\mu\text{m}$ ) and the temperature of the oven was set to 40  $^\circ\text{C}$ . The volume of the sample injected was 10  $\mu\text{L}$ , while the flow rate of the mobile phase was set to 1.5 mL/min. The mobile phase comprised appropriate ratios of Solvent A (1 %  $\text{CH}_3\text{CN}$  and 0.1 %  $\text{HCOOH}$  in double-distilled  $\text{H}_2\text{O}$ ) and Solvent B ( $\text{CH}_3\text{CN}$ ). The elution gradient was used as follows: 0–1 min, 25 % B; 1–6 min, 25%–98 % B; 6–6.5 min, 98 % B; 6.5–7 min, 98%–25 % B;

7–10 min, 25 % B. The method used on the HPLC was set up as follows: the column used was a  $\text{C}_{18}$  column (Waters Acquity UPLC $^{\text{®}}$  HSS C18 SB column, 2.1 mm  $\times$  50 mm, 1.8  $\mu\text{m}$ ) and the temperature of the oven was set to 40  $^\circ\text{C}$ . The volume of the sample injected was 5  $\mu\text{L}$ , while the flow rate of the mobile phase was set to 0.3 mL/min. The mobile phase comprised appropriate ratios of Solvent A (0.1 % TFA in  $\text{H}_2\text{O}$ ) and Solvent B ( $\text{CH}_3\text{CN}$ ). The elution gradient was used as follows: 0–7 min 5 % B; 7–8 min 95 % B. Mass spectra were recorded using Expression CMS $^{\text{L}}$  mass spectrometer (Advion Inc., Ithaca, NY, USA). For the high-resolution mass spectra Exactive Plus Orbitrap mass spectrometer (Thermo Scientific Inc., Waltham, MA, USA) was used.

#### 4.1.2. Synthetic procedures and analytical data

##### General procedures

##### General procedure A

General procedure A was applied in the synthesis of compounds **2**, **3h–3l**, **6a–6l**, and **10a–10i**. The corresponding carboxylic acid (1 eq) was dissolved in DMF. Then 1-ethyl-3-(3-dimethylaminopropyl)carbodiimide (EDC, 1.3 eq), 1-hydroxybenzotriazole (HOBT, 1.3 eq) and *N*-methylmorpholine (NMM, 2 eq) were added at 0  $^\circ\text{C}$ . After 20 minutes of stirring at 0  $^\circ\text{C}$  respective amines (1 eq) were added, and the reaction was stirred at room temperature overnight. The solvent was then evaporated, and the residue was taken up in ethyl acetate. The organic layer was then washed with 1 % citric acid, 1 M NaOH(aq) and brine. The organic layer was then dried over  $\text{Na}_2\text{SO}_4$ , filtered and the volatiles were evaporated under reduced pressure to yield compounds **2**, **6a–6l**, and **10a–10i**.

##### General procedure B

General procedure B was applied in the synthesis of compounds **2**, **6a–6l**, and **10a–10i**. Respective Boc-protected amines (1 eq) were taken up in either dichloromethane and trifluoroacetic acid (25 eq) or 1,4-dioxane and 4 M HCl in 1,4-dioxane (50 eq) was added. The reaction mixture was stirred overnight at room temperature. Either the precipitate that formed was filtered off or the volatiles were evaporated under reduced pressure. In some cases, the residue was purified by flash column chromatography to yield compounds **2**, **6a–6l**, and **10a–10i**.

##### General procedure C

General procedure C was applied in the synthesis of compounds **3a–3c**, and **6m–6n**. The corresponding aliphatic alcohol (1 eq) and sodium hydride, 60 % dispersion in mineral oil (3 eq), were taken up in dry THF at 0  $^\circ\text{C}$ . After stirring at room temperature for 30 min, propargyl bromide, 80 % solution in toluene (3 eq), was added and the reaction was stirred overnight at room temperature. After this, the solvent was

evaporated under reduced pressure and the product was taken up in dichloromethane (DCM) or ethyl acetate (EtOAc). The organic layer was then washed with 1 M NaOH(aq) and brine. Afterwards the solvent was evaporated, and the residue was purified by flash column chromatography when needed to yield compounds **3a–3c**, and **6m–6n**.

#### General procedure D

General procedure D was applied in the synthesis of compounds **3d–3g**, and **6p–6x**. The corresponding aromatic alcohol (1 eq) and potassium carbonate (3 eq), were taken up in *N,N*-dimethylformamide (DMF). After stirring at 0 °C for 30 min, propargyl bromide, 80 % solution in toluene (3 eq), was added and the reaction was stirred overnight at room temperature. After this, the solvent was evaporated under reduced pressure and the residue was purified by flash column chromatography when needed to yield compounds **3d–3g**, and **6p–6x**.

#### General procedure E

General procedure E was applied for the synthesis of compounds **3h–3l**. The corresponding aromatic carboxylic acid (1 eq) was dissolved in dry DCM under an argon atmosphere and oxalyl chloride (2 eq) was added on an ice bath. The reaction mixture was stirred overnight at room temperature and the solvent was evaporated under reduced pressure. The residue was taken up in dry DCM and triethylamine (3 eq) and propargylamine (1.2 eq) were added on an ice bath. The reaction mixture was stirred at room temperature overnight and the solvent was evaporated under reduced pressure. The residue was taken up in ethyl acetate. In some cases, a precipitate formed that was filtered off. Otherwise, the organic layer was washed with 1 M HCl(aq), 1 M NaOH (aq) and brine. The organic layer was then dried over Na<sub>2</sub>SO<sub>4</sub>, filtered and the volatiles were evaporated under reduced pressure to yield compounds **3h–3l**.

#### General procedure F

General procedure F was applied in the synthesis of compounds **4a–4l**, **5m–6x**, **8m–8g** and **9a–9d**. The corresponding azide (1 eq), corresponding alkyne (1 eq), sodium ascorbate (0.4 eq) and copper(II) sulphate (0.2 eq) were taken up in the mixture of MeOH and water (2:1). The reaction was stirred overnight at room temperature. In some cases, a precipitate formed that was filtered off. Otherwise, the solvent was evaporated under reduced pressure and the product was further purified by column chromatography. After suitable purification steps were applied when needed, compounds **4a–4l**, **5m–6x**, **8m–8g** and **9a–9d** were obtained.

*tert*-Butyl 4-(4-azidobenzoyl)piperazine-1-carboxylate (1)

Compound **1** was prepared according to General procedure A using 1-Boc-piperazine (1.72 g, 9.20 mmol) and 4-azidobenzoic acid (1.50 g, 9.20 mmol) as starting material. Yield: 89.0 % (2.7 g); <sup>1</sup>H NMR (400 MHz, CDCl<sub>3</sub>) δ 7.45–7.40 (m, 2 H), 7.09–7.05 (m, 2 H), 3.81–3.33 (m, 8 H), 1.47 (s, 9 H) ppm; MS (ESI+) C<sub>16</sub>H<sub>21</sub>N<sub>5</sub>O<sub>3</sub> 332.0 [M+H]<sup>+</sup>. HRMS calcd. for C<sub>16</sub>H<sub>22</sub>O<sub>3</sub>N<sub>5</sub> [M+H]<sup>+</sup> 332.1717, found 332.1712.

(4-Azidophenyl)(piperazin-1-yl)methanone (2)

Compound **2** was prepared according to the General procedure B from the Boc-protected amine **1** (3.0 g, 9.1 mmol). Yield: 99.0 % (2.1 g); white solid; <sup>1</sup>H NMR (400 MHz, CDCl<sub>3</sub>) δ 7.47–7.40 (m, 2 H), 7.21–7.14 (m, 2 H), 3.72–2.58 (m, 8 H) ppm; <sup>13</sup>C NMR (101 MHz, DMSO-*d*<sub>6</sub>) δ 168.20, 140.49, 132.70, 128.94, 119.03, 48.64, 45.67, 42.82 ppm; HRMS calcd. for C<sub>11</sub>H<sub>14</sub>ON<sub>5</sub> [M+H]<sup>+</sup> 232.1193, found 232.1189.

(1*R*,2*R*)-1-(Prop-2-yn-1-yloxy)-2-(trifluoromethyl)-1,2,3,4-tetrahydronaphthalene (3a)

Compound **3a** was prepared according to the literature procedure [29], starting from (*R,R*)-2-trifluoromethyl-1-tetralol. Yield: 84.0 % (0.106 g); <sup>1</sup>H NMR (400 MHz, CDCl<sub>3</sub>) δ 7.36–7.32 (m, 1 H), 7.32–7.27 (m, 1 H), 7.23–7.17 (m, 2 H), 4.92 (d, *J* = 2.0 Hz, 1 H), 4.23 (dd, *J*<sub>1</sub> = 16.1 Hz, *J*<sub>2</sub> = 2.4 Hz, 1 H), 4.06 (dd, *J*<sub>1</sub> = 16.1 Hz, *J*<sub>2</sub> = 2.4 Hz, 1 H), 3.06 (dd, *J*<sub>1</sub> = 17.3 Hz, *J*<sub>2</sub> = 6.8 Hz, 1 H), 2.86 (ddd, *J*<sub>1</sub> = 17.7 Hz, *J*<sub>2</sub> =

11.1 Hz, *J*<sub>3</sub> = 7.1 Hz, 1 H), 2.55–2.42 (m, 2 H), 2.32 (tdd, *J*<sub>1</sub> = 12.9 Hz, *J*<sub>2</sub> = 11.0 Hz, *J*<sub>3</sub> = 6.8 Hz, 1 H), 2.06–1.95 (m, 1 H) ppm; <sup>19</sup>F NMR (376 MHz, CDCl<sub>3</sub>) δ –68.67 (d, *J* = 8.8 Hz) ppm. NMR data is in accordance with the literature data [29].

(1*S*,2*S*)-7-Methoxy-1-(prop-2-yn-1-yloxy)-2-(trifluoromethyl)-1,2,3,4-tetrahydronaphthalene (3b)

Compound **3b** was prepared according to the General procedure C from (*S,S*)-7-methoxy-2-trifluoromethyl-1-tetralol [29] (79.4 mg, 0.323 mmol). Yield 70.0 % (64.6 mg); colorless oil; <sup>1</sup>H NMR (400 MHz, CDCl<sub>3</sub>) δ 7.09 (d, *J* = 8.5 Hz, 1 H), 6.91 (d, *J* = 2.8 Hz, 1 H), 6.85 (dd, *J*<sub>1</sub> = 8.4 Hz, *J*<sub>2</sub> = 2.7 Hz, 1 H), 4.87 (d, *J* = 2.2 Hz, 2 H), 4.24 (dd, *J*<sub>1</sub> = 16.1 Hz, *J*<sub>2</sub> = 2.4 Hz, 1 H), 4.09 (dd, *J*<sub>1</sub> = 16.1 Hz, *J*<sub>2</sub> = 2.4 Hz, 1 H), 3.80 (s, 3 H), 2.97 (ddd, *J*<sub>1</sub> = 17.5 Hz, *J*<sub>2</sub> = 7.0 Hz, *J*<sub>3</sub> = 2.0 Hz, 2 H), 2.83–2.70 (m, 1 H), 2.49–2.38 (m, 2 H), 2.27 (tdd, *J*<sub>1</sub> = 12.9 Hz, *J*<sub>2</sub> = 11.1 Hz, *J*<sub>3</sub> = 6.7 Hz, 1 H), 2.03–1.89 (m, 1 H). <sup>19</sup>F NMR (376 MHz, CDCl<sub>3</sub>) δ –68.55 (d, *J* = 8.9 Hz) ppm; <sup>13</sup>C NMR (101 MHz, CDCl<sub>3</sub>) δ 157.47, 133.93, 130.53, 128.39, 127.07 (q, *J* = 279.5 Hz), 115.12, 115.08, 79.77, 75.15, 71.07 (q, *J* = 2.9 Hz), 55.57, 55.43, 44.00 (q, *J* = 26.5 Hz), 26.81, 16.93 (q, *J* = 2.3 Hz) ppm; MS – non ionisable.

(1*S*,2*S*)-1-(Prop-2-yn-1-yloxy)-2-(trifluoromethyl)-indane (3c)

Compound **3c** was prepared according to the General procedure C from (*S,S*)-2-trifluoromethyl-1-indanol (108 mg, 0.534 mmol). Yield 88.0 % (0.113 mg); colourless oil; <sup>1</sup>H NMR (400 MHz, CDCl<sub>3</sub>) δ 7.46 (d, *J* = 7.3 Hz, 1 H), 7.37–7.21 (m, 3 H), 5.25 (d, *J* = 5.6 Hz, 1 H), 4.25 (dd, *J*<sub>1</sub> = 16.1 Hz, *J*<sub>2</sub> = 2.4 Hz, 1 H), 4.15 (dd, *J*<sub>1</sub> = 16.1 Hz, *J*<sub>2</sub> = 2.4 Hz, 1 H), 3.43–3.30 (m, 1 H), 3.21–2.97 (m, 2 H), 2.50 (t, *J* = 2.4 Hz, 1 H). <sup>19</sup>F NMR (376 MHz, CDCl<sub>3</sub>) δ –65.45 (d, *J* = 9.1 Hz) ppm; <sup>13</sup>C NMR (101 MHz, CDCl<sub>3</sub>) δ 141.72, 139.65, 129.58, 127.07, 126.36 (q, *J* = 277.9 Hz), 125.74, 125.31, 79.64, 78.84 (q, *J* = 2.1 Hz), 75.11, 56.08, 47.62 (q, *J* = 27.4 Hz), 30.96 (q, *J* = 2.6 Hz) ppm; HRMS calcd. for C<sub>13</sub>H<sub>11</sub>OF<sub>3</sub>Na [M+Na]<sup>+</sup> 263.0654, found 263.0648.

1-Methoxy-4-(prop-2-yn-1-yloxy)benzene (3d)

Compound **3d** was prepared according to General procedure D using 4-methoxyphenol (0.53 g, 4.3 mmol) as starting material. Yield: 56.0 % (0.389 g); brown oil; <sup>1</sup>H NMR (400 MHz, CDCl<sub>3</sub>) δ 6.96–6.90 (m, 2 H), 6.87–6.82 (m, 2 H), 4.64 (d, *J* = 2.4 Hz, 2 H), 3.77 (s, 3 H), 2.51 (t, *J* = 2.4 Hz, 1 H) ppm; MS – non ionisable.

1-(Prop-2-yn-1-yloxy)naphthalene (3e)

Compound **3e** was prepared according to General procedure D using 1-naphthol (0.50 g, 3.5 mmol) as starting material. Yield: 64.0 % (0.403 mg); brown oil; <sup>1</sup>H NMR (400 MHz, CDCl<sub>3</sub>) δ 8.29–8.26 (m, 1 H), 7.84–7.77 (m, 1 H), 7.54–7.45 (m, 3 H), 7.42–7.34 (m, 1 H), 6.95 (dd, *J*<sub>1</sub> = 7.6 Hz, *J*<sub>2</sub> = 1.0 Hz, 1 H), 4.90 (d, *J* = 2.4 Hz, 2 H), 2.55 (t, *J* = 2.4 Hz, 1 H) ppm; MS (ESI-) C<sub>13</sub>H<sub>10</sub>O m/z 181.1 [M-H]<sup>-</sup>.

2-(Prop-2-yn-1-yloxy)naphthalene (3f)

Compound **3f** was prepared according to General procedure D using 2-naphthol (0.50 g, 3.5 mmol) as starting material. Yield: 59.0 % (0.374 g); brown solid; <sup>1</sup>H NMR (400 MHz, CDCl<sub>3</sub>) δ 7.85–7.72 (m, 3 H), 7.45 (ddd, *J*<sub>1</sub> = 8.2 Hz, *J*<sub>2</sub> = 6.8 Hz, *J*<sub>3</sub> = 1.3 Hz, 1 H), 7.36 (ddd, *J*<sub>1</sub> = 8.2 Hz, *J*<sub>2</sub> = 6.8 Hz, *J*<sub>3</sub> = 1.3 Hz, 1 H), 7.24 (d, *J* = 2.6 Hz, 1 H), 7.19 (dd, *J*<sub>1</sub> = 9.0 Hz, *J*<sub>2</sub> = 2.6 Hz, 1 H), 4.82 (d, *J* = 2.4 Hz, 2 H), 2.55 (t, *J* = 2.4 Hz, 1 H) ppm; MS – non ionisable.

1,2-Dichloro-4-(prop-2-yn-1-yloxy)benzene (3g)

Compound **3g** was prepared according to General procedure D using 3,4-dichlorophenol (0.50 g, 3.1 mmol) as starting material. Yield: 62 % (0.380 g); orange oil; <sup>1</sup>H NMR (400 MHz, DMSO-*d*<sub>6</sub>) δ = 7.56 (d, 1 H, *J* = 8.9 Hz), 7.31 (d, 1 H, *J* = 3.0 Hz), 7.02 (dd, 1 H, *J*<sub>1</sub> = 8.9 Hz, *J*<sub>2</sub> = 2.9 Hz), 4.87 (d, 2 H, *J* = 2.4 Hz), 3.64 (t, 1 H, *J* = 2.4 Hz) ppm; MS –

non ionisable.

*N*-(Prop-2-yn-1-yl)-1*H*-indole-2-carboxamide (3h)

Compound **3h** was prepared according to General procedure E using 1*H*-indole-2-carboxylic acid (0.50 g, 3.1 mmol) as starting material. The precipitate that formed was further washed with water to yield a clean product **3h**. Yield: 63 % (0.385 g); light brown solid; <sup>1</sup>H NMR (400 MHz, DMSO-*d*<sub>6</sub>): δ = 11.63 (s, 1 H), 8.94 (t, 1 H, *J* = 5.7 Hz), 7.62 (dd, 1 H, *J*<sub>1</sub> = 8.1 Hz, *J*<sub>2</sub> = 1.0 Hz), 7.43 (dd, 1 H, *J*<sub>1</sub> = 8.2 Hz, *J*<sub>2</sub> = 1.0 Hz), 7.12 – 7.22 (m, 2 H), 7.04 (ddd, 1 H, *J*<sub>1</sub> = 7.9 Hz, *J*<sub>2</sub> = 6.9 Hz, *J*<sub>3</sub> = 1.0 Hz), 4.09 (dd, 2 H, *J*<sub>1</sub> = 5.6 Hz, *J*<sub>2</sub> = 2.6 Hz), 3.17 (t, 1 H, *J* = 2.5 Hz) ppm; MS (ESI+) C<sub>12</sub>H<sub>10</sub>N<sub>2</sub>O m/z 199.8 [M+H]<sup>+</sup>.

5-Methoxy-*N*-(prop-2-yn-1-yl)-1*H*-indole-2-carboxamide (3i)

Compound **3i** was prepared according to General procedure E using 5-methoxy-1*H*-indole-2-carboxylic acid (0.50 g, 2.6 mmol) as starting material. After the extraction the product was additionally purified by column chromatography using EtOAc:Hex = 1:2 as the mobile phase. Yield: 46 % (0.274 g); orange solid; <sup>1</sup>H NMR (400 MHz, DMSO-*d*<sub>6</sub>): δ = 11.47 (s, 1 H), 8.88 (t, 1 H, *J* = 5.6 Hz), 7.31 (d, 1 H, *J* = 8.9 Hz), 7.07 (dd, 2 H, *J*<sub>1</sub> = 9.1 Hz, *J*<sub>2</sub> = 1.9 Hz), 6.84 (dd, 1 H, *J*<sub>1</sub> = 8.9 Hz, *J*<sub>2</sub> = 2.5 Hz), 4.08 (dd, 2 H, *J*<sub>1</sub> = 5.6 Hz, *J*<sub>2</sub> = 2.5 Hz), 3.76 (s, 3 H), 3.17 (t, 1 H, *J* = 2.5 Hz) ppm; MS (ESI+) C<sub>13</sub>H<sub>12</sub>N<sub>2</sub>O<sub>2</sub> m/z 228.7 [M+H]<sup>+</sup>.

3,4-Dichloro-*N*-(prop-2-yn-1-yl)benzamide (3j)

Compound **3j** was prepared according to General procedure E using 3,4-dichlorobenzoic acid (0.75 g, 3.9 mmol) as starting material. The extraction yielded a clean product **3j**. Yield: 93 % (0.834 g); off-white solid; <sup>1</sup>H NMR (400 MHz, CDCl<sub>3</sub>) δ 7.89 (d, *J* = 2.0 Hz, 1 H), 7.61 (dd, *J*<sub>1</sub> = 8.3 Hz, *J*<sub>2</sub> = 2.1 Hz, 1 H), 7.53 (d, *J* = 8.3 Hz, 1 H), 6.27 (s, 1 H), 4.25 (dd, *J*<sub>1</sub> = 5.2 Hz, *J*<sub>2</sub> = 2.6 Hz, 2 H), 2.31 (t, *J* = 2.6 Hz, 1 H) ppm; MS (ESI+) C<sub>10</sub>H<sub>7</sub>Cl<sub>2</sub>NO m/z 227.9 [M+H]<sup>+</sup>.

2-(3,4-Dichlorophenyl)-*N*-(prop-2-yn-1-yl)acetamide (3k)

Compound **3k** was prepared according to General procedure E using 2-(3,4-dichlorophenyl)acetic acid (0.40 g, 2.0 mmol) as starting material. The extraction yielded a clean product **3k**. Yield: 64 % (0.304 g); light red solid; <sup>1</sup>H NMR (400 MHz, CDCl<sub>3</sub>) δ 7.43 (d, *J* = 8.2 Hz, 1 H), 7.38 (d, *J* = 2.1 Hz, 1 H), 7.13 (dd, *J*<sub>1</sub> = 8.2 Hz, *J*<sub>2</sub> = 2.1 Hz, 1 H), 5.66 (s, 1 H), 4.04 (dd, *J*<sub>1</sub> = 5.3 Hz, *J*<sub>2</sub> = 2.5 Hz, 2 H), 3.53 (s, 2 H), 2.23 (t, *J* = 2.6 Hz, 1 H) ppm; MS (ESI+) C<sub>11</sub>H<sub>9</sub>Cl<sub>2</sub>NO m/z 242.4 [M+H]<sup>+</sup>.

*N*-(Prop-2-yn-1-yl)-2-naphthamide (3l)

Compound **3l** was prepared according to General procedure E using 2-(3,4-dichlorophenyl)acetic acid (0.50 g, 2.9 mmol) as starting material. The precipitate that formed was further washed with water to yield a clean product **3l**. Yield: 69 % (0.420 g); white solid; <sup>1</sup>H NMR (400 MHz, DMSO-*d*<sub>6</sub>): δ = 9.12 (t, 1 H, *J* = 5.6 Hz), 8.48 (d, 1 H, *J* = 1.7 Hz), 8.08 – 7.90 (m, 4 H), 7.67 – 7.55 (m, 2 H), 4.12 (dd, 2 H, *J*<sub>1</sub> = 5.6 Hz, *J*<sub>2</sub> = 2.5 Hz), 3.17 (t, 1 H, *J* = 2.5 Hz) ppm; MS (ESI+) C<sub>14</sub>H<sub>11</sub>NO m/z 209.7 [M+H]<sup>+</sup>.

1-(Prop-2-yn-1-yloxy)-1,2,3,4-tetrahydronaphthalene (3m)

Compound **3m** was prepared according to the General procedure C from *rac*-1-tetralol (200 mg, 1.35 mmol). After purification by flash chromatography, eluent hexane/EtOAc 9:1, the title compound was isolated as a colorless oil. Yield: 84 % (210 mg); <sup>1</sup>H NMR (400 MHz, CDCl<sub>3</sub>) δ 7.43–7.33 (m, 1 H), 7.25–7.13 (m, 2 H), 7.15–7.05 (m, 1 H), 4.68 (t, *J* = 4.5 Hz, 1 H), 4.24 (d, *J* = 2.4 Hz, 2 H), 2.89–2.78 (m, 1 H), 2.76–2.65 (m, 1 H), 2.46 (t, *J* = 2.4 Hz, 1 H), 2.08–1.94 (m, 2 H), 1.94–1.84 (m, 1 H), 1.80–1.69 (m, 1 H) ppm; <sup>13</sup>C NMR (101 MHz, CDCl<sub>3</sub>) δ 137.81, 135.89, 129.78, 129.11, 127.83, 125.82, 80.63, 74.29, 73.80, 55.46, 29.10, 27.81, 18.68 ppm; MS – non ionisable.

(1*S*,2*S*)-6-Methoxy-1-(prop-2-yn-1-yloxy)-2-(trifluoromethyl)-1,2,3,4-tetrahydronaphthalene (3n)

Compound **3n** was prepared according to the General procedure C from (*S,S*)-6-methoxy-2-trifluoromethyl-1-tetralol (125 mg, 0.508 mmol). The crude product was purified by flash chromatography, eluent hexane/EtOAc 9:1. Yield: 76 % (110 mg); light yellow oil; <sup>1</sup>H NMR (400 MHz, CDCl<sub>3</sub>) δ 7.27 (d, *J* = 8.3 Hz, 1 H), 6.75 (dd, *J*<sub>1</sub> = 8.3 Hz, *J*<sub>2</sub> = 2.7 Hz, 1 H), 6.71 (d, *J* = 2.5 Hz, 1 H), 4.88 (d, *J* = 2.1 Hz, 1 H), 4.20 (dd, *J*<sub>1</sub> = 16.1 Hz, *J*<sub>2</sub> = 2.4 Hz, 1 H), 4.03 (dd, *J*<sub>1</sub> = 16.1 Hz, *J*<sub>2</sub> = 2.4 Hz, 1 H), 3.80 (s, 3 H), 3.02 (dd, *J*<sub>1</sub> = 17.1 Hz, *J*<sub>2</sub> = 6.4 Hz, 1 H), 2.83 (ddd, *J*<sub>1</sub> = 17.6 Hz, *J*<sub>2</sub> = 11.2 Hz, *J*<sub>3</sub> = 7.1 Hz, 1 H), 2.49 (t, *J* = 2.4 Hz, 1 H), 2.55–2.38 (m, 1 H), 2.30 (tdd, *J*<sub>1</sub> = 12.9 Hz, *J*<sub>2</sub> = 11.2 Hz, *J*<sub>3</sub> = 6.8 Hz, 1 H), 2.04–1.89 (m, 1 H) ppm; <sup>19</sup>F NMR (376 MHz, CDCl<sub>3</sub>) δ –68.71 (d, *J* = 9.0 Hz) ppm; MS – non ionisable.

1-(Prop-2-yn-1-yloxy)-2,3-dihydro-1*H*-indene (3o)

Compound **3m** was prepared according to the General procedure C from *rac*-1-indanol (200 mg, 1.49 mmol). After purification by flash chromatography, eluent hexane/EtOAc 5:1, the title compound was isolated as a light yellow oil. Yield: 34 % (87 mg); <sup>1</sup>H NMR (400 MHz, CDCl<sub>3</sub>) δ 7.42 (d, *J* = 7.2 Hz, 1 H), 7.29 – 7.16 (m, 3 H), 5.14 (dd, *J*<sub>1</sub> = 6.5 Hz, *J*<sub>2</sub> = 3.6 Hz, 1 H), 4.22 (d, *J* = 2.4 Hz, 2 H), 3.10 (ddd, *J*<sub>1</sub> = 15.1 Hz, *J*<sub>2</sub> = 8.2 Hz, *J*<sub>3</sub> = 6.5 Hz, 1 H), 2.81 (ddd, *J*<sub>1</sub> = 15.9 Hz, *J*<sub>2</sub> = 8.4 Hz, *J*<sub>3</sub> = 4.7 Hz, 1 H), 2.46 (t, *J* = 2.4 Hz, 1 H), 2.35 (ddt, *J*<sub>1</sub> = 13.2 Hz, *J*<sub>2</sub> = 8.4 Hz, *J*<sub>3</sub> = 6.5 Hz, 1 H), 2.13 (dddd, *J*<sub>1</sub> = 13.4 Hz, *J*<sub>2</sub> = 8.2 Hz, *J*<sub>3</sub> = 4.7 Hz, *J*<sub>4</sub> = 3.6 Hz, 1 H) ppm; <sup>13</sup>C NMR (101 MHz, CDCl<sub>3</sub>) δ 144.40, 141.97, 128.71, 126.38, 125.36, 125.07, 82.08, 80.34, 74.38, 55.76, 32.43, 30.32 ppm; MS – non ionisable.

3-(Prop-2-yn-1-yloxy)-1,1'-biphenyl (3p)

Compound **3p** was prepared according to the General procedure D from 3-hydroxybiphenyl (340 mg, 2.00 mmol). Yield: 95 % (397 mg); orange oil; <sup>1</sup>H NMR (400 MHz, CDCl<sub>3</sub>) δ 7.62–7.55 (m, 2 H), 7.48–7.39 (m, 2 H), 7.42–7.30 (m, 2 H), 7.27–7.18 (m, 2 H), 6.97 (ddd, *J*<sub>1</sub> = 8.2 Hz, *J*<sub>2</sub> = 2.6 Hz, *J*<sub>3</sub> = 1.0 Hz, 1 H), 4.74 (d, *J* = 2.4 Hz, 2 H), 2.54 (t, *J* = 2.4 Hz, 1 H) ppm; <sup>13</sup>C NMR (101 MHz, CDCl<sub>3</sub>) δ 158.02, 142.92, 140.97, 129.89, 128.89, 127.61, 127.30, 120.66, 114.03, 113.69, 78.70, 75.77, 55.97 ppm; MS – non ionisable.

4-(Prop-2-yn-1-yloxy)-1,1'-biphenyl (3r)

Compound **3r** was prepared according to the General procedure D from 4-hydroxybiphenyl (340 mg, 2.00 mg). Yield: 94 % (435 mg); orange solid; <sup>1</sup>H NMR (400 MHz, CDCl<sub>3</sub>) δ 7.59–7.50 (m, 4 H), 7.47–7.37 (m, 2 H), 7.36–7.26 (m, 1 H), 7.06 (d, *J* = 8.8 Hz, 2 H), 4.74 (d, *J* = 2.4 Hz, 2 H), 2.55 (t, *J* = 2.4 Hz, 1 H) ppm; MS – non ionisable.

2-Chloro-1-fluoro-4-(prop-2-yn-1-yloxy)benzene (3s)

Compound **3s** was prepared according to the General procedure D from 3-chloro-4-fluorophenol (293 mg, 2.00 mmol). Yield: 53 % (194 mg); light yellow oil; <sup>1</sup>H NMR (400 MHz, CDCl<sub>3</sub>) δ 7.29 (t, *J* = 8.7 Hz, 1 H), 6.80 (dd, *J*<sub>1</sub> = 10.6 Hz, *J*<sub>2</sub> = 2.8 Hz, 1 H), 6.73 (ddd, *J*<sub>1</sub> = 8.9 Hz, *J*<sub>2</sub> = 2.9 Hz, *J*<sub>3</sub> = 1.3 Hz, 1 H), 4.67 (d, *J* = 2.4 Hz, 2 H), 2.55 (t, *J* = 2.4 Hz, 1 H). <sup>13</sup>C NMR (101 MHz, CDCl<sub>3</sub>) δ 159.71, 157.24, 130.74 (d, *J* = 1.5 Hz), 113.41 (d, *J* = 18.0 Hz), 111.72 (d, *J* = 3.4 Hz), 104.24 (d, *J* = 24.6 Hz), 77.76, 76.40, 56.42; MS – non ionisable.

1-Bromo-2-chloro-4-(prop-2-yn-1-yloxy)benzene (3t)

Compound **3t** was prepared according to the General procedure D from 4-bromo-3-chlorophenol (415 mg, 2.00 mmol). Yield: 95 % (514 mg); light yellow oil; <sup>1</sup>H NMR (400 MHz, CDCl<sub>3</sub>) δ 7.35 (d, *J* = 8.8 Hz, 1 H), 7.24 (d, *J* = 2.9 Hz, 1 H), 6.88 (dd, *J*<sub>1</sub> = 8.8 Hz, *J*<sub>2</sub> = 2.9 Hz, 1 H), 4.67 (d, *J* = 2.4 Hz, 2 H), 2.56 (t, *J* = 2.4 Hz, 1 H) ppm; <sup>13</sup>C NMR (101 MHz, CDCl<sub>3</sub>) δ 156.45, 130.63, 127.03, 122.71, 120.22, 115.66, 77.72, 76.44, 56.39 ppm; MS – non ionisable.



## 2-Chloro-1-iodo-4-(prop-2-yn-1-yloxy)benzene (3u)

Compound **3u** was prepared according to the General procedure D from 3-chloro-4-iodophenol (509 mg, 2.00 mmol). Yield: 93 % (545 mg); light yellow oil;  $^1\text{H NMR}$  (400 MHz,  $\text{CDCl}_3$ )  $\delta$  7.45 (d,  $J = 2.9$  Hz, 1 H), 7.34 (d,  $J = 8.8$  Hz, 1 H), 6.92 (dd,  $J_1 = 8.9$  Hz,  $J_2 = 2.9$  Hz, 1 H), 4.66 (d,  $J = 2.4$  Hz, 2 H), 2.55 (t,  $J = 2.4$  Hz, 1 H) ppm;  $^{13}\text{C NMR}$  (101 MHz,  $\text{CDCl}_3$ )  $\delta$  156.09, 131.19, 129.42, 126.51, 116.60, 98.03, 77.75, 76.41, 56.38 ppm; MS – non ionisable.

## 1-Fluoro-4-(prop-2-yn-1-yloxy)benzene (3v)

Compound **3v** was prepared according to the General procedure D from 4-fluorophenol (224 mg, 2.00 mmol). Yield: 50 % (74 mg); light yellow oil;  $^1\text{H NMR}$  (400 MHz,  $\text{CDCl}_3$ )  $\delta$  7.05–6.88 (m, 4 H), 4.66 (d,  $J = 2.4$  Hz, 2 H), 2.52 (t,  $J = 2.4$  Hz, 1 H).  $^{19}\text{F NMR}$  (376 MHz,  $\text{CDCl}_3$ )  $\delta$  –122.85 (tt,  $J_1 = 8.7$  Hz,  $J_2 = 4.4$  Hz) ppm; MS – non ionisable.

## 1-Isopropyl-4-(prop-2-yn-1-yloxy)benzene (3w)

Compound **3w** was prepared according to the General procedure D from 4-isopropylphenol (272 mg, 2.00 mmol). Yield: 82 % (285 mg); light yellow oil;  $^1\text{H NMR}$  (400 MHz,  $\text{CDCl}_3$ )  $\delta$  7.15 (d,  $J = 8.5$  Hz, 2 H), 6.91 (d,  $J = 8.8$  Hz, 2 H), 4.66 (d,  $J = 2.4$  Hz, 2 H), 2.86 (hept,  $J = 6.8$  Hz, 1 H), 2.50 (t,  $J = 2.4$  Hz, 1 H), 1.22 (d,  $J = 6.9$  Hz, 6 H) ppm;  $^{13}\text{C NMR}$  (101 MHz,  $\text{CDCl}_3$ )  $\delta$  155.76, 142.11, 127.41, 114.80, 78.98, 75.44, 55.98, 33.42, 24.30 ppm; MS – non ionisable.

## 2-methoxy-7-(prop-2-yn-1-yloxy)naphthalene (3x)

Compound **3x** was prepared according to General procedure D using 7-methoxyphenol (2.0 g, 11.5 mmol) as starting material. Yield: 97 % (2362 g); light brown solid;  $^1\text{H NMR}$  (400 MHz,  $\text{CDCl}_3$ )  $\delta$  7.74 – 7.63 (m, 2 H), 7.16 (d,  $J = 2.5$  Hz, 1 H), 7.10 – 6.98 (m, 3 H), 4.80 (d,  $J = 2.4$  Hz, 2 H), 3.92 (s, 3 H), 2.56 (t,  $J = 2.4$  Hz, 1 H) ppm;  $^{13}\text{C NMR}$  (101 MHz,  $\text{CDCl}_3$ )  $\delta$  158.36, 156.20, 135.76, 129.42, 129.26, 124.77, 116.66, 116.15, 107.00, 105.46, 78.71, 75.73, 55.89, 55.37; HRMS (ESI+) calcd. for  $\text{C}_{14}\text{H}_{13}\text{O}_2$   $[\text{M}+\text{H}]^+$ : 213.0910, found: 213.0905.

*tert*-Butyl 4-(4-(4-(((1*R*,2*R*)-2-(trifluoromethyl)-1,2,3,4-tetrahydronaphthalen-1-yl)oxy)methyl)-1*H*-1,2,3-triazol-1-yl)benzoyl)piperazine-1-carboxylate (4a)

Compound **4a** was prepared according to the literature procedure, starting from (*R,R*)-**3a**. [29] NMR data is in accordance with the literature data.

*tert*-Butyl 4-(4-(4-(((1*S*,2*S*)-7-methoxy-2-(trifluoromethyl)-1,2,3,4-tetrahydronaphthalen-1-yl)oxy)methyl)-1*H*-1,2,3-triazol-1-yl)benzoyl)piperazine-1-carboxylate (4b)

Compound **4b** was prepared according to the General procedure F from **3b** (65 mg, 0.23 mmol). The crude product was purified by flash chromatography, eluent hexane/EtOAc 1:1. Yield: 86 % (120 mg); white solid;  $^1\text{H NMR}$  (400 MHz,  $\text{CDCl}_3$ )  $\delta$  7.95 (s, 1 H), 7.80 (d,  $J = 8.6$  Hz, 2 H), 7.58 (d,  $J = 8.6$  Hz, 2 H), 7.11 (d,  $J = 9.2$  Hz, 1 H), 6.95–6.84 (m, 2 H), 4.88 (d,  $J = 12.7$  Hz, 1 H), 4.82 (d,  $J = 12.7$  Hz, 1 H), 4.71 (d,  $J = 2.6$  Hz, 1 H), 3.82 (s, 3 H), 3.80–3.66 (m, 2 H), 3.62–3.30 (m, 6 H), 3.01 (dd,  $J_1 = 16.9$  Hz,  $J_2 = 5.8$  Hz, 1 H), 2.89–2.72 (m, 1 H), 2.58–2.43 (m, 1 H), 2.43–2.27 (m, 1 H), 2.10–1.95 (m, 1 H), 1.48 (s, 9 H).  $^{19}\text{F NMR}$  (376 MHz,  $\text{CDCl}_3$ )  $\delta$  –68.41 (d,  $J = 8.8$  Hz).  $^{13}\text{C NMR}$  (101 MHz,  $\text{CDCl}_3$ )  $\delta$  169.31, 157.60, 154.64, 146.91, 138.12, 135.84, 134.18, 130.60, 128.95, 128.14, 127.28 (q,  $J = 279.7$  Hz), 120.77, 120.67, 115.45, 114.94, 80.64, 73.08 (q,  $J = 2.5$  Hz), 62.87, 55.58, 47.68, 44.22 (q,  $J = 26.4$  Hz), 44.17, 43.19, 42.46, 28.50, 26.90, 17.11 (q,  $J = 2.1$  Hz). HRMS calcd. for  $\text{C}_{31}\text{H}_{37}\text{O}_5\text{N}_5\text{F}_3$   $[\text{M}+\text{H}]^+$  616.2741, found 616.2729.

*tert*-Butyl 4-(4-(4-(((1*S*,2*S*)-2-(trifluoromethyl)-2,3-dihydro-1*H*-inden-1-yl)oxy)methyl)-1*H*-1,2,3-triazol-1-yl)benzoyl)piperazine-1-carboxylate (4c)

Compound **4c** was prepared according to the General procedure F from **3c** (94 mg, 0.39 mmol). The crude product was purified by flash chromatography, eluent hexane/EtOAc 1:1. Yield: 80 % (180 mg); white solid;  $^1\text{H NMR}$  (400 MHz,  $\text{CDCl}_3$ )  $\delta$  7.97 (s, 1 H), 7.81 (d,  $J = 8.6$  Hz, 2 H), 7.58 (d,  $J = 8.6$  Hz, 2 H), 7.46 (d,  $J = 7.4$  Hz, 1 H), 7.38–7.31 (m, 2 H), 7.31–7.25 (m, 1 H), 5.13 (d,  $J = 5.6$  Hz, 1 H), 4.88 (d,  $J = 12.5$  Hz, 1 H), 4.83 (d,  $J = 12.5$  Hz, 1 H), 3.87–3.64 (m, 2 H), 3.62–3.31 (m, 7 H), 3.24–3.05 (m, 2 H), 1.48 (s, 9 H).  $^{19}\text{F NMR}$  (376 MHz,  $\text{CDCl}_3$ )  $\delta$  –65.29 (d,  $J = 8.9$  Hz) ppm;  $^{13}\text{C NMR}$  (101 MHz,  $\text{CDCl}_3$ )  $\delta$  169.27, 154.61, 146.76, 141.61, 139.86, 138.07, 135.82, 129.68, 128.93, 127.19, 126.52 (q,  $J = 277.9$  Hz), 125.59, 125.38, 120.65, 120.62, 80.60, 80.58, 63.04, 47.80, 47.78 (q,  $J = 27.3$  Hz), 44.03, 43.50, 42.26, 30.98 (d,  $J = 2.3$  Hz), 28.47 ppm; MS – non ionisable.

*tert*-Butyl 4-(4-(4-((4-methoxyphenoxy)methyl)-1*H*-1,2,3-triazol-1-yl)benzoyl)piperazine-1-carboxylate (4d)

Compound **4d** was prepared according to General procedure F using **3d** (0.20 g, 1.2 mmol) as starting material. The product was additionally purified by column chromatography using EtOAc:Hex = 4:1 as the mobile phase. Yield: 29 % (0.126 g); white solid;  $^1\text{H NMR}$  (400 MHz,  $\text{DMSO}-d_6$ )  $\delta$  9.00 (s, 1 H), 8.05 – 7.97 (m, 2 H), 7.68 – 7.62 (m, 2 H), 7.04 – 6.97 (m, 2 H), 6.93 – 6.84 (m, 2 H), 5.18 (s, 2 H), 3.70 (s, 3 H), 3.65 – 3.35 (m, 8 H), 1.41 (s, 9 H) ppm; MS (ESI+)  $\text{C}_{26}\text{H}_{31}\text{N}_5\text{O}_5$   $m/z$  494.5  $[\text{M}+\text{H}]^+$ .

*tert*-Butyl 4-(4-(4-((naphthalen-1-yloxy)methyl)-1*H*-1,2,3-triazol-1-yl)benzoyl)piperazine-1-carboxylate (4e)

Compound **4e** was prepared according to General procedure F using **3e** (0.19 g, 1.0 mmol) as starting material. A precipitate formed during the reaction that was filtered off and dried to yield a clean product **4e**. Yield: 78 % (0.412 g); light grey solid;  $^1\text{H NMR}$  (400 MHz,  $\text{DMSO}-d_6$ )  $\delta$  9.15 (s, 1 H), 8.27 – 8.18 (m, 1 H), 8.10 – 8.02 (m, 2 H), 7.89 (dd,  $J_1 = 7.7$  Hz,  $J_2 = 1.6$  Hz, 1 H), 7.70 – 7.62 (m, 2 H), 7.58 – 7.42 (m, 4 H), 7.27 – 7.20 (m, 1 H), 5.46 (s, 2 H), 3.71 – 3.35 (m, 8 H), 1.41 (s, 9 H) ppm; MS (ESI+)  $\text{C}_{29}\text{H}_{31}\text{N}_5\text{O}_4$   $m/z$  514.4  $[\text{M}+\text{H}]^+$ .

*tert*-Butyl 4-(4-(4-((naphthalen-2-yloxy)methyl)-1*H*-1,2,3-triazol-1-yl)benzoyl)piperazine-1-carboxylate (4f)

Compound **4f** was prepared according to General procedure F using **3f** (0.10 g, 0.55 mmol) as starting material. A precipitate formed during the reaction that was filtered off and dried to yield a clean product **4f**. Yield: 69 % (0.195 g);  $^1\text{H NMR}$  (400 MHz,  $\text{DMSO}-d_6$ )  $\delta$  9.09 (s, 1 H), 8.06 – 7.98 (m, 2 H), 7.90 – 7.82 (m, 3 H), 7.69 – 7.62 (m, 2 H), 7.56 (d,  $J = 2.7$  Hz, 1 H), 7.49 (ddd,  $J_1 = 8.2$  Hz,  $J_2 = 6.9$  Hz,  $J_3 = 1.3$  Hz, 1 H), 7.37 (ddd,  $J_1 = 8.2$  Hz,  $J_2 = 6.9$  Hz,  $J_3 = 1.3$  Hz, 1 H), 7.24 (dd,  $J_1 = 8.9$  Hz,  $J_2 = 2.6$  Hz, 1 H), 5.38 (s, 2 H), 3.67 – 3.35 (m, 8 H), 1.41 (s, 9 H) ppm; MS (ESI+)  $\text{C}_{29}\text{H}_{31}\text{N}_5\text{O}_4$   $m/z$  513.9  $[\text{M}+\text{H}]^+$ .

*tert*-Butyl 4-(4-(4-((3,4-dichlorophenoxy)methyl)-1*H*-1,2,3-triazol-1-yl)benzoyl)piperazine-1-carboxylate (4g)

Compound **4g** was prepared according to General procedure F using **3g** (0.20 g, 1.0 mmol) as starting material. A precipitate formed during the reaction that was filtered off and dried to yield a clean product **4g**. Yield: 96 % (0.487 g); yellow solid;  $^1\text{H NMR}$  ( $\text{DMSO}-d_6$ , 400 MHz):  $\delta$  = 9.04 (s, 1 H), 8.05 – 7.96 (m, 2 H), 7.70 – 7.61 (m, 2 H), 7.57 (d, 1 H,  $J = 8.9$  Hz), 7.43 (d, 1 H,  $J = 2.9$  Hz), 7.11 (dd, 1 H,  $J_1 = 9.0$  Hz,  $J_2 = 2.9$  Hz), 5.31 (s, 2 H), 3.61 – 3.39 (m, 8 H), 1.41 (s, 9 H) ppm; MS (ESI+)  $\text{C}_{25}\text{H}_{27}\text{Cl}_2\text{N}_5\text{O}_4$   $m/z$  531.7  $[\text{M}+\text{H}]^+$ .

*tert*-Butyl 4-(4-(4-((1*H*-indole-2-carboxamido)methyl)-1*H*-1,2,3-triazol-1-yl)benzoyl)piperazine-1-carboxylate (4h)

Compound **4h** was prepared according to General procedure F using **3h** (0.20 g, 1.0 mmol) as starting material. A precipitate formed during the reaction that was filtered off and dried to yield a clean product **4h**. Yield: 54 % (0.287 g); white solid;  $^1\text{H}$  NMR (DMSO- $d_6$ , 400 MHz):  $\delta$  = 11.60 (s, 1 H), 9.09 (t, 1 H,  $J$  = 5.7 Hz), 8.79 (s, 1 H), 7.96 – 8.06 (m, 2 H), 7.57 – 7.67 (m, 3 H), 7.40 – 7.47 (m, 1 H), 7.15 – 7.22 (m, 2 H), 7.03 (td, 1 H,  $J_1$  = 7.5 Hz,  $J_2$  = 7.0 Hz,  $J_3$  = 0.9 Hz), 4.66 (d, 2 H,  $J$  = 5.7 Hz), 3.60 – 3.37 (m, 8 H) ppm; MS (ESI+)  $\text{C}_{28}\text{H}_{31}\text{N}_7\text{O}_4$  m/z 530.0  $[\text{M}+\text{H}]^+$ .

*tert*-Butyl 4-(4-((5-methoxy-1*H*-indole-2-carboxamido)methyl)-1*H*-1,2,3-triazol-1-yl)benzoyl)piperazine-1-carboxylate (4i)

Compound **4i** was prepared according to General procedure F using **3i** (0.20 g, 0.88 mmol) as starting material. A precipitate formed during the reaction that was filtered off and dried. The residue was further purified by column chromatography using DCM:MeOH = 20:1 as the mobile phase to yield a clean product **4i**. Yield: 50 % (0.247 g); light yellow solid;  $^1\text{H}$  NMR DMSO- $d_6$ , 400 MHz):  $\delta$  = 11.45 (d, 1 H,  $J$  = 1.4 Hz), 9.04 (t, 1 H,  $J$  = 5.7 Hz), 8.78 (s, 1 H), 8.00 (d, 2 H,  $J$  = 8.7 Hz), 7.62 (d, 2 H,  $J$  = 8.6 Hz), 7.32 (d, 1 H,  $J$  = 8.9 Hz), 7.09 (dd, 2 H,  $J_1$  = 7.0 Hz,  $J_2$  = 2.0 Hz), 6.83 (dd, 1 H,  $J_1$  = 8.9 Hz,  $J_2$  = 2.5 Hz), 4.64 (d, 2 H,  $J$  = 5.6 Hz), 3.75 (s, 3 H), 3.60 – 3.39 (m, 8 H), 1.41 (s, 9 H) ppm; MS (ESI+)  $\text{C}_{29}\text{H}_{33}\text{N}_7\text{O}_5$  m/z 559.6  $[\text{M}+\text{H}]^+$ .

*tert*-Butyl 4-(4-((3,4-dichlorobenzamido)methyl)-1*H*-1,2,3-triazol-1-yl)benzoyl)piperazine-1-carboxylate (4j)

Compound **4j** was prepared according to General procedure F using **3j** (0.20 g, 0.88 mmol) as starting material. A precipitate formed during the reaction that was filtered off and dried to yield a clean product **4j**. Yield: 69 % (0.339 g); light yellow solid;  $^1\text{H}$  NMR (400 MHz, DMSO- $d_6$ )  $\delta$  9.31 (t,  $J$  = 5.6 Hz, 1 H), 8.79 (s, 1 H), 8.15 (d,  $J$  = 2.1 Hz, 1 H), 8.04 – 7.94 (m, 2 H), 7.88 (dd,  $J_1$  = 8.4 Hz,  $J_2$  = 2.1 Hz, 1 H), 7.78 (d,  $J$  = 8.4 Hz, 1 H), 7.67 – 7.58 (m, 2 H), 4.62 (d,  $J$  = 5.6 Hz, 2 H), 3.49 (m, 8 H), 1.41 (s, 9 H) ppm; MS (ESI+)  $\text{C}_{26}\text{H}_{28}\text{Cl}_2\text{N}_6\text{O}_4$  m/z 559.3  $[\text{M}+\text{H}]^+$ .

*tert*-Butyl 4-(4-((2-(3,4-dichlorophenyl)acetamido)methyl)-1*H*-1,2,3-triazol-1-yl)benzoyl)piperazine-1-carboxylate (4k)

Compound **4k** was prepared according to General procedure F using **3k** (0.15 g, 0.62 mmol) as starting material. A precipitate formed during the reaction that was filtered off and dried to yield a clean product **4k**. Yield: 88 % (0.312 g); brown solid;  $^1\text{H}$  NMR (400 MHz, DMSO- $d_6$ )  $\delta$  8.74 – 8.66 (m, 2 H), 7.97 (d,  $J$  = 8.3 Hz, 2 H), 7.64 (d,  $J$  = 8.4 Hz, 2 H), 7.58 – 7.50 (m, 2 H), 7.27 (dd,  $J_1$  = 8.3 Hz,  $J_2$  = 2.1 Hz, 1 H), 4.41 (d,  $J$  = 5.5 Hz, 2 H), 3.72 – 3.39 (m, 10 H), 1.41 (s, 9 H) ppm; MS (ESI+)  $\text{C}_{27}\text{H}_{30}\text{Cl}_2\text{N}_6\text{O}_4$  m/z 573.4  $[\text{M}+\text{H}]^+$ .

*tert*-Butyl 4-(4-((2-naphthamido)methyl)-1*H*-1,2,3-triazol-1-yl)benzoyl)piperazine-1-carboxylate (4l)

Compound **4l** was prepared according to General procedure F using **3l** (0.20 g, 0.96 mmol) as starting material. A precipitate formed during the reaction that was filtered off and dried to yield a clean product **4l**. Yield: 75 % (0.388 g); beige solid;  $^1\text{H}$  NMR (400 MHz, DMSO- $d_6$ )  $\delta$  = 9.28 (t, 1 H,  $J$  = 5.6 Hz), 8.81 (s, 1 H), 8.52 (s, 1 H), 8.07 – 7.94 (m, 6 H), 7.67 – 7.56 (m, 4 H), 4.69 (d, 2 H,  $J$  = 5.5 Hz), 3.60 – 3.38 (m, 8 H), 1.41 (s, 9 H) ppm; MS (ESI+)  $\text{C}_{30}\text{H}_{32}\text{N}_6\text{O}_4$  m/z 540.7  $[\text{M}+\text{H}]^+$ .

Piperazin-1-yl(4-(4-(((1*R*,2*R*)-2-(trifluoromethyl)-1,2,3,4-tetrahydronaphthalen-1-yl)oxy)methyl)-1*H*-1,2,3-triazol-1-yl)phenyl)methanone (5a)

Compound **5a** was prepared according to the General procedure F from the alkyne **4a** (17.0 mg, 0.0669 mmol) and the azide **2** (15.5 mg, 0.0669 mmol). The crude product was purified by flash chromatography, eluent DCM/MeOH/NH<sub>4</sub>OH 9:1:0.1. Yield: 34 % (11 mg); light-yellow solid;  $^1\text{H}$  NMR (400 MHz, CDCl<sub>3</sub>)  $\delta$  7.93 (s, 1 H), 7.79 (d,  $J$  =

8.6 Hz, 2 H), 7.58 (d,  $J$  = 8.6 Hz, 2 H), 7.37–7.29 (m, 2 H), 7.25–7.17 (m, 2 H), 4.84 (d,  $J$  = 12.7 Hz, 1 H), 4.79 (d,  $J$  = 12.7 Hz, 1 H), 4.74 (d,  $J$  = 2.0 Hz, 1 H), 3.80 (s, 2 H), 3.48 (d,  $J$  = 13.1 Hz, 2 H), 3.09 (dd,  $J_1$  = 17.5 Hz,  $J_2$  = 6.6 Hz, 1 H), 3.03–2.78 (m, 5 H), 2.69–2.45 (m, 3 H), 2.44–2.29 (m, 1 H), 2.08–1.97 (m, 1 H) ppm;  $^{19}\text{F}$  NMR (376 MHz, CDCl<sub>3</sub>)  $\delta$  –68.47 (d,  $J$  = 8.6 Hz) ppm; HRMS calcd. for  $\text{C}_{25}\text{H}_{27}\text{O}_2\text{N}_5\text{F}_3$   $[\text{M}+\text{H}]^+$  486.2111, found 486.2096. HPLC:  $t_r$  5.1 min (94.9 % at 254 nm)

(4-(4-(((1*S*,2*S*)-7-Methoxy-2-(trifluoromethyl)-1,2,3,4-tetrahydronaphthalen-1-yl)oxy)methyl)-1*H*-1,2,3-triazol-1-yl)phenyl)piperazin-1-yl)methanone (5b)

Prepared according to the General procedure B from **4b** (100 mg, 0.162 mmol). The crude product was purified by flash chromatography, eluent DCM/MeOH/NH<sub>4</sub>OH 9:1:0.1. Yield: 41 % (34 mg); white solid;  $^1\text{H}$  NMR (400 MHz, CDCl<sub>3</sub>)  $\delta$  7.94 (s, 1 H), 7.80 (d,  $J$  = 8.6 Hz, 2 H), 7.58 (d,  $J$  = 8.6 Hz, 2 H), 7.11 (d,  $J$  = 9.2 Hz, 1 H), 6.92–6.84 (m, 2 H), 4.87 (d,  $J$  = 12.8 Hz, 1 H), 4.81 (d,  $J$  = 12.9 Hz, 1 H), 4.71 (d,  $J$  = 2.2 Hz, 1 H), 3.82 (s, 3 H), 4.02–3.37 (m, 4 H), 3.13–2.74 (m, 6 H), 2.56–2.43 (m, 1 H), 2.34 (tdd,  $J_1$  = 12.8 Hz,  $J_2$  = 11.3 Hz,  $J_3$  = 6.6 Hz, 1 H), 2.09–1.95 (m, 1 H) ppm;  $^{19}\text{F}$  NMR (376 MHz, CDCl<sub>3</sub>)  $\delta$  –68.41 (d,  $J$  = 8.8 Hz) ppm;  $^{13}\text{C}$  NMR (101 MHz, CDCl<sub>3</sub>)  $\delta$  169.16, 157.60, 146.89, 138.07, 135.84, 134.18, 130.60, 128.93 (2 C), 128.14, 127.28 (q,  $J$  = 279.7 Hz), 120.80, 120.67 (2 C), 115.44, 114.95, 73.08 (q,  $J$  = 2.8 Hz), 62.87, 55.58, 47.92, 45.69, 44.22 (q,  $J$  = 26.3 Hz), 42.50 (2 C), 26.90, 17.11 (q,  $J$  = 2.1 Hz) ppm; HRMS calcd. for  $\text{C}_{26}\text{H}_{29}\text{O}_3\text{N}_5\text{F}_3$   $[\text{M}+\text{H}]^+$  516.2217, found 516.2208. HPLC:  $t_r$  5.2 min (97.8 % at 254 nm).

4-(4-(4-(((1*S*,2*S*)-2-(Trifluoromethyl)-2,3-dihydro-1*H*-inden-1-yl)oxy)methyl)-1*H*-1,2,3-triazol-1-yl)benzoyl)piperazin-1-ium chloride (5c)

Prepared according to the General procedure B from **4c** (120 mg, 0.210 mmol). The crude product was purified by flash chromatography, eluent DCM/MeOH/NH<sub>4</sub>OH 9:1:0.1, then the product was converted to a chloride salt by titration with 1 M HCl in diethyl ether. Yield: quant. (110 mg); white solid;  $^1\text{H}$  NMR (400 MHz, CDCl<sub>3</sub>)  $\delta$  7.97 (s, 1 H), 7.81 (d,  $J$  = 8.5 Hz, 2 H), 7.58 (d,  $J$  = 8.5 Hz, 2 H), 7.46 (d,  $J$  = 7.4 Hz, 1 H), 7.39–7.31 (m, 2 H), 7.31–7.24 (m, 1 H), 5.13 (d,  $J$  = 5.5 Hz, 1 H), 4.88 (d,  $J$  = 12.4 Hz, 1 H), 4.83 (d,  $J$  = 12.5 Hz, 1 H), 4.53 (s, 1 H), 3.81 (s, 4 H), 3.42 (dd,  $J_1$  = 14.6 Hz,  $J_2$  = 8.4 Hz, 1 H), 3.25–2.91 (m, 6 H) ppm;  $^{19}\text{F}$  NMR (376 MHz, CDCl<sub>3</sub>)  $\delta$  –65.29 (d,  $J$  = 8.9 Hz) ppm;  $^{13}\text{C}$  NMR (101 MHz, CDCl<sub>3</sub>)  $\delta$  169.17, 146.78, 141.62, 139.85, 138.13, 135.53, 129.69, 128.95, 127.21, 126.53 (d,  $J$  = 278.0 Hz), 125.60, 125.39, 120.67, 120.59, 80.63 (d,  $J$  = 2.2 Hz), 63.04, 47.78 (q,  $J$  = 27.3 Hz), 45.30, 41.97, 30.99 (d,  $J$  = 2.7 Hz) ppm; HRMS calcd. for  $\text{C}_{24}\text{H}_{25}\text{O}_2\text{N}_5\text{F}_3$   $[\text{M}-\text{Cl}]^+$  472.1955, found 472.1947. HPLC:  $t_r$  4.9 min (99.2 % at 254 nm).

(4-(4-((4-Methoxyphenoxy)methyl)-1*H*-1,2,3-triazol-1-yl)phenyl)(piperazin-1-yl)methanone (5d)

Compound **5d** was prepared according to General procedure B using TFA as a reagent and **4d** (0.075 g, 0.15 mmol) as starting material. The product was further purified by column chromatography using DCM: MeOH:NH<sub>4</sub>OH = 20:1:0.1 as the mobile phase to yield a clean product **5d**. Yield: 35 % (0.021 g); white solid;  $^1\text{H}$  NMR (400 MHz, CDCl<sub>3</sub>)  $\delta$  8.07 (s,  $J$  = 0.8 Hz, 1 H), 7.83 – 7.78 (m, 2 H), 7.62 – 7.56 (m, 2 H), 7.00 – 6.93 (m, 2 H), 6.88 – 6.83 (m, 2 H), 5.26 (s, 2 H), 3.78 (s, 5 H), 3.43 (s, 2 H), 3.04 – 2.76 (m, 4 H) ppm;  $^{13}\text{C}$  NMR (101 MHz, DMSO- $d_6$ )  $\delta$  168.27, 154.12, 152.41, 144.75, 137.37, 136.80, 129.07, 123.25, 120.49, 116.22, 115.08, 62.00, 55.81, 49.06, 46.30, 45.90, 43.38 ppm; HRMS (ESI+) calcd. for  $\text{C}_{21}\text{H}_{24}\text{O}_3\text{N}_5$   $[\text{M}+\text{H}]^+$ : 394.18737, found: 394.18602; HPLC:  $t_r$ : 4.24 min (99.8 % at 254 nm).

(4-(4-((Naphthalen-1-yloxy)methyl)-1*H*-1,2,3-triazol-1-yl)phenyl)(piperazin-1-yl)methanone (5e)

Compound **5e** was prepared according to General procedure B using TFA as a reagent and **4e** (0.10 g, 0.19 mmol) as starting material. The product was purified by column chromatography using DCM:MeOH: NH<sub>4</sub>OH = 20:1:0.1 as the mobile phase to yield a clean product **5e**. Yield: 78 % (0.063 g); brown solid; <sup>1</sup>H NMR (400 MHz, CDCl<sub>3</sub>) δ 8.31 – 8.25 (m, 1 H), 8.17 – 8.12 (m, 1 H), 7.87 – 7.79 (m, 3 H), 7.62 – 7.57 (m, 2 H), 7.53 – 7.45 (m, 3 H), 7.43 – 7.38 (m, 1 H), 7.04 – 6.98 (m, 1 H), 5.52 (s, 2 H), 3.78 (s, 2 H), 3.43 (s, 2 H), 3.04 – 2.80 (m, 4 H) ppm; <sup>13</sup>C NMR (101 MHz, DMSO-*d*<sub>6</sub>) δ 168.29, 153.90, 144.69, 137.41, 136.82, 134.52, 129.07, 127.93, 126.99, 126.62, 125.84, 125.36, 123.27, 122.16, 120.95, 120.57, 106.33, 62.15, 49.07, 46.32, 45.91, 43.35 ppm; HRMS (ESI+) calcd. for C<sub>24</sub>H<sub>24</sub>O<sub>2</sub>N<sub>5</sub> [M+H]<sup>+</sup>: 414.19245, found: 414.19102; HPLC: t<sub>r</sub>: 5.71 min (99.0 % at 254 nm).

(4-(4-((Naphthalen-2-yloxy)methyl)-1H-1,2,3-triazol-1-yl)phenyl) (piperazin-1-yl)methanone × HCl (5f)

Compound **5f** was prepared according to General procedure B using 4 M HCl in 1,4-dioxane as a reagent and **4f** (0.095 g, 0.18 mmol) as starting material. The precipitate that formed during the reaction was filtered off, washed with diethyl ether and dried to yield a clean product **5f**. Yield: 83 % (0.069 g); orange solid; <sup>1</sup>H NMR (400 MHz, DMSO-*d*<sub>6</sub>) δ 9.16 – 9.04 (m, 3 H), 8.08 – 7.99 (m, 2 H), 7.90 – 7.81 (m, 3 H), 7.75 – 7.67 (m, 2 H), 7.56 (d, *J* = 2.7 Hz, 1 H), 7.49 (ddd, *J*<sub>1</sub> = 8.3 Hz, *J*<sub>2</sub> = 6.8 Hz, *J*<sub>3</sub> = 1.3 Hz, 1 H), 7.37 (ddd, *J*<sub>1</sub> = 8.2 Hz, *J*<sub>2</sub> = 6.9 Hz, *J*<sub>3</sub> = 1.3 Hz, 1 H), 7.24 (dd, *J*<sub>1</sub> = 9.0 Hz, *J*<sub>2</sub> = 2.6 Hz, 1 H), 5.38 (s, 2 H), 3.95 – 3.56 (m, 4 H), 3.24 – 3.10 (m, 4 H) ppm; <sup>13</sup>C NMR (101 MHz, DMSO-*d*<sub>6</sub>) δ 168.64, 156.31, 144.48, 137.80, 135.56, 134.65, 129.92, 129.46, 129.14, 128.02, 127.27, 126.97, 124.29, 123.57, 120.56, 119.13, 107.77, 61.54, 44.31, 42.90 ppm; HRMS (ESI+) calcd. for C<sub>24</sub>H<sub>26</sub>O<sub>2</sub>N<sub>7</sub> [M+H]<sup>+</sup>: 414.19245, found: 414.19170; HPLC: t<sub>r</sub>: 5.38 min (98.0 % at 254 nm).

(4-(4-((3,4-Dichlorophenoxy)methyl)-1H-1,2,3-triazol-1-yl)phenyl) (piperazin-1-yl)methanone × HCl (5g)

Compound **5g** was prepared according to General procedure B using 4 M HCl in 1,4-dioxane as a reagent and **4g** (0.20 g, 0.38 mmol) as starting material. The precipitate that formed during the reaction was filtered off, washed with acetonitrile, and dried to yield a clean product **5g**. Yield: 75 % (0.132 g); yellow solid; <sup>1</sup>H NMR (400 MHz, DMSO-*d*<sub>6</sub>) δ = 9.45 (s, 2 H), 9.06 (s, 1 H), 8.08 – 7.99 (m, 2 H), 7.76 – 7.67 (m, 2 H), 7.57 (d, 1 H, *J* = 8.9 Hz), 7.43 (d, 1 H, *J* = 2.9 Hz), 7.11 (dd, 1 H, *J*<sub>1</sub> = 8.9 Hz, *J*<sub>2</sub> = 2.9 Hz), 5.31 (s, 2 H), 3.82 (s, 2 H), 3.57 (s, 2 H), 3.17 (s, 4 H) ppm; <sup>13</sup>C NMR (101 MHz, DMSO-*d*<sub>6</sub>): δ = 168.65, 157.88, 143.95, 137.73, 135.63, 132.13, 131.53, 129.47, 123.72, 123.38, 120.60, 117.28, 116.35, 62.17, 42.88 ppm, signal for one aliphatic carbon is not visible; HRMS calcd. for C<sub>20</sub>H<sub>20</sub>O<sub>2</sub>N<sub>5</sub>Cl<sub>2</sub> [M+H]<sup>+</sup>: 432.09886, found 432.09823; UPLC: t<sub>r</sub> = 4.06 min (97.5 % at 254 nm)

*N*-((1-(4-(piperazine-1-carbonyl)phenyl)-1H-1,2,3-triazol-4-yl)methyl)-1H-indole-2-carboxamide × HCl (5h)

Compound **5h** was prepared according to General procedure B using 4 M HCl in 1,4-dioxane as a reagent and **4h** (0.17 g, 0.31 mmol) as starting material. The precipitate that formed during the reaction was filtered off, washed with acetonitrile, and dried to yield a clean product **5h**. Yield: 62 % (0.090 g); white solid; <sup>1</sup>H NMR (400 MHz, DMSO-*d*<sub>6</sub>): δ = 11.65 (d, 1 H, *J* = 2.2 Hz), 9.53 (s, 2 H), 9.16 (t, 1 H, *J* = 5.7 Hz), 8.81 (s, 1 H), 8.06 – 7.96 (m, 2 H), 7.74 – 7.65 (m, 2 H), 7.61 (d, 1 H, *J* = 8.0 Hz), 7.44 (d, 1 H, *J* = 8.3 Hz), 7.23 – 7.13 (m, 2 H), 7.04 (ddd, 1 H, *J*<sub>1</sub> = 7.9 Hz, *J*<sub>2</sub> = 6.8 Hz, *J*<sub>3</sub> = 1.0 Hz), 4.66 (d, 2 H, *J* = 5.6 Hz), 3.66 – 3.16 (m, 8 H) ppm; <sup>13</sup>C NMR (101 MHz, DMSO-*d*<sub>6</sub>): δ 168.70, 161.59, 146.91, 137.90, 136.95, 135.34, 131.94, 129.43, 127.53, 123.83, 122.00, 121.79, 120.33, 120.20, 112.77, 103.50, 42.84, 34.83 ppm, signal for one aliphatic carbon is not visible; HRMS calcd. for C<sub>23</sub>H<sub>24</sub>O<sub>2</sub>N<sub>7</sub> [M+H]<sup>+</sup>: 430.19860, found: 430.19791; HPLC: t<sub>r</sub>: 2.41 min (96.2 % at 254 nm).

5-Methoxy-*N*-((1-(4-(piperazine-1-carbonyl)phenyl)-1H-1,2,3-triazol-4-yl)methyl)-1H-indole-2-carboxamide × HCl (5i)

Compound **5i** was prepared according to General procedure B using 4 M HCl in 1,4-dioxane as a reagent and **4i** (0.10 g, 0.18 mmol) as starting material. The product was purified by column chromatography using DCM:MeOH:NH<sub>4</sub>OH = 20:1:0.1 as the mobile phase. The solvent was evaporated under reduced pressure and the residue was taken up in mixture of MeOH and DCM. 1 mL of 1 M HCl in diethyl ether was added to transform the product back into HCl salt form and the solvent was evaporated *in vacuo* to yield a clean product **5i**. Yield: 32 % (0.028 g); yellow solid; <sup>1</sup>H NMR (DMSO-*d*<sub>6</sub>, 400 MHz): δ = 11.47 (s, 1 H), 9.26 (s, 2 H), 9.07 (t, 1 H, *J* = 5.7 Hz), 8.79 (s, 1 H), 8.03 (d, 2 H, *J* = 8.6 Hz), 7.69 (d, 2 H, *J* = 8.6 Hz), 7.32 (d, 1 H, *J* = 8.9 Hz), 7.09 (dd, 2 H, *J*<sub>1</sub> = 9.4 Hz, *J*<sub>2</sub> = 2.0 Hz), 6.84 (dd, 1 H, *J*<sub>1</sub> = 8.9 Hz, *J*<sub>2</sub> = 2.4 Hz), 4.65 (d, 2 H, *J* = 5.6 Hz), 3.76 (s, 3 H), 3.68 (br s, 4 H), 3.17 (br s, 4 H) ppm; <sup>13</sup>C NMR (DMSO-*d*<sub>6</sub>, 101 MHz): δ = 168.70, 161.55, 154.20, 146.94, 137.90, 135.34, 132.23, 132.21, 129.43, 127.83, 121.79, 120.32, 115.02, 113.58, 103.22, 102.44, 55.72, 42.85, 34.80 ppm, signal for one aliphatic carbon is not visible; HRMS calcd. for C<sub>24</sub>H<sub>26</sub>O<sub>3</sub>N<sub>7</sub> [M+H]<sup>+</sup>: 460.20916, found 460.20814; HPLC: t<sub>r</sub> = 2.21 min (96.3 % at 254 nm).

3,4-Dichloro-*N*-((1-(4-(piperazine-1-carbonyl)phenyl)-1H-1,2,3-triazol-4-yl)methyl)benzamide (5j)

Compound **5j** was prepared according to General procedure B using TFA as a reagent and **4j** (0.070 g, 0.13 mmol) as starting material. The residue was taken up in DCM. The organic layer was washed with 1 M NaOH (3 × 25 mL), brine (25 mL), dried over Na<sub>2</sub>SO<sub>4</sub> and filtered. Then the solvent was evaporated under reduced pressure to yield a clean product **5j**. Yield: 83 % (0.048 g); light yellow solid; <sup>1</sup>H NMR (400 MHz, DMSO-*d*<sub>6</sub>) δ 9.31 (t, *J* = 5.6 Hz, 1 H), 8.78 (s, 1 H), 8.15 (d, *J* = 2.0 Hz, 1 H), 8.03 – 7.95 (m, 2 H), 7.88 (dd, *J*<sub>1</sub> = 8.4 Hz, *J*<sub>2</sub> = 2.1 Hz, 1 H), 7.78 (d, *J* = 8.4 Hz, 1 H), 7.61 (dd, *J*<sub>1</sub> = 8.4 Hz, *J*<sub>2</sub> = 6.3 Hz, 2 H), 4.62 (d, *J* = 5.5 Hz, 2 H), 3.62 (s, 2 H), 2.82 (s, 4 H) ppm, signal for the remaining CH<sub>2</sub> group is covered with solvent. <sup>13</sup>C NMR (101 MHz, MeOD) δ 169.79, 166.26, 145.88, 138.08, 135.46, 135.26, 134.14, 132.34, 130.44, 129.31, 128.61, 126.78, 121.20, 120.18, 44.20, 34.87 ppm, signal for one aliphatic carbon is not visible; HRMS calcd. for C<sub>21</sub>H<sub>21</sub>O<sub>2</sub>N<sub>6</sub>Cl<sub>2</sub> [M+H]<sup>+</sup>: 459.1098, found 459.2089; HPLC: t<sub>r</sub> = 4.29 min (97.7 % at 254 nm).

2-(3,4-Dichlorophenyl)-*N*-((1-(4-(piperazine-1-carbonyl)phenyl)-1H-1,2,3-triazol-4-yl)methyl)acetamide × HCl (5k)

Compound **5k** was prepared according to General procedure B using 4 M HCl in 1,4-dioxane as a reagent and **4k** (0.10 g, 0.17 mmol) as starting material. No additional purification was needed after the evaporation of the solvent. Yield 95 % (0.079 g); brown solidified oil; <sup>1</sup>H NMR (400 MHz, DMSO-*d*<sub>6</sub>) δ 9.13 (s, 2 H), 8.73 (t, *J* = 5.7 Hz, 1 H), 8.71 (s, 1 H), 8.02 – 7.96 (m, 2 H), 7.73 – 7.66 (m, 2 H), 7.59 – 7.52 (m, 2 H), 7.27 (dd, *J*<sub>1</sub> = 8.3 Hz, *J*<sub>2</sub> = 2.1 Hz, 1 H), 4.41 (d, *J* = 5.6 Hz, 2 H), 3.96 – 3.59 (m, 4 H), 3.52 (s, 2 H), 3.18 (s, 4 H) ppm; <sup>13</sup>C NMR (101 MHz, DMSO-*d*<sub>6</sub>) δ 169.32, 168.17, 146.01, 137.35, 137.33, 134.87, 131.12, 130.61, 130.27, 129.62, 129.09, 128.97, 121.21, 119.82, 62.78, 42.42, 40.80, 34.28 ppm; HRMS (ESI+) calcd. for C<sub>22</sub>H<sub>23</sub>O<sub>2</sub>N<sub>6</sub>Cl<sub>2</sub> [M+H]<sup>+</sup>: 473.12541, found: 473.12412; HPLC: t<sub>r</sub>: 4.36 min (97.7 % at 254 nm).

*N*-((1-(4-(Piperazine-1-carbonyl)phenyl)-1H-1,2,3-triazol-4-yl)methyl)-2-naphthamide × HCl (5l)

Compound **5l** was prepared according to General procedure B using 4 M HCl in 1,4-dioxane as a reagent and **4l** (0.26 g, 0.55 mmol) as starting material. The precipitate that formed during the reaction was filtered off and dried to yield a clean product **5l**. Yield: 72 % (0.164 g); white solid; <sup>1</sup>H NMR (400 MHz, DMSO-*d*<sub>6</sub>): δ = 9.49 (s, 2 H), 9.32 (t, 1 H, *J* = 5.7 Hz), 8.82 (s, 1 H), 8.54 (d, 1 H, *J* = 1.2 Hz), 8.07 – 7.96 (m, 6 H), 7.72 – 7.66 (m, 2 H), 7.66 – 7.56 (m, 2 H), 4.69 (d, 2 H, *J* =

5.6 Hz), 3.80 (s, 2 H), 3.65 (s, 2 H), 3.16 (s, 4 H) ppm;  $^{13}\text{C}$  NMR (101 MHz, DMSO- $d_6$ ):  $\delta$  = 168.71, 166.77, 147.00, 137.91, 135.33, 134.66, 132.60, 131.93, 129.41, 129.34, 128.32, 128.21, 128.13, 128.10, 127.22, 124.75, 121.82, 120.32, 42.80, 35.42 ppm, signal for one aliphatic carbon is not visible; HRMS (ESI $^{+}$ ) calcd. for  $\text{C}_{25}\text{H}_{25}\text{O}_2\text{N}_6$  ( $[\text{M}+\text{H}]^{+}$ ): 441.20335, found 441.20259. UPLC:  $t_r$  2.23 min (96.4 % at 254 nm).

Piperazin-1-yl(4-(4-(((1,2,3,4-tetrahydronaphthalen-1-yl)oxy)methyl)-1H-1,2,3-triazol-1-yl)phenyl)methanone (5m)

Compound **5o** was prepared according to the General procedure F from the alkyne **3m** (80.5 mg, 0.432 mmol) and the azide **2** (100 mg, 0.432 mmol). The crude product was purified by flash chromatography, eluent DCM/MeOH/NH $_4$ OH 9:1:0.1. Yield: 23 % (42 mg); brown solid;  $^1\text{H}$  NMR (400 MHz,  $\text{CDCl}_3$ )  $\delta$  8.02 (s, 1 H), 7.80 (d,  $J$  = 8.6 Hz, 2 H), 7.57 (d,  $J$  = 8.2 Hz, 2 H), 7.37 (dd,  $J_1$  = 7.0 Hz,  $J_2$  = 2.1 Hz, 1 H), 7.25–7.13 (m, 2 H), 7.12 (dd,  $J_1$  = 7.1 Hz,  $J_2$  = 1.9 Hz, 1 H), 4.92 (d,  $J$  = 12.3 Hz, 1 H), 4.82 (d,  $J$  = 12.3 Hz, 1 H), 4.70–4.61 (m, 1 H), 3.93–3.66 (m, 2 H), 3.57–3.33 (m, 2 H), 3.07–2.81 (m, 4 H), 2.80–2.68 (m, 1 H), 2.69–2.43 (m, 1 H), 2.22–1.93 (m, 4 H), 1.85–1.70 (m, 1 H) ppm;  $^{13}\text{C}$  NMR (101 MHz,  $\text{CDCl}_3$ )  $\delta$  169.12, 147.26, 137.95, 137.82, 136.23, 136.10, 129.52, 129.19, 128.89, 127.88, 125.90, 120.63, 120.59, 75.65, 62.18, 48.73, 45.91, 29.17, 28.06, 18.84 ppm; HRMS (ESI $^{+}$ )  $m/z$ :  $[\text{M}+\text{H}]^{+}$  calcd for  $\text{C}_{24}\text{H}_{28}\text{O}_2\text{N}_5$  418.2238; found 418.2232. HPLC:  $t_r$  5.1 min (96.1 % at 254 nm).

(4-(4-(((1,2,3,4-tetrahydronaphthalen-1-yl)oxy)methyl)-1H-1,2,3-triazol-1-yl)phenyl)(piperazin-1-yl)methanone (5n)

Compound **5n** was prepared according to the General procedure F from the alkyne **3n** (50 mg, 0.18 mmol) and the azide **2** (41 mg, 0.18 mmol). The crude product was purified by flash chromatography, eluent DCM/MeOH/NH $_4$ OH 20:1:0.1. Yield: 56 % (51 mg); beige solid;  $^1\text{H}$  NMR (400 MHz,  $\text{CDCl}_3$ )  $\delta$  7.92 (s, 1 H), 7.79 (d,  $J$  = 8.6 Hz, 2 H), 7.58 (d,  $J$  = 8.7 Hz, 2 H), 7.27 (d,  $J$  = 8.3 Hz, 1 H), 6.78 (dd,  $J_1$  = 8.4 Hz,  $J_2$  = 2.7 Hz, 1 H), 6.73 (d,  $J$  = 2.6 Hz, 1 H), 4.81 (d,  $J$  = 12.9 Hz, 1 H), 4.76 (d,  $J$  = 12.8 Hz, 1 H), 4.70 (d,  $J$  = 2.1 Hz, 1 H), 3.81 (s, 3 H), 3.92–3.71 (m, 2 H), 3.50–3.35 (m, 2 H), 3.11–2.76 (m, 6 H), 2.57–2.42 (m, 1 H), 2.43–2.28 (m, 1 H), 2.09–1.93 (m, 1 H) ppm;  $^{19}\text{F}$  NMR (376 MHz,  $\text{CDCl}_3$ )  $\delta$  –68.51 (d,  $J$  = 8.8 Hz) ppm;  $^{13}\text{C}$  NMR (101 MHz,  $\text{CDCl}_3$ )  $\delta$  169.12, 160.10, 146.98, 137.95, 137.89, 136.08, 131.54, 128.87, 127.23 (q,  $J$  = 279.7 Hz), 125.71, 120.70, 120.60, 114.35, 111.75, 72.19 (q,  $J$  = 2.9 Hz), 62.27, 55.39, 48.77, 46.31, 46.00, 44.41 (q,  $J$  = 26.4 Hz), 43.22, 28.02, 16.78 (q,  $J$  = 2.5 Hz) ppm; HRMS (ESI $^{+}$ )  $m/z$ :  $[\text{M}+\text{H}]^{+}$  calcd for  $\text{C}_{26}\text{H}_{29}\text{O}_3\text{N}_5\text{F}_3$  516.2217; found 516.2202. HPLC:  $t_r$  5.1 min (97.3 % at 254 nm).

(4-(4-(((2,3-Dihydro-1H-inden-1-yl)oxy)methyl)-1H-1,2,3-triazol-1-yl)phenyl)(piperazin-1-yl)methanone (5o)

Compound **5o** was prepared according to the General procedure F from the alkyne **3o** (59 mg, 0.34 mmol) and the azide **2** (78 mg, 0.34 mmol). The crude product was purified by flash chromatography, eluent DCM/MeOH/NH $_4$ OH 9:1:0.1. Yield: 11 % (15 mg); light yellow crispy foam;  $^1\text{H}$  NMR (400 MHz,  $\text{CDCl}_3$ )  $\delta$  7.99 (s, 1 H), 7.79 (d,  $J$  = 8.8 Hz, 2 H), 7.57 (d,  $J$  = 8.6 Hz, 2 H), 7.45 (d,  $J$  = 7.3 Hz, 1 H), 7.32–7.25 (m, 2 H), 7.27–7.18 (m, 1 H), 5.13 (dd,  $J_1$  = 6.6 Hz,  $J_2$  = 3.9 Hz, 1 H), 4.86 (d,  $J$  = 12.9 Hz, 1 H), 4.83 (d,  $J$  = 12.7 Hz, 1 H), 3.93–3.65 (m, 2 H), 3.55–3.35 (m, 2 H), 3.19–3.07 (m, 1 H), 3.04–2.77 (m, 5 H), 2.42 (ddt,  $J_1$  = 13.0 Hz,  $J_2$  = 8.5 Hz,  $J_3$  = 6.4 Hz, 1 H), 2.19 (dddd,  $J_1$  = 13.3 Hz,  $J_2$  = 8.5 Hz,  $J_3$  = 5.0 Hz,  $J_4$  = 3.8 Hz, 1 H) ppm; HRMS (ESI $^{+}$ )  $m/z$ :  $[\text{M}+\text{H}]^{+}$  calcd for  $\text{C}_{23}\text{H}_{26}\text{O}_2\text{N}_5$  404.2081; found 404.2076. HPLC:  $t_r$  4.9 min (97.0 % at 254 nm).

(4-(4-(((1,1'-Biphenyl)-3-yloxy)methyl)-1H-1,2,3-triazol-1-yl)phenyl)(piperazin-1-yl)methanone (5p)

Compound **5p** was prepared according to the General procedure F from the alkyne **3p** (90 mg, 0.43 mmol) and the azide **2** (100 mg, 0.43 mmol). The crude product was purified by flash chromatography, eluent DCM/MeOH/NH $_4$ OH 20:1:0.1. Yield: 27 % (51 mg); light yellow solid;  $^1\text{H}$  NMR (400 MHz,  $\text{CDCl}_3$ )  $\delta$  8.11 (s, 1 H), 7.81 (d,  $J$  = 8.6 Hz, 2 H), 7.63–7.55 (m, 4 H), 7.49–7.33 (m, 4 H), 7.29–7.20 (m, 2 H), 7.02 (ddd,  $J_1$  = 8.2 Hz,  $J_2$  = 2.6 Hz,  $J_3$  = 1.0 Hz, 1 H), 5.37 (s, 2 H), 3.90–3.69 (m, 2 H), 3.58–3.35 (m, 2 H), 3.09–2.70 (m, 4 H) ppm;  $^{13}\text{C}$  NMR (101 MHz,  $\text{CDCl}_3$ )  $\delta$  169.04, 158.60, 145.45, 143.05, 140.88, 137.76, 136.44, 130.06, 128.92, 127.67, 127.27, 120.93, 120.66, 120.53, 115.17, 113.94, 113.47, 62.15, 49.19, 46.54, 46.03, 43.47 ppm; HRMS (ESI $^{+}$ )  $m/z$ :  $[\text{M}+\text{H}]^{+}$  calcd for  $\text{C}_{26}\text{H}_{26}\text{O}_2\text{N}_5$  440.2081; found 440.2076; HPLC:  $t_r$  5.77 min (95.9 % at 254 nm).

(4-(4-(((1,1'-Biphenyl)-4-yloxy)methyl)-1H-1,2,3-triazol-1-yl)phenyl)(piperazin-1-yl)methanone (5r)

Compound **5r** was prepared according to the General procedure F from the alkyne **3r** (90 mg, 0.43 mmol) and the azide **2** (100 mg, 0.43 mmol). The crude product was purified by flash chromatography, eluent DCM/MeOH/NH $_4$ OH 20:1:0.1. Yield: 4.2 % (7.6 mg); light yellow solid;  $^1\text{H}$  NMR (400 MHz,  $\text{CDCl}_3$ )  $\delta$  8.11 (s, 1 H), 7.82 (d,  $J$  = 8.6 Hz, 2 H), 7.63–7.52 (m, 6 H), 7.47–7.38 (m, 2 H), 7.36–7.27 (m, 1 H), 7.10 (d,  $J$  = 8.8 Hz, 2 H), 5.36 (s, 2 H), 3.87–3.70 (m, 2 H), 3.55–3.27 (m, 2 H), 3.09–2.71 (m, 4 H) ppm;  $^{13}\text{C}$  NMR (101 MHz, DMSO- $d_6$ )  $\delta$  167.91, 157.60, 144.05, 139.72, 137.03, 136.12, 135.97, 133.02, 128.88, 128.73, 128.69, 127.82, 126.80, 126.22, 122.98, 120.07, 115.23, 61.09 ppm; HRMS (ESI $^{+}$ )  $m/z$ :  $[\text{M}+\text{H}]^{+}$  calcd. for  $\text{C}_{26}\text{H}_{26}\text{O}_2\text{N}_5$  440.2081; found 440.2077. HPLC:  $t_r$  6.2 min (96.1 % at 254 nm).

(4-(4-(((3-Chloro-4-fluorophenoxy)methyl)-1H-1,2,3-triazol-1-yl)phenyl)(piperazin-1-yl)methanone (5s)

Compound **5s** was prepared according to the General procedure F from the alkyne **3s** (79.7 mg, 0.432 mmol) and the azide **2** (100 mg, 0.432 mmol). The crude product was purified by flash chromatography, eluent DCM/MeOH/NH $_4$ OH 9:1:0.1. Yield: 29 % (52 mg); light yellow solid;  $^1\text{H}$  NMR (400 MHz,  $\text{CDCl}_3$ )  $\delta$  8.08 (s, 1 H), 7.81 (d,  $J$  = 8.6 Hz, 2 H), 7.59 (d,  $J$  = 8.6 Hz, 2 H), 7.31 (t,  $J$  = 8.6 Hz, 1 H), 6.85 (dd,  $J_1$  = 10.6 Hz,  $J_2$  = 2.8 Hz, 1 H), 6.79 (ddd,  $J_1$  = 8.9 Hz,  $J_2$  = 2.9 Hz,  $J_3$  = 1.2 Hz, 1 H), 3.90–3.65 (m, 2 H), 3.54–3.34 (m, 2 H), 3.07–2.76 (m, 4 H);  $^{19}\text{F}$  NMR (376 MHz,  $\text{CDCl}_3$ )  $\delta$  (–112.51)–(–112.59) (m);  $^{13}\text{C}$  NMR (100 MHz,  $\text{CDCl}_3$ )  $\delta$  168.99, 158.57 (d,  $J$  = 248.5 Hz), 157.90 (d,  $J$  = 9.6 Hz), 144.49, 137.64, 136.61 (d,  $J$  = 4.9 Hz), 130.91, 128.96, 121.09, 120.69, 113.28 (d,  $J$  = 17.8 Hz), 111.47 (d,  $J$  = 3.4 Hz), 104.14 (d,  $J$  = 24.5 Hz), 62.49, 49.18, 46.56, 46.00, 43.49. HRMS (ESI $^{+}$ )  $m/z$ :  $[\text{M}+\text{H}]^{+}$  calcd. for  $\text{C}_{20}\text{H}_{20}\text{O}_2\text{N}_5\text{ClF}$  416.1284; found 416.1279. HPLC:  $t_r$  5.2 min (97.7 % at 254 nm).

(4-(4-(((4-Bromo-3-chlorophenoxy)methyl)-1H-1,2,3-triazol-1-yl)phenyl)(piperazin-1-yl)methanone (5t)

Compound **5t** was prepared according to the General procedure F from the alkyne **3t** (106 mg, 0.432 mmol) and the azide **2** (100 mg, 0.432 mmol). The crude product was purified by flash chromatography, eluent DCM/MeOH/NH $_4$ OH 20:1:0.1. Yield: 25 % (52 mg); off-white solid;  $^1\text{H}$  NMR (400 MHz,  $\text{CDCl}_3$ )  $\delta$  8.08 (s, 1 H), 7.81 (d,  $J$  = 8.5 Hz, 2 H), 7.59 (d,  $J$  = 8.5 Hz, 2 H), 7.36 (d,  $J$  = 8.9 Hz, 1 H), 7.31 (d,  $J$  = 2.9 Hz, 1 H), 6.94 (dd,  $J_1$  = 8.9 Hz,  $J_2$  = 2.9 Hz, 1 H), 5.27 (s, 2 H), 3.95–3.64 (m, 2 H), 3.54–3.33 (m, 2 H), 3.05–2.75 (m, 4 H); HRMS (ESI $^{+}$ )  $m/z$ :  $[\text{M}+\text{H}]^{+}$  calcd for  $\text{C}_{20}\text{H}_{20}\text{O}_2\text{N}_5\text{BrCl}$  476.0483; found 476.0480. HPLC:  $t_r$  5.8 min (99.8 % at 254 nm).

(4-(4-(((3-Chloro-4-iodophenoxy)methyl)-1H-1,2,3-triazol-1-yl)phenyl)(piperazin-1-yl)methanone (5u)

Compound **5u** was prepared according to the General procedure F from the alkyne **3u** (106 mg, 0.432 mmol) and the azide **2** (100 mg, 0.432 mmol). The crude product was purified by flash chromatography,

eluent DCM/MeOH/NH<sub>4</sub>OH 20:1:0.1. Yield: 25 % (52 mg); off-white solid; <sup>1</sup>H NMR (400 MHz, CDCl<sub>3</sub>) δ 8.07 (s, 1 H), 7.86–7.77 (m, 2 H), 7.65–7.56 (m, 2 H), 7.52 (d, *J* = 2.9 Hz, 1 H), 7.35 (d, *J* = 8.8 Hz, 1 H), 6.98 (dd, *J*<sub>1</sub> = 8.8 Hz, *J*<sub>2</sub> = 2.9 Hz, 1 H), 5.26 (s, 2 H), 3.99–3.68 (m, 2 H), 3.61–3.31 (m, 2 H), 3.18–2.80 (m, 2 H), 2.73–2.36 (m, 2 H) ppm; <sup>13</sup>C NMR (100 MHz, DMSO-*d*<sub>6</sub>) representatives peaks δ 167.90, 156.86, 143.56, 136.98, 136.04, 129.58, 129.29, 128.73, 125.93, 123.11, 120.11, 116.87, 99.11, 61.59 ppm; HRMS (ESI+) *m/z*: [M+H]<sup>+</sup> calcd for C<sub>20</sub>H<sub>20</sub>O<sub>2</sub>N<sub>5</sub>Cl 524.03447; found 524.03407; HPLC: t<sub>r</sub> 6.41 min (92.2 % at 254 nm)

(4-(4-((4-Fluorophenoxy)methyl)-1*H*-1,2,3-triazol-1-yl)phenyl)(piperazin-1-yl)methanone (5v)

Compound **5v** was prepared according to the General procedure F from the alkyne **3v** (45 mg, 0.30 mmol) and the azide **2** (58 mg, 0.25 mmol). The crude product was purified by flash chromatography, eluent DCM/MeOH/NH<sub>4</sub>OH 9:1:0.1. Yield: 2.4 % (2.3 mg); off-white solid. Note: NMR data was acquired from less pure fractions. <sup>1</sup>H NMR (400 MHz, DMSO-*d*<sub>6</sub>) δ 9.02 (s, 1 H), 8.00 (d, *J* = 8.6 Hz, 2 H), 7.63 (d, *J* = 8.6 Hz, 2 H), 7.21–7.06 (m, 4 H), 5.24 (s, 2 H), 3.45–3.23 (m, 4 H), 2.89–2.62 (m, 4 H) ppm; <sup>13</sup>C NMR (101 MHz, DMSO-*d*<sub>6</sub>) δ 167.86, 157.92, 155.57, 154.29 (d, *J* = 1.9 Hz), 143.95, 136.58 (d, *J* = 74.6 Hz), 128.67, 122.96, 120.07, 116.13 (d, *J* = 8.1 Hz), 115.91 (d, *J* = 23.0 Hz), 61.57, 48.05, 45.36, 45.04, 42.29 ppm; HRMS (ESI+) *m/z*: [M+H]<sup>+</sup> calcd for C<sub>20</sub>H<sub>21</sub>O<sub>2</sub>N<sub>5</sub>F 382.1674; found 382.1669. HPLC: t<sub>r</sub> 4.4 min (98.1 % at 254 nm).

(4-(4-((4-Isopropylphenoxy)methyl)-1*H*-1,2,3-triazol-1-yl)phenyl)(piperazin-1-yl)methanone (5w)

Compound **5w** was prepared according to the General procedure F from the alkyne **3w** (75.3 mg, 0.432 mmol) and the azide **2** (100 mg, 0.432 mmol). The crude product was purified by flash chromatography, eluent DCM/MeOH/NH<sub>4</sub>OH 9:1:0.1. Yield: 21 % (37 mg); off-white solid; <sup>1</sup>H NMR (400 MHz, CDCl<sub>3</sub>) δ 8.08 (s, 1 H), 7.81 (d, *J* = 8.6 Hz, 2 H), 7.58 (d, *J* = 8.5 Hz, 2 H), 7.17 (d, *J* = 8.5 Hz, 2 H), 6.96 (d, *J* = 8.7 Hz, 2 H), 5.29 (s, 2 H), 3.87–3.65 (m, 2 H), 3.53–3.29 (m, 2 H), 3.06–2.77 (m, 5 H), 1.23 (d, *J* = 6.9 Hz, 6 H) ppm; <sup>13</sup>C NMR (101 MHz, DMSO-*d*<sub>6</sub>) δ 167.88, 156.08, 144.27, 140.89, 136.99, 136.12, 128.68, 127.22, 122.84, 120.05, 114.55, 60.99, 47.87, 45.24, 44.95, 42.12, 32.59, 24.12 ppm; HRMS (ESI+) *m/z*: [M+H]<sup>+</sup> calcd for C<sub>23</sub>H<sub>28</sub>O<sub>2</sub>N<sub>5</sub> 406.2238; found 406.2233; HPLC: t<sub>r</sub> 5.5 min (99.3 % at 254 nm).

(4-(4-(((7-Methoxynaphthalen-2-yl)oxy)methyl)-1*H*-1,2,3-triazol-1-yl)phenyl)(piperazin-1-yl)methanone (5x)

Compound **5x** was prepared according to the General procedure F from the alkyne **3x** (92 mg, 0.432 mmol) and the azide **2** (100 mg, 0.432 mmol). The crude product was purified by flash chromatography, eluent DCM/MeOH/NH<sub>4</sub>OH 9:1:0.1. Yield: 2.1 % (9.2 mg); off-white solid; <sup>1</sup>H NMR (400 MHz, DMSO-*d*<sub>6</sub>) δ 9.07 (s, 1 H), 8.00 (d, *J* = 8.3 Hz, 2 H), 7.76 (dd, *J*<sub>1</sub> = 8.9 Hz, *J*<sub>2</sub> = 6.7 Hz, 2 H), 7.62 (d, *J* = 8.2 Hz, 2 H), 7.46 (d, *J* = 2.6 Hz, 1 H), 7.25 (d, *J* = 2.6 Hz, 1 H), 7.04 (ddd, *J*<sub>1</sub> = 21.8 Hz, *J*<sub>2</sub> = 8.9 Hz, *J*<sub>3</sub> = 2.5 Hz, 2 H), 5.35 (s, 2 H), 3.87 (s, 3 H), 3.66–3.48 (m, 2 H), 3.43–3.14 (m, 2 H), 2.72 (d, *J* = 30.7 Hz, 4 H) ppm; <sup>13</sup>C NMR (100 MHz, DMSO-*d*<sub>6</sub>) δ 167.82, 157.81, 156.44, 143.99, 136.92, 136.35, 135.66, 129.18, 129.05, 128.62, 123.96, 123.03, 120.09, 116.05, 115.89, 106.73, 105.46, 61.01, 55.11, 48.58, 45.78, 45.37, 42.78, 40.15 ppm; HRMS (ESI+) *m/z*: [M+H]<sup>+</sup> calcd. for C<sub>25</sub>H<sub>26</sub>O<sub>3</sub>N<sub>5</sub> 444.2030; found 444.2025. HPLC: t<sub>r</sub> 5.7 min (97.4 % at 254 nm).

4-(4-(((7-Methoxynaphthalen-2-yl)oxy)methyl)-1*H*-1,2,3-triazol-1-yl)benzoic acid (6)

Compound **6** was prepared according to General procedure F using **3x** (1.2 g, 5.7 mmol) as starting material. The precipitate that formed during the reaction was filtered off and dried to yield a clean product **6**.

Yield: 96 % (2,05 g); yellow solid; <sup>1</sup>H NMR (400 MHz, DMSO-*d*<sub>6</sub>) δ 13.27 (s, 1 H), 9.12 (s, 1 H), 8.15 (s, 4 H), 7.75 (dd, *J*<sub>1</sub> = 8.9 Hz, *J*<sub>2</sub> = 6.4 Hz, 2 H), 7.45 (d, *J* = 2.5 Hz, 1 H), 7.25 (d, *J* = 2.6 Hz, 1 H), 7.10–6.97 (m, 2 H), 5.35 (s, 2 H), 3.87 (s, 3 H) ppm; MS (ESI+) C<sub>21</sub>H<sub>13</sub>N<sub>3</sub>O<sub>4</sub> *m/z*: 375.4 [M+H]<sup>+</sup>.

4-(4-(((7-Methoxynaphthalen-2-yl)oxy)methyl)-1*H*-1,2,3-triazol-1-yl)aniline (7)

Compound **7** was prepared according to General procedure F using **3x** (1.7 g, 8.0 mmol) as starting material. The precipitate that formed during the reaction was filtered off and dried. The residue was further purified by flash column chromatography using EtOAc:hexane = 1:2 as the mobile phase to yield a clean product **7**. Yield: 86 % (2.40 g); light brown solid; <sup>1</sup>H NMR (400 MHz, DMSO-*d*<sub>6</sub>) δ 8.71 (s, 1 H), 7.79–7.71 (m, 2 H), 7.51–7.46 (m, 2 H), 7.44 (d, *J* = 2.6 Hz, 1 H), 7.24 (d, *J* = 2.5 Hz, 1 H), 7.06–6.98 (m, 2 H), 6.73–6.65 (m, 2 H), 5.51 (s, 2 H), 5.28 (s, 2 H), 3.87 (s, 3 H) ppm; MS (ESI+) C<sub>20</sub>H<sub>18</sub>N<sub>4</sub>O<sub>2</sub> *m/z*: 346.6 [M+H]<sup>+</sup>.

*tert*-Butyl (1-(4-(4-(((7-methoxynaphthalen-2-yl)oxy)methyl)-1*H*-1,2,3-triazol-1-yl)benzoyl)piperidin-4-yl)carbamate (8a)

Compound **8a** was prepared according to General procedure A using **6** (0.40 g, 1.1 mmol) as starting material. The product was purified by flash column chromatography using DCM:MeOH = 20:1 as the mobile phase to yield a clean product **8a**. Yield: 34 % (203 mg); light red solid; <sup>1</sup>H NMR (400 MHz, DMSO-*d*<sub>6</sub>) δ 9.07 (s, 1 H), 8.05–7.97 (m, 2 H), 7.82–7.71 (m, 2 H), 7.68–7.55 (m, 2 H), 7.46 (d, *J* = 2.5 Hz, 1 H), 7.25 (d, *J* = 2.6 Hz, 1 H), 7.06 (dd, *J*<sub>1</sub> = 8.9 Hz, *J*<sub>2</sub> = 2.5 Hz, 1 H), 7.01 (dd, *J*<sub>1</sub> = 8.9 Hz, *J*<sub>2</sub> = 2.5 Hz, 1 H), 6.92 (d, *J* = 7.7 Hz, 1 H), 5.35 (s, 2 H), 4.41–4.26 (m, 1 H), 3.60–3.49 (m, 2 H), 3.21–2.90 (m, 2 H), 1.87–1.65 (m, 2 H), 1.44–1.20 (m, 11 H) ppm; MS (ESI+) C<sub>31</sub>H<sub>35</sub>N<sub>5</sub>O<sub>5</sub> *m/z*: 557.6 [M+H]<sup>+</sup>.

*tert*-Butyl (1-(4-(4-(((7-methoxynaphthalen-2-yl)oxy)methyl)-1*H*-1,2,3-triazol-1-yl)benzoyl)piperidin-4-yl)(methyl)carbamate (8b)

Compound **8b** was prepared according to General procedure A using **6** (0.18 g, 0.48 mmol) as starting material. The product was purified by flash column chromatography using DCM:MeOH = 20:1 as the mobile phase to yield a clean product **8b**. Yield: 40 % (109 mg); white solid; <sup>1</sup>H NMR (400 MHz, DMSO-*d*<sub>6</sub>) δ 9.07 (s, 1 H), 8.05–7.97 (m, 2 H), 7.80–7.71 (m, 2 H), 7.69–7.61 (m, 2 H), 7.46 (d, *J* = 2.5 Hz, 1 H), 7.25 (d, *J* = 2.5 Hz, 1 H), 7.06 (dd, *J*<sub>1</sub> = 8.9 Hz, *J*<sub>2</sub> = 2.6 Hz, 1 H), 7.01 (dd, *J* = 8.9, 2.5 Hz, 1 H), 5.35 (s, 2 H), 4.69–4.50 (m, 1 H), 4.18–3.98 (m, 1 H), 3.72–3.54 (m, 1 H), 3.21–3.06 (m, 1 H), 2.89–2.73 (m, 1 H), 2.70 (s, 3 H), 1.73–1.46 (m, 4 H), 1.40 (s, 9 H) ppm; MS (ESI+) C<sub>32</sub>H<sub>37</sub>N<sub>5</sub>O<sub>5</sub> *m/z*: 571.6 [M+H]<sup>+</sup>.

*tert*-Butyl 4-(4-(4-(((7-methoxynaphthalen-2-yl)oxy)methyl)-1*H*-1,2,3-triazol-1-yl)benzamido)piperidine-1-carboxylate (8c)

Compound **8c** was prepared according to General procedure A using **6** (0.18 g, 0.48 mmol) as starting material. The product was purified by flash column chromatography using DCM:MeOH = 20:1 as the mobile phase to yield a clean product **8c**. Yield: 45 % (120 mg); white solid; <sup>1</sup>H NMR (400 MHz, DMSO-*d*<sub>6</sub>) δ 9.12 (s, 1 H), 8.45 (d, *J* = 7.8 Hz, 1 H), 8.06 (s, 4 H), 7.76 (dd, *J*<sub>1</sub> = 8.9 Hz, *J*<sub>2</sub> = 6.7 Hz, 2 H), 7.46 (d, *J* = 2.6 Hz, 1 H), 7.25 (d, *J* = 2.5 Hz, 1 H), 7.06 (dd, *J*<sub>1</sub> = 8.9 Hz, *J*<sub>2</sub> = 2.5 Hz, 1 H), 7.01 (dd, *J*<sub>1</sub> = 8.9 Hz, *J*<sub>2</sub> = 2.5 Hz, 1 H), 5.35 (s, 2 H), 4.06–3.90 (m, 3 H), 3.87 (s, 3 H), 2.95–2.77 (m, 2 H), 1.85–1.77 (m, 2 H), 1.49–1.33 (m, 11 H) ppm; MS (ESI+) C<sub>31</sub>H<sub>35</sub>N<sub>5</sub>O<sub>5</sub> *m/z*: 557.2 [M+H]<sup>+</sup>.

*tert*-Butyl 7-(4-(4-(((7-methoxynaphthalen-2-yl)oxy)methyl)-1*H*-1,2,3-triazol-1-yl)benzoyl)-2,7-diazaspiro[4.4]nonane-2-carboxylate (8d)

Compound **8d** was prepared according to General procedure A using **6** (0.25 g, 0.67 mmol) as starting material. The product was purified by

flash column chromatography using DCM:MeOH = 20:1 as the mobile phase to yield a clean product **8d**. Yield: 61 % (238 mg); white solid; <sup>1</sup>H NMR (400 MHz, DMSO-*d*<sub>6</sub>) δ 9.09 (d, *J* = 7.6 Hz, 1 H), 8.04 – 7.93 (m, 2 H), 7.83 – 7.71 (m, 4 H), 7.46 (d, *J* = 2.5 Hz, 1 H), 7.25 (d, *J* = 2.5 Hz, 1 H), 7.06 (dd, *J*<sub>1</sub> = 8.9 Hz, *J*<sub>2</sub> = 2.5 Hz, 1 H), 7.01 (dd, *J*<sub>1</sub> = 8.9 Hz, *J*<sub>2</sub> = 2.5 Hz, 1 H), 5.35 (s, 2 H), 3.63 – 3.52 (m, 2 H), 3.47 – 3.13 (m, 6 H), 1.96 – 1.74 (m, 4 H), 1.45 – 1.32 (m, 9 H); MS (ESI+) C<sub>33</sub>H<sub>37</sub>N<sub>5</sub>O<sub>5</sub> *m/z*: 583.5 [M+H]<sup>+</sup>.

*tert*-Butyl 3-(4-(4-(((7-methoxynaphthalen-2-yl)oxy)methyl)-1*H*-1,2,3-triazol-1-yl)benzamido)propyl)carbamate (8e)

Compound **8e** was prepared according to General procedure A using **6** (0.25 g, 0.67 mmol) as starting material. The product was purified by flash column chromatography using DCM:MeOH = 30:1 as the mobile phase to yield a clean product **8e**. Yield: 46 % (163 mg); white solid; <sup>1</sup>H NMR (400 MHz, DMSO-*d*<sub>6</sub>) δ 9.11 (s, 1 H), 8.61 (t, *J* = 5.7 Hz, 1 H), 8.06 (s, 4 H), 7.80 – 7.71 (m, 2 H), 7.46 (d, *J* = 2.5 Hz, 1 H), 7.25 (d, *J* = 2.5 Hz, 1 H), 7.06 (dd, *J*<sub>1</sub> = 8.9 Hz, *J*<sub>2</sub> = 2.5 Hz, 1 H), 7.01 (dd, *J*<sub>1</sub> = 8.9 Hz, *J*<sub>2</sub> = 2.5 Hz, 1 H), 6.83 (d, *J* = 6.1 Hz, 1 H), 5.35 (s, 2 H), 3.87 (s, 3 H), 3.33 – 3.23 (m, 2 H), 2.99 (q, *J* = 6.6 Hz, 2 H), 1.69 – 1.61 (m, 2 H), 1.38 (s, 9 H) ppm; MS (ESI+) C<sub>29</sub>H<sub>33</sub>N<sub>5</sub>O<sub>5</sub> *m/z*: 531.5 [M+H]<sup>+</sup>.

(4-(4-(((7-Methoxynaphthalen-2-yl)oxy)methyl)-1*H*-1,2,3-triazol-1-yl)phenyl)(morpholino)methanone (8f)

Compound **8f** was prepared according to General procedure A using **6** (0.25 g, 0.67 mmol) as starting material. The product was purified by flash column chromatography using DCM:MeOH = 30:1 as the mobile phase to yield a clean product **8f**. Yield: 49 % (145 mg); light yellow solid; <sup>1</sup>H NMR (400 MHz, DMSO-*d*<sub>6</sub>) δ 9.08 (s, 1 H), 8.06 – 7.98 (m, 2 H), 7.80 – 7.71 (m, 2 H), 7.70 – 7.61 (m, 2 H), 7.46 (d, *J* = 2.5 Hz, 1 H), 7.25 (d, *J* = 2.5 Hz, 1 H), 7.06 (dd, *J*<sub>1</sub> = 8.9 Hz, *J*<sub>2</sub> = 2.5 Hz, 1 H), 7.01 (dd, *J*<sub>1</sub> = 8.9 Hz, *J*<sub>2</sub> = 2.5 Hz, 1 H), 5.35 (s, 2 H), 3.87 (s, 3 H), 3.73 – 3.36 (m, 8 H) ppm; <sup>13</sup>C NMR (101 MHz, DMSO-*d*<sub>6</sub>) δ 167.99, 157.83, 156.46, 144.03, 137.12, 135.76, 135.68, 129.20, 129.08, 128.84, 123.98, 123.06, 120.11, 116.07, 115.91, 106.74, 105.47, 66.05, 61.01, 55.13, 47.71, 42.12 ppm; HRMS (ESI+) calcd. for C<sub>25</sub>H<sub>25</sub>N<sub>4</sub>O<sub>4</sub> [M+H]<sup>+</sup>: 445.1870, found: 445.1858; UPLC: *t*<sub>r</sub> = 4.86 min (97.6 % at 254 nm).

(4-Hydroxypiperidin-1-yl)(4-(4-(((7-methoxynaphthalen-2-yl)oxy)methyl)-1*H*-1,2,3-triazol-1-yl)phenyl)methanone (8g)

Compound **8g** was prepared according to General procedure A using **6** (0.25 g, 0.67 mmol) as starting material. The product was purified by flash column chromatography using DCM:MeOH = 20:1 as the mobile phase to yield a clean product **8g**. Yield: 46 % (141 mg); white solid; <sup>1</sup>H NMR (400 MHz, DMSO-*d*<sub>6</sub>) δ 9.07 (s, 1 H), 8.03 – 7.96 (m, 2 H), 7.80 – 7.72 (m, 2 H), 7.65 – 7.57 (m, 2 H), 7.46 (s, 1 H), 7.25 (s, 1 H), 7.06 (dd, *J*<sub>1</sub> = 8.9 Hz, *J*<sub>2</sub> = 2.4 Hz, 1 H), 7.01 (dd, *J*<sub>1</sub> = 8.9 Hz, *J*<sub>2</sub> = 2.4 Hz, 1 H), 5.35 (s, 2 H), 4.85 – 4.79 (m, 1 H), 4.08 – 3.97 (m, 1 H), 3.87 (s, 3 H), 3.79 – 3.71 (m, 1 H), 3.58 – 3.45 (m, 1 H), 3.26 – 3.10 (m, 2 H), 1.88 – 1.64 (m, 2 H), 1.47 – 1.26 (m, 2 H) ppm; <sup>13</sup>C NMR (101 MHz, DMSO-*d*<sub>6</sub>) δ 167.82, 157.83, 156.46, 144.00, 136.92, 136.58, 135.68, 129.20, 129.07, 128.41, 123.98, 123.05, 120.13, 116.07, 115.91, 106.74, 105.47, 65.41, 61.01, 55.12, 44.68, 34.41 ppm; HRMS (ESI+) calcd. for C<sub>26</sub>H<sub>27</sub>N<sub>4</sub>O<sub>4</sub> [M+H]<sup>+</sup>: 459.2026, found: 459.2013; UPLC: *t*<sub>r</sub> = 4.57 min (98.3 % at 254 nm).

*tert*-Butyl 4-((4-(4-(((7-methoxynaphthalen-2-yl)oxy)methyl)-1*H*-1,2,3-triazol-1-yl)phenyl)carbamoyl)piperidine-1-carboxylate (9a)

Compound **9a** was prepared according to General procedure A using **7** (0.25 g, 0.72 mmol) as starting material. The product was purified by flash column chromatography using DCM:MeOH = 30:1 as the mobile phase to yield a clean product **9a**. Yield: 38 % (154 mg); orange solid; <sup>1</sup>H NMR (400 MHz, DMSO-*d*<sub>6</sub>) δ 10.21 (s, 1 H), 8.92 (s, 1 H), 7.88 – 7.78 (m, 4 H), 7.79 – 7.71 (m, 2 H), 7.45 (d, *J* = 2.6 Hz, 1 H), 7.24 (d, *J* = 2.5 Hz, 1 H), 7.05 (dd, *J*<sub>1</sub> = 8.9 Hz, *J*<sub>2</sub> = 2.6 Hz, 1 H), 7.01 (dd, *J*<sub>1</sub> =

8.9 Hz, *J*<sub>2</sub> = 2.6 Hz, 1 H), 5.32 (s, 2 H), 4.04 – 3.97 (m, 2 H), 3.87 (s, 3 H), 2.86 – 2.74 (m, 2 H), 2.59 – 2.51 (m, 1 H), 1.84 – 1.76 (m, 2 H), 1.57 – 1.42 (m, 2 H), 1.41 (s, 9 H); MS (ESI+) C<sub>31</sub>H<sub>35</sub>N<sub>5</sub>O<sub>5</sub> *m/z*: 557.4 [M+H]<sup>+</sup>.

*tert*-Butyl 3-((4-(4-(((7-methoxynaphthalen-2-yl)oxy)methyl)-1*H*-1,2,3-triazol-1-yl)phenyl)carbamoyl)bicyclo[1.1.1]pentan-1-yl)carbamate (9b)

Compound **9b** was prepared according to General procedure A using **7** (0.25 g, 0.72 mmol) as starting material. The product was purified by flash column chromatography using DCM:MeOH = 20:1 as the mobile phase to yield a clean product **9b**. Yield: 34 % (135 mg); off-white solid; <sup>1</sup>H NMR (400 MHz, DMSO-*d*<sub>6</sub>) δ 9.80 (s, 1 H), 8.93 (s, 1 H), 7.86 (s, 3 H), 7.79 – 7.71 (m, 2 H), 7.67 – 7.61 (m, 1 H), 7.45 (d, *J* = 2.5 Hz, 1 H), 7.24 (d, *J* = 2.5 Hz, 1 H), 7.05 (dd, *J*<sub>1</sub> = 8.9 Hz, *J*<sub>2</sub> = 2.5 Hz, 1 H), 7.01 (dd, *J*<sub>1</sub> = 8.9 Hz, *J*<sub>2</sub> = 2.5 Hz, 1 H), 5.32 (s, 2 H), 3.87 (s, 3 H), 2.22 (s, 6 H), 1.40 (s, 9 H); MS (ESI+) C<sub>31</sub>H<sub>33</sub>N<sub>5</sub>O<sub>5</sub> *m/z*: 555.5 [M+H]<sup>+</sup>.

*tert*-Butyl 3-((4-(4-(((7-methoxynaphthalen-2-yl)oxy)methyl)-1*H*-1,2,3-triazol-1-yl)phenyl)carbamoyl)azetidine-1-carboxylate (9c)

Compound **9c** was prepared according to General procedure A using **7** (0.25 g, 0.72 mmol) as starting material. The product was purified by flash column chromatography using DCM:MeOH = 30:1 as the mobile phase to yield a clean product **9c**. Yield: 27 % (102 mg); yellow solid; <sup>1</sup>H NMR (400 MHz, DMSO-*d*<sub>6</sub>) δ 10.32 (s, 1 H), 8.93 (s, 1 H), 7.90 – 7.85 (m, 2 H), 7.85 – 7.80 (m, 2 H), 7.78 – 7.72 (m, 2 H), 7.45 (d, *J* = 2.6 Hz, 1 H), 7.24 (d, *J* = 2.5 Hz, 1 H), 7.05 (dd, *J*<sub>1</sub> = 8.9 Hz, *J*<sub>2</sub> = 2.5 Hz, 1 H), 7.01 (dd, *J*<sub>1</sub> = 8.9 Hz, *J*<sub>2</sub> = 2.6 Hz, 1 H), 5.33 (s, 2 H), 4.07 – 3.90 (m, 4 H), 3.87 (s, 3 H), 3.56 – 3.45 (m, 1 H), 1.39 (s, 9 H); MS (ESI+) C<sub>29</sub>H<sub>31</sub>N<sub>5</sub>O<sub>5</sub> *m/z*: 529.3 [M+H]<sup>+</sup>.

*tert*-Butyl 3-((4-(4-(((7-methoxynaphthalen-2-yl)oxy)methyl)-1*H*-1,2,3-triazol-1-yl)phenyl)amino)-3-oxopropyl)carbamate (9d)

Compound **9d** was prepared according to General procedure A using **7** (0.25 g, 0.72 mmol) as starting material. The product was purified by flash column chromatography using DCM:MeOH = 30:1 as the mobile phase to yield a clean product **9d**. Yield: 36 % (134 mg); yellow solid; <sup>1</sup>H NMR (400 MHz, DMSO-*d*<sub>6</sub>) δ 10.22 (s, 1 H), 8.92 (s, 1 H), 7.88 – 7.70 (m, 6 H), 7.45 (d, *J* = 2.6 Hz, 1 H), 7.24 (d, *J* = 2.6 Hz, 1 H), 7.05 (dd, *J*<sub>1</sub> = 8.9 Hz, *J*<sub>2</sub> = 2.5 Hz, 1 H), 7.01 (dd, *J*<sub>1</sub> = 8.9 Hz, *J*<sub>2</sub> = 2.5 Hz, 1 H), 6.91 (t, *J* = 5.6 Hz, 1 H), 5.32 (s, 2 H), 3.87 (s, 3 H), 3.24 (q, *J* = 6.7 Hz, 2 H), 1.38 (s, 9 H); MS (ESI+) C<sub>28</sub>H<sub>31</sub>N<sub>5</sub>O<sub>5</sub> *m/z*: 517.5 [M+H]<sup>+</sup>.

(4-Aminopiperidin-1-yl)(4-(4-(((7-methoxynaphthalen-2-yl)oxy)methyl)-1*H*-1,2,3-triazol-1-yl)phenyl)methanone (10a)

Compound **10a** was prepared according to General procedure B using TFA as a reagent and **8a** (0.050 g, 0.090 mmol) as starting material. The product was purified by flash column chromatography using DCM:MeOH:NH<sub>4</sub>OH = 9:1:0.1 as the mobile phase to yield a clean product **10a**. Yield: 97 % (40 mg); white solid; <sup>1</sup>H NMR (400 MHz, DMSO-*d*<sub>6</sub>) δ 9.07 (s, 1 H), 8.04 – 7.96 (m, 2 H), 7.81 – 7.71 (m, 2 H), 7.64 – 7.56 (m, 2 H), 7.46 (d, *J* = 2.6 Hz, 1 H), 7.25 (d, *J* = 2.5 Hz, 1 H), 7.06 (dd, *J*<sub>1</sub> = 8.9 Hz, *J*<sub>2</sub> = 2.5 Hz, 1 H), 7.01 (dd, *J*<sub>1</sub> = 8.9 Hz, *J*<sub>2</sub> = 2.5 Hz, 1 H), 5.35 (s, 2 H), 4.36 – 4.22 (m, 1 H), 3.87 (s, 3 H), 3.61 – 3.47 (m, 1 H), 3.14 – 2.89 (m, 2 H), 2.89 – 2.79 (m, 1 H), 1.88 – 1.59 (m, 4 H), 1.29 – 1.11 (m, 2 H) ppm; <sup>13</sup>C NMR (101 MHz, DMSO-*d*<sub>6</sub>) δ 167.76, 157.82, 156.45, 143.99, 136.90, 136.64, 135.67, 129.18, 129.06, 128.36, 123.96, 123.03, 120.13, 116.06, 115.90, 106.73, 105.46, 61.01, 55.11, 47.90, 45.80, 35.32, 34.65 ppm; HRMS (ESI+) calcd. for C<sub>26</sub>H<sub>28</sub>N<sub>5</sub>O<sub>3</sub> [M+H]<sup>+</sup>: 458.2186, found 458.2171; UPLC: *t*<sub>r</sub> = 3.84 min (97.5 % at 254 nm).

(4-(4-(((7-Methoxynaphthalen-2-yl)oxy)methyl)-1*H*-1,2,3-triazol-1-yl)phenyl)(4-(methylamino)piperidin-1-yl)methanone (10b)

Compound **10b** was prepared according to General procedure B using TFA as a reagent and **8b** (0.050 g, 0.087 mmol) as starting material. The product was purified by flash column chromatography using DCM:MeOH:NH<sub>4</sub>OH = 9:1:0.1 as the mobile phase to yield a clean product **10b**. Yield: 74 % (31 mg); white solid; <sup>1</sup>H NMR (400 MHz, DMSO-*d*<sub>6</sub>) δ 9.07 (s, 1 H), 8.04 – 7.96 (m, 2 H), 7.80 – 7.71 (m, 2 H), 7.65 – 7.57 (m, 2 H), 7.46 (d, *J* = 2.5 Hz, 1 H), 7.06 (dd, *J*<sub>1</sub> = 8.9 Hz, *J*<sub>2</sub> = 2.5 Hz, 1 H), 7.01 (dd, *J*<sub>1</sub> = 8.9 Hz, *J*<sub>2</sub> = 2.6 Hz, 1 H), 5.35 (s, 2 H), 4.31 – 4.18 (m, 1 H), 3.87 (s, 3 H), 3.62 – 3.47 (m, 1 H), 3.14 – 2.96 (m, 2 H), 2.28 (s, 3 H), 1.93 – 1.70 (m, 3 H), 1.28 – 1.13 (m, 2 H) ppm; <sup>13</sup>C NMR (101 MHz, DMSO-*d*<sub>6</sub>) δ 167.75, 157.82, 156.45, 143.99, 136.90, 136.62, 135.67, 129.18, 129.06, 128.39, 123.96, 123.04, 120.12, 116.06, 115.90, 106.73, 105.46, 61.01, 55.68, 55.11, 45.63, 33.22, 31.89, 31.23 ppm; HRMS (ESI+) calcd. for C<sub>27</sub>H<sub>30</sub>N<sub>5</sub>O<sub>3</sub> [M+H]<sup>+</sup>: 472.2343, found 472.2328; UPLC: t<sub>r</sub> = 3.94 min (98.1 % at 254 nm).

4-(4-(((7-Methoxynaphthalen-2-yl)oxy)methyl)-1*H*-1,2,3-triazol-1-yl)-*N*-(piperidin-4-yl)benzamide (10c)

Compound **10c** was prepared according to General procedure B using TFA as a reagent and **8c** (0.050 g, 0.090 mmol) as starting material. Yield: 83 % (34 mg); white solid; <sup>1</sup>H NMR (400 MHz, DMSO-*d*<sub>6</sub>) δ 9.12 (s, 1 H), 8.43 (d, *J* = 7.8 Hz, 1 H), 8.11 – 8.01 (m, 4 H), 7.80 – 7.71 (m, 2 H), 7.46 (d, *J* = 2.5 Hz, 1 H), 7.25 (d, *J* = 2.5 Hz, 1 H), 7.06 (dd, *J*<sub>1</sub> = 8.9 Hz, *J*<sub>2</sub> = 2.5 Hz, 1 H), 7.01 (dd, *J*<sub>1</sub> = 8.9 Hz, *J*<sub>2</sub> = 2.5 Hz, 1 H), 5.35 (s, 2 H), 3.91 – 3.79 (m, 4 H), 3.02 – 2.94 (m, 2 H), 1.80 – 1.72 (m, 2 H), 1.51 – 1.37 (m, 2 H) ppm, the signal for the remaining 2 protons is covered by DMSO; <sup>13</sup>C NMR (101 MHz, DMSO-*d*<sub>6</sub>) δ 164.22, 157.83, 156.45, 144.10, 138.19, 135.67, 134.63, 129.19, 129.08, 129.06, 123.97, 123.02, 119.53, 116.07, 115.89, 106.72, 105.46, 61.02, 55.11, 47.45, 45.16, 32.66 ppm; HRMS (ESI+) calcd. for C<sub>26</sub>H<sub>28</sub>N<sub>5</sub>O<sub>3</sub> [M+H]<sup>+</sup>: 458.2186, found: 458.2172; UPLC: t<sub>r</sub> = 3.99 min (99.5 % at 254 nm).

4-(4-(((7-Methoxynaphthalen-2-yl)oxy)methyl)-1*H*-1,2,3-triazol-1-yl)phenyl(2,7-diazaspiro[4.4]nonan-2-yl)methanone (10d)

Compound **10d** was prepared according to General procedure B using TFA as a reagent and **8d** (0.13 g, 0.22 mmol) as starting material. The product was purified by flash column chromatography using DCM:MeOH:NH<sub>4</sub>OH = 9:1:0.1 as the mobile phase to yield a clean product **10d**. Yield: 84 % (91 mg); white solid; <sup>1</sup>H NMR (400 MHz, DMSO-*d*<sub>6</sub>) δ 9.08 (d, *J* = 6.4 Hz, 1 H), 8.04 – 7.96 (m, 2 H), 7.81 – 7.71 (m, 4 H), 7.46 (d, *J* = 2.5 Hz, 1 H), 7.25 (d, *J* = 2.5 Hz, 1 H), 7.06 (dd, *J*<sub>1</sub> = 8.9 Hz, *J*<sub>2</sub> = 2.5 Hz, 1 H), 7.01 (dd, *J*<sub>1</sub> = 8.9 Hz, *J*<sub>2</sub> = 2.5 Hz, 1 H), 5.35 (s, 2 H), 3.87 (s, 3 H), 3.65 – 3.37 (m, 4 H), 2.92 – 2.79 (m, 1 H), 2.79 – 2.53 (m, 4 H), 1.91 – 1.52 (m, 4 H) ppm; <sup>13</sup>C NMR (101 MHz, DMSO-*d*<sub>6</sub>) δ 167.57, 158.28, 156.90, 144.46, 137.67, 137.53, 137.39, 136.13, 129.65, 129.52, 129.37, 124.42, 123.50, 120.37, 120.26, 116.52, 116.36, 107.19, 105.92, 61.47, 59.27, 56.66 (d, *J* = 36.6 Hz), 55.58, 50.50, 48.71 (d, *J* = 39.5 Hz), 46.16 (d, *J* = 18.9 Hz), 36.71 (d, *J* = 29.5 Hz), 35.54 (d, *J* = 154.1 Hz) ppm; HRMS (ESI+) calcd. for C<sub>28</sub>H<sub>30</sub>N<sub>5</sub>O<sub>3</sub> [M+H]<sup>+</sup>: 484.2343, found: 484.2332; UPLC: t<sub>r</sub> = 3.98 min (99.1 % at 254 nm).

*N*-(3-Aminopropyl)-4-(4-(((7-methoxynaphthalen-2-yl)oxy)methyl)-1*H*-1,2,3-triazol-1-yl)benzamide (10e)

Compound **10e** was prepared according to General procedure B using TFA as a reagent and **8e** (0.050 g, 0.094 mmol) as starting material. The product was purified by flash column chromatography using DCM:MeOH:NH<sub>4</sub>OH = 9:1:0.1 as the mobile phase to yield a clean product **10e**. Yield: 92 % (37 mg); white solid; <sup>1</sup>H NMR (400 MHz, DMSO-*d*<sub>6</sub>) δ 9.10 (s, 1 H), 8.69 (t, *J* = 5.5 Hz, 1 H), 8.05 (s, 4 H), 7.80 – 7.71 (m, 2 H), 7.46 (d, *J* = 2.5 Hz, 1 H), 7.25 (d, *J* = 2.5 Hz, 1 H), 7.06 (dd, *J*<sub>1</sub> = 8.9 Hz, *J*<sub>2</sub> = 2.5 Hz, 1 H), 7.01 (dd, *J*<sub>1</sub> = 8.9 Hz, *J*<sub>2</sub> = 2.6 Hz, 1 H), 5.35 (s, 2 H), 3.87 (s, 3 H), 2.60 (t, *J* = 6.6 Hz, 2 H), 1.91 – 1.54 (m, 4 H) ppm; <sup>13</sup>C NMR (101 MHz, DMSO-*d*<sub>6</sub>) δ 164.94, 157.81, 156.44, 144.08, 138.19, 135.66, 134.55, 129.18, 129.05, 128.86, 123.96,

123.01, 119.67, 116.06, 115.88, 106.72, 105.46, 61.02, 55.11, 37.23, 32.85 ppm; HRMS (ESI+) za C<sub>24</sub>H<sub>26</sub>N<sub>5</sub>O<sub>3</sub> [M+H]<sup>+</sup>: calcd. for 432.2030, found 432.2018; UPLC: t<sub>r</sub> = 4.57 min (98.3 % at 254 nm).

*N*-(4-(4-(((7-Methoxynaphthalen-2-yl)oxy)methyl)-1*H*-1,2,3-triazol-1-yl)phenyl)piperidine-4-carboxamide (10f)

Compound **10f** was prepared according to General procedure B using TFA as a reagent and **9a** (0.060 g, 0.11 mmol) as starting material. The product was purified by flash column chromatography using DCM:MeOH:NH<sub>4</sub>OH = 9:1:0.1 as the mobile phase to yield a clean product **10f**. Yield: 65 % (32 mg); white solid; <sup>1</sup>H NMR (400 MHz, DMSO-*d*<sub>6</sub>) δ 10.12 (s, 1 H), 8.92 (s, 1 H), 7.88 – 7.80 (m, 4 H), 7.77 – 7.71 (m, 1 H), 7.45 (d, *J* = 2.5 Hz, 1 H), 7.24 (d, *J* = 2.5 Hz, 1 H), 7.05 (dd, *J*<sub>1</sub> = 8.9 Hz, *J*<sub>2</sub> = 2.5 Hz, 1 H), 7.01 (dd, *J*<sub>1</sub> = 8.9 Hz, *J*<sub>2</sub> = 2.5 Hz, 1 H), 5.32 (s, 2 H), 3.87 (s, 3 H), 3.04 – 2.97 (m, 2 H), 1.75 – 1.68 (m, 2 H), 1.61 – 1.47 (m, 2 H) ppm, the remaining 3 aliphatic protons are covered by solvent; <sup>13</sup>C NMR (101 MHz, DMSO-*d*<sub>6</sub>) δ 174.00, 157.82, 156.48, 143.68, 139.83, 135.68, 131.51, 129.18, 129.06, 123.95, 122.74, 120.73, 119.80, 116.04, 115.91, 106.69, 105.46, 61.04, 55.12, 45.37, 43.49, 29.11 ppm; HRMS (ESI+) calcd. for C<sub>26</sub>N<sub>28</sub>N<sub>5</sub>O<sub>3</sub> [M+H]<sup>+</sup>: 458.2186, found: 458.2173; UPLC: t<sub>r</sub> = 4.06 min (99.7 % at 254 nm).

3-Amino-*N*-(4-(4-(((7-methoxynaphthalen-2-yl)oxy)methyl)-1*H*-1,2,3-triazol-1-yl)phenyl)bicyclo[1.1.1]pentane-1-carboxamide (10g)

Compound **10g** was prepared according to General procedure B using TFA as a reagent and **9b** (0.060 g, 0.11 mmol) as starting material. The product was purified by flash column chromatography using DCM:MeOH:NH<sub>4</sub>OH = 9:1:0.1 as the mobile phase to yield a clean product **10g**. Yield: 68 % (33 mg); yellow solid; <sup>1</sup>H NMR (400 MHz, DMSO-*d*<sub>6</sub>) δ 9.71 (s, 1 H), 8.92 (s, 1 H), 7.90 – 7.80 (m, 4 H), 7.80 – 7.71 (m, 2 H), 7.45 (d, *J* = 2.5 Hz, 1 H), 7.24 (d, *J* = 2.5 Hz, 1 H), 7.05 (dd, *J*<sub>1</sub> = 8.9 Hz, *J*<sub>2</sub> = 2.5 Hz, 1 H), 7.01 (dd, *J*<sub>1</sub> = 8.9 Hz, *J*<sub>2</sub> = 2.5 Hz, 1 H), 5.32 (s, 2 H), 3.87 (s, 3 H), 2.41 – 2.30 (m, 2 H), 2.00 (s, 6 H) ppm; <sup>13</sup>C NMR (101 MHz, DMSO-*d*<sub>6</sub>) δ 168.86, 157.82, 156.48, 143.70, 139.32, 135.68, 131.75, 129.19, 129.07, 123.96, 122.73, 120.59, 120.47, 116.05, 115.92, 106.71, 105.47, 61.05, 55.12, 54.33, 48.89, 35.59; HRMS (ESI+) calcd. for C<sub>26</sub>H<sub>26</sub>N<sub>5</sub>O<sub>3</sub> [M+H]<sup>+</sup>: 456.2030, found: 456.2014; UPLC: t<sub>r</sub> = 4.00 min (99.5 % at 254 nm).

*N*-(4-(4-(((7-Methoxynaphthalen-2-yl)oxy)methyl)-1*H*-1,2,3-triazol-1-yl)phenyl)azetidine-3-carboxamide (10h)

Compound **10h** was prepared according to General procedure B using TFA as a reagent and **9c** (0.050 g, 0.094 mmol) as starting material. The product was purified by flash column chromatography using DCM:MeOH:NH<sub>4</sub>OH = 9:1:0.1 as the mobile phase to yield a clean product **10h**. Yield: 65 % (26 mg); white solid; <sup>1</sup>H NMR (400 MHz, DMSO-*d*<sub>6</sub>) δ 10.22 – 10.07 (m, 1 H), 8.92 (s, 1 H), 7.89 – 7.79 (m, 4 H), 7.78 – 7.73 (m, 2 H), 7.45 (d, *J* = 2.6 Hz, 1 H), 7.24 (d, *J* = 2.6 Hz, 1 H), 7.05 (dd, *J*<sub>1</sub> = 8.9 Hz, *J*<sub>2</sub> = 2.5 Hz, 1 H), 7.01 (dd, *J*<sub>1</sub> = 8.9 Hz, *J*<sub>2</sub> = 2.5 Hz, 1 H), 5.32 (s, 2 H), 3.87 (s, 3 H), 3.76 (t, *J* = 7.0 Hz, 2 H), 3.60 (p, *J* = 7.4 Hz, 1 H), 3.51 (t, *J* = 7.6 Hz, 2 H) ppm; <sup>13</sup>C NMR (101 MHz, DMSO-*d*<sub>6</sub>) δ 171.50, 157.82, 156.48, 143.69, 139.58, 135.67, 131.65, 129.17, 129.05, 123.95, 122.75, 120.81, 119.90, 116.04, 115.91, 106.69, 105.46, 61.04, 55.11, 54.73, 48.67 ppm; HRMS (ESI+) calcd. for C<sub>24</sub>H<sub>24</sub>N<sub>5</sub>O<sub>3</sub> [M+H]<sup>+</sup>: 430.1873, found: 430.1861; UPLC: t<sub>r</sub> = 3.97 min (98.7 % at 254 nm).

3-Amino-*N*-(4-(4-(((7-methoxynaphthalen-2-yl)oxy)methyl)-1*H*-1,2,3-triazol-1-yl)phenyl)propenamide (10i)

Compound **10i** was prepared according to General procedure B using TFA as a reagent and **9d** (0.060 g, 0.12 mmol) as starting material. The product was purified by flash column chromatography using DCM:MeOH:NH<sub>4</sub>OH = 9:1:0.1 as the mobile phase to yield a clean product **10i**. Yield: 92 % (37 mg); white solid; <sup>1</sup>H NMR (400 MHz, DMSO-*d*<sub>6</sub>) δ 10.30 (s, 0 H), 7.87 – 7.78 (m, 4 H), 7.78 – 7.70 (m, 2 H), 7.45 (d, *J* =

2.6 Hz, 1 H), 7.05 (dd,  $J_1 = 8.9$  Hz,  $J_2 = 2.5$  Hz, 1 H), 7.01 (dd,  $J_1 = 8.9$  Hz,  $J_2 = 2.5$  Hz, 1 H), 5.32 (s, 2 H), 3.87 (s, 3 H), 2.86 (t,  $J = 6.5$  Hz, 2 H), 2.43 (t,  $J = 6.5$  Hz, 2 H), 2.01 (s, 2 H) ppm;  $^{13}\text{C}$  NMR (101 MHz, DMSO- $d_6$ )  $\delta$  170.93, 157.82, 156.48, 143.68, 139.66, 135.68, 131.52, 129.18, 129.06, 123.95, 122.75, 120.79, 119.76, 116.04, 115.91, 106.69, 105.46, 61.05, 55.11, 38.07 ppm; HRMS (ESI+) calcd. for  $\text{C}_{24}\text{H}_{26}\text{N}_5\text{O}_3$   $[\text{M}+\text{H}]^+$ : 432.2030, found: 432.2018; UPLC:  $t_r = 3.92$  min (98.3 % at 254 nm).

#### 4.2. Lipophilicity, drug-plasma proteins binding, and phospholipids affinity assays

All measurements were carried out using protocols proposed by Valko and co-workers [33,34] and adopted in our laboratory [62–64]. Briefly, these methods offered the determination of Chromatographic Hydrophobicity Index (CHI) indices and % of plasma protein binding (% PPB) using one gradient elution experiment and comparison to reference substances. Each chromatographic experiment was carried out using the Prominence-1 LC-2030 C 3D HPLC system (Shimadzu, Japan) controlled by LabSolution system (version 5.90 Shimadzu, Japan). During the study, three chromatographic columns varied in terms of chemical modification of stationary phases were applied:

- IAM.PC.DD2 (10 × 4.6 mm × 10.0  $\mu\text{m}$  with a guard column; Regis Technologies; USA);
- $\text{C}_{18}$  Hypersil GOLD™ (50 mm × 4.6 mm; 5.0  $\mu\text{m}$  with a guard column; Thermo Scientific, USA);
- Chiralpak® HSA (100 × 4 mm; 5  $\mu\text{m}$  with safety guard column; Daicel Chiral Technologies, USA)

The reference substances for calibration of HSA,  $\text{C}_{18}$ , and IAM columns were purchased, respectively: acetanilide, butyphenone, diclofenac and octanophenone (Alfa Aesar, Haverhill, USA); acetophenone, benzimidazole, colchicine, indole, indomethacin, paracetamol and theophylline (Sigma-Aldrich, Steinheim, Germany); nicardipine and nizatidine (Cayman Chemical, Michigan, USA); carbamazepine, heptanophenone, hexanophenone, propiophenone and valerophenone (Acros Organic, Pittsburg, USA). For all measurements, mobile phase A was a water solution of 50 mM ammonium acetate (VWR International, Leuven, Belgium) adjusted to pH 7.4 with concentrated ammonia solution (Avantor Performance Materials Poland S.A., Gliwice, Poland). Ultrapure water to a resistivity of 18.2 M $\Omega$  was obtained from a Milli-Q water purification system (Merck Millipore, Darmstadt, Germany). For measurements of phospholipids binding, mobile phase B was HPLC-grade acetonitrile (Chempur, Piekary Śląskie, Poland) with the linear gradient from 0 % to 85 % B in 5.25 min was applied and then held at 85 % ACN for 0.5 minutes. The mobile phase flow rate was 1.5 mL/min and IAM.PC.DD2 column was maintained at 30 °C. For lipophilicity measurements, solvents, and flow rate were the same as in the case of IAM chromatography. The  $\text{C}_{18}$  Hypersil GOLD™ column was maintained at a temperature of 40 °C. Similarly, from 0 to 5.25 min, the linear gradient was applied, but in this case, from 2 % to 98 % ACN and held maximum phase B concentration for 1.75 minutes. For determination of %PPB binding, HPLC grade isopropanol (VWR International, Leuven, Belgium) was used as a mobile phase B. For the first 15 minutes, the linear gradient from 0 % to 20 % isopropanol was applied and then held at 20 % isopropanol for 12 minutes. In the last 5 minutes of the sequence, the mobile phase mixture returned to pure ammonium acetate solution. The column temperature was held at 30 °C, whereas the flow rate was 0.9 mL/min. Before chromatographic experiments, solutes were dissolved in dimethyl sulfoxide (Avantor Performance Materials Poland S.A., Poland) to obtain a 200  $\mu\text{g}/\text{mL}$  concentration. The detection was performed in the UV region at the wavelength from 190 nm to 300 nm. The injected volume was 5  $\mu\text{L}$ , and each compound was analysed at triplicate. Retention times for studied molecules and reference standards are collected in [supplementary materials](#), Table 2S and 3S.

#### 4.3. Molecular modelling

##### 4.3.1. Molecular docking

The Hsp90 $\beta$  C-terminal domain binding site at the dimer interface (PDB entry: 5FWK) was created using MAKE RECEPTOR (Release 4.1.0.1, OpenEye Scientific Software, Inc., Santa Fe, NM, USA; [www.eyesopen.com](http://www.eyesopen.com)). The grid box with dimensions 21.7 Å × 24.7 Å × 16.0 Å and the volume of 8551 Å<sup>3</sup> was generated around the Hsp90 CTD inhibitor [65]. For “Cavity detection”, the “Molecular” method was used. The outer contours of the binding site were calculated with the “Balanced” settings. Libraries of conformers of compounds **C** and **5x** were generated using OMEGA software (Release 4.2.2.1, OpenEye Scientific Software, Inc., Santa Fe, NM, USA; [www.eyesopen.com](http://www.eyesopen.com)) [66] using default settings. The OMEGA library of ligand conformers was then rigidly docked to the Hsp90 CTD using FRED (OEDOCKING 4.2.1.1: OpenEye Scientific Software, Santa Fe, NM, USA. <http://www.eyesopen.com>) [67,68] with the default settings. Ten docking poses per compound were visualised and analysed with VIDA (version 5.0.4.0, OpenEye Scientific Software, Inc., Santa Fe, NM, USA, [www.eyesopen.com](http://www.eyesopen.com)).

##### 4.3.2. Molecular dynamics simulations

MD simulation of Hsp90 $\beta$  dimer in complex with compound **5x** was performed using NAMD package (version 3.0) [69] and the CHARMM36m [70] force field. Parameters for molecular mechanics calculations for compound **5x** were estimated using the ParamChem tool [71–73]. Removal of potential steric clashes and optimisation of the atomic coordinates of the Hsp90 $\beta$ -**5x** complex were performed by 10,000 steps of steepest descent and adopted basis Newton–Raphson energy minimisations. Psfgen in VMD (version 1.9.1.) was used to prepare the system for MD simulation [74]. Structure of the Hsp90 $\beta$ -**5x** complex was embedded in a box of TIP3P water molecules and neutralised by addition of KCl. The MD simulation was run in the NPT ensemble using the periodic boundary conditions. Temperature (300 K) and pressure (1 atm) were controlled using the Langevin dynamics and Langevin piston methods, respectively. Short-range and long-range forces were calculated every 1 and 2 time steps, respectively, with a time step of 2.0 ps. The smooth particle mesh Ewald method was used to calculate the electrostatic interactions [75]. The short-range interactions were cut off at 12 Å. All of the chemical bonds between hydrogen and the heavy atoms were held fixed using the SHAKE algorithm [76]. The simulation consisted of three consecutive steps: (i) solvent equilibration for 1 ns with ligand and protein constrained harmonically around the initial structure; (ii) equilibration of the complete system for 1 ns with ligand and protein released; and (iii) an unconstrained 500 ns production run. The MD simulation was repeated twice.

##### 4.3.3. Structure-based pharmacophore modelling

For structure-based pharmacophore modelling, 2500 frames from the production run of Hsp90 $\beta$ -**5x** MD trajectory run were saved separately and used for interaction analysis. The MD trajectory was then used for pharmacophore feature analysis using LigandScout 4.5 Expert [77], which resulted in 2500 structure-based pharmacophore models.

#### 4.4. Protein expression and purification

##### 4.4.1. Full-length Hsp90 $\alpha$ and Hsp90 $\beta$ expression and purification

For the protein expression of full-length Hsp90 $\alpha$  and Hsp90 $\beta$ , plasmids were kindly gifted to us by dr. Asta Zubrienė, Institute of Biotechnology, Vilnius University, Lithuania. Both proteins, including N-terminal 6×His-tags, were expressed in *Escherichia coli* strain BL21 (DE3). The cells were grown in TB media at 37 °C, and protein expression was achieved by induction with 0.5 mM isopropyl  $\beta$ -D-1-thiogalactopyranoside (IPTG) at OD<sub>600</sub> = 0.8. The induction was followed by an 18 h incubation at 18 °C. Afterwards the cells were harvested by centrifugation. They were then resuspended in lysis buffer that comprised 40 mM potassium phosphate pH 8.0, 400 mM KCl, 10 mM



imidazole and protease inhibitors (Sigma). They were additionally lysed by sonication. Following the centrifugation, proteins were first purified with a Ni<sup>2+</sup>-affinity HisTrap column (GE Healthcare). To wash away the impurities the lysis buffer containing 20–40 mM imidazole was used, then Hsp90 was eluted with lysis buffer containing 300 mM imidazole. Next the purification was continued by SEC with a Superdex-200 (16/600) column (GE Healthcare) and running buffer (50 mM Tris pH 7.5 at RT, 300 mM KCl). The purity of the fractions was assessed by SDS-PAGE and then they were concentrated. Hsp90 $\alpha$  and Hsp90 $\beta$  were then dialysed against NMR buffer (50 mM potassium phosphate pD 7.5, 100 mM KCl, 1 mM DTT (98 %, D10) in D<sub>2</sub>O) and frozen in liquid nitrogen.

#### 4.4.2. Expression and purification of the Hsp90 $\alpha$ and Hsp90 $\beta$ N-terminal domains

The plasmid encoding for the N-terminal domains of Hsp90 $\beta$  and Hsp90 $\alpha$  (Hsp90 $\beta$  NTD and Hsp90 $\alpha$  NTD) were constructed by inserting the DNA sequence encoding the NTD of human Hsp90 $\beta$  (corresponding to amino acids 1–239) or Hsp90 $\alpha$  (corresponding to amino acids 1–241) into the pET21b vector (Novagen, Madison, WI, USA). The resulting protein constructs also included an N-terminal 6 $\times$ His tag with a thrombin cleavage site. The Hsp90 NTDs were then expressed in *Escherichia coli* BL21 (DE3) strain. Bacterial cultures transformed by the plasmid were grown in shaker flasks in LB media supplemented with ampicillin until OD<sub>600</sub> of 0.6 at 37 °C. Then temperature was reduced to 30 °C and target protein expression was induced by the addition of 1 mM IPTG. 4 hours post-induction, bacteria were centrifuged and resuspended in buffer that comprised 25 mM Tris-HCl, 100 mM NaCl, 100 mM imidazole, pH 7.5. The bacteria were lysed by sonication. Protein was purified from the soluble fraction using a Ni-IDA immobilized metal affinity column (Cytiva) followed by Q-Sepharose anion-exchange column (Cytiva). SDS-PAGE analysis determined protein purity to be higher than 95 %. Protein concentrations were determined by UV-VIS spectrophotometry.

#### 4.5. Ligand-observed protein NMR studies

High-resolution NMR spectra were acquired with the Bruker Avance Neo 600 MHz spectrometer, using cryoprobe, at 25 °C. Data was collected using the pulse sequences provided by the Bruker library of pulse programs and analysed using Bruker Topspin 4.2.0. The residual water signal was suppressed by excitation sculpting [78] with 2 ms selective pulse and a T<sub>1</sub> $\rho$  filter of 100 ms was used to eliminate the background protein resonances. The <sup>1</sup>H spectral widths were 5882 Hz. NMR samples were prepared in a buffer of 50 mM potassium phosphate (pD 7.5), 100 mM KCl in D<sub>2</sub>O, complemented with 5 mM MgSO<sub>4</sub>, 2 mM DTT-d<sub>10</sub>, 0.02 % NaN<sub>3</sub>, and 2 % DMSO-d<sub>6</sub>. Full assignment of protons (Supplementary information Fig. 9S-10S and Tables 4–7S) was achieved by a combination of TOCSY, NOESY, ROESY, and HSQC spectra. The <sup>1</sup>H STD spectra were recorded at a protein:ligand ratio of 1:100. The protein concentration was 1  $\mu$ M and the ligand concentration was 0.1 mM.

The <sup>1</sup>H STD ligand epitope mapping experiments [79] were performed with 65,536 data points (5.57 s acquisition time), a relaxation delay of 1.63 s, and 4400 (5x) and 5840 (10b) scans. The short protein saturation time of 0.5 s was used to avoid the influence of relaxation on the STD amplification factors [80]. In the case of 5x, the saturation time was increased to 1 s to reduce the errors of STD amplification factors for individual protons to below 10 %. Selective on-resonance saturation of Hsp90 $\beta$  was performed at – 0.827 ppm with a transmitter offset referenced to 4.70 ppm. The off-resonance irradiation was applied at 30 ppm for the reference spectrum. The spectra were zero-filled and apodized with an exponential line-broadening function of 3 Hz. Errors in the STD amplification factor were estimated according to the formula [81]:

STD amplification factor absolute error

$$= \text{STD amplification factor} \times \left[ \left( \frac{N_{\text{STD}}}{I_{\text{STD}}} \right)^2 + \left( \frac{N_{\text{REF}}}{I_{\text{REF}}} \right)^2 \right]^{\frac{1}{2}}$$

N<sub>STD</sub> and N<sub>REF</sub> are noise levels in STD and reference spectra. I<sub>STD</sub> and I<sub>REF</sub> are signal intensities in STD and reference spectra. The relative errors of the STD amplification factors for all protons are below 4 % (5x) and 7 % (10b).

#### 4.6. Hsp90 C-terminal domain binding TR-FRET (time-resolved fluorescence resonance energy transfer) assay

The TR-FRET kit for evaluating the binding to Hsp90 $\beta$  and Hsp90 $\alpha$  C-terminal domain was acquired from BPS Bioscience (San Diego, CA, USA). The kit measures the protein-protein interaction among the CTD of Hsp90 and cyclophilin D which can be blocked by C-terminal Hsp90 inhibitors. The assay was performed according to the manufacturer's instructions as follows. Consequently terbium-labelled donor, dye-labelled acceptor, Hsp90 $\beta$  C-terminal domain or Hsp90 $\alpha$  C-terminal domain, PPID and respective newly prepared compound or novobiocin a known inhibitor of the C-terminal domain of Hsp90. For positive control assay buffer was in place of inhibitor solution while negative control contained no Hsp90-interacting protein PPID. Both samples and controls were prepared in duplicates. After everything was added the solutions were incubated for 2 h at room temperature. Following the incubation, time-resolved fluorescence resonance energy transfer (TR-FRET) was measured using Tecan's Spark Multimode Microplate reader (Tecan Trading AG, Switzerland). The results are obtained as percentages of residual Hsp90 CTD activity which was calculated by the following equation: %Activity = 100  $\times$  (FRET<sub>sample</sub> – FRET<sub>negative control</sub>) / (FRET<sub>positive control</sub> – FRET<sub>negative control</sub>). In this formula FRET value is the ratio between dye-acceptor emission and Tb-donor emission.

#### 4.7. Microscale thermophoresis

The full-length Hsp90 $\beta$  and Hsp90 $\alpha$  were labeled with the Monolith His-Tag Labeling Kit RED-tris-NTA according to the manufacturers labeling instructions (NanoTemper Technologies GmbH, Munich, Germany). The protein was first diluted to 8 nM concentration by the assay buffer (50 mM Tris-HCl, pH 7.4 containing 150 mM NaCl, 5 % EtOH and 10 mM MgCl<sub>2</sub>). To determine the K<sub>d</sub> values, the protein was mixed with the solution of the compound in question in a ratio 1:1. The final concentration of Hsp90 $\beta$  was 4 nM and compounds were added as follows: 300  $\mu$ M – 18.75  $\mu$ M for 5x; 625  $\mu$ M – 7.8 for 5s; 5 mM – 0.00031 mM for novobiocin. The final concentration of Hsp90 $\alpha$  was 4 nM and compounds were added as follows: 275  $\mu$ M – 18.75  $\mu$ M for 5x and 10 mM – 0.00031 mM for novobiocin. At higher concentrations of the compounds, aggregation was observed due to insufficient solubility, therefore these measurements were disregarded (MST curves colored in grey). The compounds were incubated with the protein for 15 minutes in the dark at room temperature. The mixtures were then inserted into Monolith NT.115 Premium Capillaries (NanoTemper Technologies GmbH, Munich, Germany). Thermophoresis of each mixture was induced at 1475  $\pm$  15 nm and measured using a Monolith NT.115 pico instrument (NanoTemper Technologies GmbH, Munich, Germany). The temperature of the measurement was kept at ambient temperature (24–25 °C), the excitation power was set to 20 %, while the MST power was set to 40 % with 5 second laser on time). Two independent K<sub>d</sub> determinations were performed for both compounds. The average fluorescence responses for each concentration were then plotted against the logarithm of compound concentration using GraphPad Prism software (GraphPad Software, Inc. La Jolla, CA).

#### 4.8. Luciferase refolding assay in PC3-MM2luc cell line

Luciferase Refolding Assay was carried out in PC3-MM2luc cells expressing firefly luciferase. Cells were grown to 80 % confluency and then harvested. Cell pellets were suspended in prewarmed medium (50 °C) for 2 min to induce firefly luciferase unfolding. The cells were plated in 96-well plates at a density of 50,000 cells per well in the presence of

selected compounds, vehicle control (1 % DMSO) or positive control (50  $\mu$ M 17-DMAG). The plates were incubated for 60 min at 37 °C to allow for luciferase refolding. After incubation 100  $\mu$ L of ONE-Glo™ Luciferase Assay System (Promega, Madison, WI, USA) was added to each well of the plate and incubated for another 5 min. Luciferase activity was determined by measuring luminescence with Tecan's Spark Multimode Microplate reader (Tecan Trading AG, Switzerland). Independent experiments were repeated two times, each performed in triplicate. IC<sub>50</sub> values (concentration of the inhibitor that gives a half-maximal response) are given as average values from the independent measurements, and were determined using GraphPad Prism 9.2.0 software (San Diego, CA, USA).

#### 4.9. Fluorescence-based thermal shift assay with the Hsp90 $\beta$ NTD

Compound binding to Hsp90 $\beta$  and Hsp90 $\alpha$  N-terminal domain was determined by the fluorescence-based thermal shift assay (FTSA) which determines the thermal stability of the free and ligand-bound protein. The experiments were performed using Rotor-Gene Q 6-Plex spectrofluorimeter (excitation 365 nm, detection 460 nm). Solutions containing 10  $\mu$ M of protein and various concentrations of ligand (0–500  $\mu$ M) were heated up from 25 °C to 80 °C at a rate of 1 °C/min. Protein unfolding was detected using 8-anilino-1-naphthalenesulphonate fluorescent dye at 100  $\mu$ M concentration. Experiments were carried out in a buffer composed of 50 mM sodium phosphate, 100 mM sodium chloride, 2 % DMSO, pH 7.5. Fitting of melting curves ( $T_m$  values) were performed using Thermott [82].

#### 4.10. Cell Culture

Six different cell lines were cultured in order to perform all the experiments: hormone positive breast cancer cell line MCF-7 (ATCC-HTB-22; ATCC), Ewing sarcoma cell line SK-N-MC (a kind gift from Beat Schäfer), hepatocellular carcinoma cell line Hep-G2 (ATCC-HB-8065, ATCC), colorectal carcinoma cell line HCT-116 (ATCC-CCL-247), glioblastoma multiforme cell line U-251 (a kind gift from Dr. Marijeta Kralj), and embryonic kidney cells HEK-293 T (ATCC-CRL-3216). All cell lines were cultured as monolayers and maintained in DMEM (Sigma – Aldrich, St. Louis, MO, USA) for MCF-7, HepG2, HCT116 and Hek293T or RPMI 1640 (Sigma – Aldrich, St. Louis, MO, USA) for SK-N-MC and U251. Both medium types were additionally supplemented with 10 % heat inactivated fetal bovine serum albumin, 100 U/mL penicillin, and 100  $\mu$ g/mL streptomycin and the cells were grown in a humidified atmosphere containing 5 % CO<sub>2</sub> at 37 °C.

#### 4.11. Cell viability assay MTS and MTT

MTS assay was used to determine the antiproliferative activity of the prepared compounds on SK-N-MC and MCF-7 cell lines. Reagent 3-(4,5-dimethylthiazol-2-yl)-2,5-diphenyltetrazolium bromide (MTS) used in the test was purchased from Promega (Madison, WI, USA) and the experiments were carried out according to the manufacturer's instructions [23].

Meanwhile, MTT assay was used to determine the antiproliferative activity of the prepared compounds on HepG2, HCT-116, U-251 and Hek-293T cell lines. Reagent 3-(4,5-dimethylthiazol-2-yl)-2,5-diphenyltetrazolium bromide (MTT) used in the test was purchased from Abcam (Cambridge, MA, USA) and the experiments were carried out according to the manufacturer's instructions [83].

More details on both protocols for cell viability assays can be found in [Supplementary information](#).

#### 4.12. Apoptosis assay

Apoptosis of MCF-7 and SK-N-MC cells was assessed by detection of phosphatidylserines, by R-phycoerythrin – Annexin V conjugate (R-PE

Annexin V; Invitrogen, Carlsbad, CA, USA) and nucleic acids in dead cells by SYTOX Blue Dead Cell Stain (Invitrogen, Carlsbad, CA, USA), following manufacturer instructions. Briefly, 250,000 MCF-7 or SK-N-MC cells were seeded in a six-well plate. After 24 h, cells were washed with PBS and treated with 7–70  $\mu$ M 5x for 24–72 hours. Next, the medium with detached cells was collected and the attached cells were harvested and merged with the cells from the medium. After two washing steps with cold PBS, cells were resuspended in a 100  $\mu$ L annexin-binding buffer (Invitrogen, Carlsbad, CA, USA) containing 2.5  $\mu$ L R-PE Annexin V solution and 750 nM SytoxBlue and incubated in the dark for 15 minutes at room temperature. Before the measurement, 200  $\mu$ L of annexin-binding buffer was added. A minimum of 10,000 events were collected with a flow cytometer (Attune NxT; Invitrogen, Carlsbad, CA, USA). Annexin V (ANV)-/SYTOX Blue (SB)- indicates viable cells that are not undergoing apoptosis, ANV+/SB- indicates early apoptotic or proapoptotic cells, ANV+/SB+ indicates late apoptotic cells, and ANV-/SB+ indicates necrotic cells.

#### 4.13. Cell cycle assay

The cell cycle analysis was performed using propidium iodide (PI, Sigma-Aldrich, St. Louis, MO, USA). 250,000 MCF-7 or SK-N-MC cells were seeded in a six-well plate. After 24 h, cells were washed with PBS and treated with 7–70  $\mu$ M 5x for 24–72 hour. Next, the medium with detached cells was collected and the attached cells were harvested and merged with the cells from the medium. Cells were washed twice with PBS. Next, cells were fixed and permeabilized by 15-minute incubation with ice-cold 85 % ethanol at –20 °C and rehydrated with PBS at room temperature. Cells were then incubated in 500  $\mu$ L of PI-binding buffer containing 1  $\mu$ M PI and 1 mg/mL Ribonuclease A (Qiagen, Hilden, Germany) in the dark for 15 minutes at room temperature. Finally, a minimum of 10,000 events were collected with a flow cytometer (Attune NxT; Invitrogen, Carlsbad, CA, USA).

#### 4.14. Western blot

The treatment of MCF-7 cells was carried out with 25  $\mu$ M, 10  $\mu$ M and 2  $\mu$ M of compound 5x, 1000  $\mu$ M, 500  $\mu$ M and 100  $\mu$ M of novobiocin, 0.5  $\mu$ M of 17-DMAG or 0.5 % DMSO. The cells were incubated for 24 h and were rinsed with 1  $\times$  DPBS (Gibco, Thermo Fisher Scientific, Waltham, MA, USA) after the incubation. Then the cells were lysed using RIPA buffer which consisted of 50 mM Tris-HCl pH 7.4, 150 mM NaCl, 1 % NP-40, 0.5 % sodium deoxycholate, 1 mM EDTA, containing 1:100 Halt™ Protease Inhibitor Cocktail (Thermo Fisher Scientific, Waltham, MA, USA) and 1:100 Halt™ Phosphatase Inhibitor Cocktail (Thermo Fisher Scientific, Waltham, MA, USA). The lysates were then frozen for the minimal amount of 24 hours. Afterwards they were thawed and sonicated and then centrifuged at 15,000 rpm for 20 min at 4 °C. For further work, only supernatants were collected. From the supernatants protein concentration was measured using DC protein assay (Bio-Rad, Hercules, California, USA). Isolated proteins (20  $\mu$ g) were then separated using SDS PAGE (10 % acrylamide/bisacrylamide gel). Electrophoresis was performed at 80 V for 15 min and afterwards at 130 V for 60 min. After the separation a transfer onto PVDF membrane was carried out using iBlot 3 Dry Blotting System (Thermo Fisher Scientific, Waltham, MA, USA). The membranes were first exposed to 5 % BSA for 1 h at room temperature to block nonspecific binding sites. Then the membranes were incubated with solutions of primary antibodies at 4 °C for overnight duration. Primary antibodies that were used in the experiments encompassed anti-Hsp90 Rabbit mAb (1:1000), anti-Hsp70 Mouse mAb (1:1000), anti-GAPDH Rabbit mAb (1:2500), anti-IGF1R Rabbit (1:1000), anti-MEK Rabbit (1:1000), ERK Rabbit mAb (1:1000), anti ER $\alpha$  Rabbit mAb (1:1000). All antibodies were acquired from Cell Signaling (Danvers, MA, USA). For detection, the membranes were incubated with secondary antibodies for 1 h at room temperature. anti-rabbit IgG, HRP-linked antibody (1:10000) and anti-mouse IgG,

Hrp-linked antibody (1:10000) were used as secondary antibodies (these were also acquired from Cell Signaling, Danvers, MA, USA). After washing, the SuperSignal™ West Femto Maximum Sensitivity Substrate was added (Thermo Fisher Scientific, Waltham, MA, USA). The blots were then visualized by UVITEC Cambridge Imaging System (UVITEC, Cambridge, UK). For quantification densitometric analysis of western blot bands was performed. This was done by NineAlliance software. GAPDH was used as a loading control and the relative densities were calculated in relation to this protein.

#### 4.15. *In vivo* efficacy study and NOEC determination in zebrafish larvae

For determination of NOEC mitfa<sup>b692/b692</sup>; ednrba<sup>b140/b140</sup> zebrafish larvae were raised until 2 days post fertilization (dpf) at 28 °C and then kept at 34 °C similar to the actual xenotransplantation procedure. At 3 dpf larvae were transferred into a 12-well plate (8–12 per well) (VWR, Avantor, Cat No. 10062–894) and treated with different concentrations of compounds as indicated. To increase solubility and to have comparable controls, DMSO concentrations were maintained at equal levels in all wells (1 %). For final compound concentrations, the respective amounts of 5x from 10 mM stock solution were pre-diluted in DMSO, mixed with E3 larvae medium to a volume of 0.5 mL that was then added to 1 mL E3 per well containing the allotted fish larvae. Survival rate and potential aberrations in development were documented on 4 and 5 dpf after visual inspection. Experiments were conducted twice in technical triplicates.

For transplantation embryos from mitfa<sup>b692/b692</sup>; ednrba<sup>b140/b140</sup> strains were raised until 2 dpf at 28 °C, dechorionated, and anesthetised using 1x Tricaine (0.16 g/l Tricaine, Sigma-Aldrich Chemie GmbH, Germany, Cat No. E1052110G, adjusted to pH 7 with 1 M Tris pH 9.5 in E3). Anesthetized larvae were positioned on a petri dish lid coated with solidified 2 % agarose, as previously described [84], for transplantation. For tumour cell injection, borosilicate glass capillaries (GB100T-8 P, without filament, Science Products GmbH, Germany) pulled with a needle puller (P-97, Sutter Instruments, USA) were utilised. Ewing sarcoma cells were harvested and resuspended to a concentration of 100 cells/nL in PBS. Approximately 5 µL of tumour cell suspension was loaded into the needles, which were then attached to a micromanipulator (M3301R, World Precision Instruments Inc., Germany) and connected to a microinjector (FemtoJet 4i, Eppendorf, Germany). Ewing sarcoma cells were injected into the perivitelline space (PVS) of zebrafish larvae. Xenotransplanted larvae were screened at 2 hours post-injection (hpi) to identify those displaying exclusively tumour cells in the PVS, and subsequently, these larvae were maintained at 34 °C.

For automated imaging, larvae were anesthetised using 1x Tricaine and placed in a 96-well ZF plate (Hashimoto Electronic Industry Co, Japan) containing 0.5 % ultra-low gelling agarose (Sigma-Aldrich Chemie GmbH, Germany, Cat. No. A2576–25 G). Image acquisition was performed using the Operetta CLS high-content imager (Revvity, USA) with a 5x air objective. Images were acquired in brightfield (40 ms and 10 % intensity) and fluorescence for GFP (excitation: 460–490 nm at 100 %, emission: 500–550 nm for 400 ms). A total of 21 planes with a 25 µm spacing were imaged per field. Right after image acquisition larvae were taken out of the imaging plate and placed into the corresponding multi-well plate well. Then a freshly prepared compound/ solvent master mix in E3 was added for a final concentration of 70 µM 5x/ 1 % DMSO or 1 % DMSO as control to the larvae. The experiment was repeated 3 times. Tumour size was quantified using Harmony Software 4.9 (Revvity, USA), with the footprint area of the tumour projected along the z-axis onto the x-y-plane selected for further analysis. Relative change in tumour size was calculated as footprint area at 3 dpi divided by area at 1 dpi.

#### CRediT authorship contribution statement

Asta Zubrienė: Supervision, Investigation. Simona Golič

Grdadolnik: Writing – review & editing, Methodology, Investigation, Funding acquisition. Jaka Dernovšek: Writing – review & editing, Writing – original draft, Visualization, Methodology, Investigation, Conceptualization. Irena Mlinarič-Rašcan: Writing – review & editing, Funding acquisition. Živa Zajec: Writing – review & editing, Visualization, Methodology, Investigation. Goran Poje: Writing – review & editing, Methodology, Investigation. Sarah Grissenberger: Writing – review & editing, Methodology, Investigation. Tihomir Tomašič: Writing – review & editing, Visualization, Supervision, Resources, Methodology, Investigation, Funding acquisition, Formal analysis, Data curation, Conceptualization. Krzesimir Ciura: Writing – review & editing, Methodology, Investigation. Mateusz Woziński: Investigation. Marius Gedgudas: Methodology, Investigation. Zrinka Rajić: Writing – review & editing, Methodology, Investigation. Andrej Emanuel Corman: Writing – review & editing, Investigation. Dunja Urbančič: Writing – review & editing, Visualization, Methodology, Investigation. Nace Zidar: Writing – review & editing, Supervision, Investigation. Caterina Sturtzel: Writing – review & editing, Visualization, Methodology, Investigation. Tjaša Goričan: Writing – review & editing, Visualization, Methodology, Investigation. Martin Distel: Writing – review & editing, Methodology, Investigation, Funding acquisition.

#### Declaration of Competing Interest

The authors declare that they have no known competing financial interests or personal relationships that could have appeared to influence the work reported in this paper.

#### Data Availability

Data will be made available on request.

#### Acknowledgements

This work was supported by the Slovenian Research Agency (Grant No. P1-0208, J1-1717, BI-AT/23-24-008, J1-4400, J1-50038) and the BMBWF through OeAD grant SI 29/2023 (M.D. and T.T.). This research was also supported by the Ministry of Education, Science and Sport (MIZŠ) and the European Regional Development Fund OP20.05187 RISI-EATRIS. K.C. gratefully acknowledges the funding by 2022/47/D/NZ7/01043 from The National Science Centre of Poland, which supported the chromatographic analysis. T.T. acknowledges OpenEye Scientific Software, Santa Fe, NM, for free academic licenses for the use of their software. Jure Lavrič, Zala Kovačič, Kaja Cej, Nataša Šuklje and Monika Smrečnik are acknowledged for their contributions in the synthetic part of the work and Maja Frelj is acknowledged for acquisition of HRMS spectra.

#### Appendix A. Supporting information

Supplementary data associated with this article can be found in the online version at [doi:10.1016/j.biopha.2024.116941](https://doi.org/10.1016/j.biopha.2024.116941).

#### References

- [1] C. Mattiuzzi, G. Lippi, *Current Cancer Epidemiology*, *J. Epidemiol. Glob. Health* 9 (2019) 217–222, <https://doi.org/10.2991/jegh.k.191008.001>.
- [2] P. Jaaks, E.A. Coker, D.J. Vis, O. Edwards, E.F. Carpenter, S.M. Leto, L. Dwane, F. Sassi, H. Lightfoot, S. Barthorpe, D. van der Meer, W. Yang, A. Beck, T. Mironenko, C. Hall, J. Hall, I. Mali, L. Richardson, C. Tolley, J. Morris, F. Thomas, E. Lleshi, N. Aben, C.H. Benes, A. Bertotti, L. Trusolino, L. Wessels, M. J. Garnett, *Effective drug combinations in breast, colon and pancreatic cancer cells*, *Nature* 603 (2022) 166–173, <https://doi.org/10.1038/s41586-022-04437-2>.
- [3] R.B. Mokhtari, T.S. Homayouni, N. Baluch, E. Morgatskaya, S. Kumar, B. Das, H. Yeger, *Combination therapy in combating cancer*, *Oncotarget* 8 (2017) 38022–38043, <https://doi.org/10.18632/oncotarget.16723>.
- [4] D. Shi, F. Khan, R. Abagyan, *Extended Multitarget Pharmacology of Anticancer Drugs*, *J. Chem. Inf. Model.* 59 (2019) 3006–3017, <https://doi.org/10.1021/acs.jcim.9b00031>.



- non-water-soluble HSP90 inhibitor, 17-AAG, in breast cancer cell lines, *Int. J. Mol. Med.* 38 (2016) 1296–1302, <https://doi.org/10.3892/ijmm.2016.2696>.
- [53] M. MORI, T. HITORA, O. NAKAMURA, Y. YAMAGAMI, R. HORIE, H. NISHIMURA, T. YAMAMOTO, Hsp90 inhibitor induces autophagy and apoptosis in osteosarcoma cells, *Int. J. Oncol.* 46 (2014) 47–54, <https://doi.org/10.3892/ijo.2014.2727>.
- [54] C. Peng, F. Zhao, H. Li, L. Li, Y. Yang, F. Liu, HSP90 mediates the connection of multiple programmed cell death in diseases, *Cell Death Dis.* 13 (2022) 1–12, <https://doi.org/10.1038/s41419-022-05373-9>.
- [55] M. Niu, B. Zhang, L. Li, Z. Su, W. Pu, C. Zhao, L. Wei, P. Lian, R. Lu, R. Wang, J. Wazir, Q. Gao, S. Song, H. Wang, Targeting HSP90 Inhibits Proliferation and Induces Apoptosis Through AKT1/ERK Pathway in Lung Cancer, *art.* 724192, *Front. Pharmacol.* 12 (2022), <https://doi.org/10.3389/fphar.2021.724192>.
- [56] S. Terracciano, A. Russo, M.G. Chini, M.C. Vaccaro, M. Potenza, A. Vassallo, R. Riccio, G. Bifulco, I. Bruno, Discovery of new molecular entities able to strongly interfere with Hsp90 C-terminal domain, *Sci. Rep.* 8 (2018) 1709, <https://doi.org/10.1038/s41598-017-14902-y>.
- [57] H.G. Lee, W.J. Park, S.J. Shin, S.H. Kwon, S.D. Cha, Y.H. Seo, J.H. Jeong, J.Y. Lee, C.H. Cho, Hsp90 inhibitor SY-016 induces G2/M arrest and apoptosis in paclitaxel-resistant human ovarian cancer cells, *Oncol. Lett.* 13 (2017) 2817–2822, <https://doi.org/10.3892/ol.2017.5794>.
- [58] P.C. Echeverria, K. Bhattacharya, A. Joshi, T. Wang, D. Picard, The sensitivity to Hsp90 inhibitors of both normal and oncogenically transformed cells is determined by the equilibrium between cellular quiescence and activity, *PLOS ONE* 14 (2019) e0208287, <https://doi.org/10.1371/journal.pone.0208287>.
- [59] F.Z. Zhang, D.H.-H. Ho, R.H.-F. Wong, Triptolide, a HSP90 middle domain inhibitor, induces apoptosis in triple manner, *Oncotarget* 9 (2018) 22301–22315, <https://doi.org/10.18632/oncotarget.24737>.
- [60] C. Sturtzel, S. Grissenberger, P. Bozatzki, E. Scheuringer, A. Wenninger-Weinzierl, Z. Zajec, J. Dernovšek, S. Pascoal, V. Gehl, A. Kutsch, A. Granig, F. Rifatbegovic, M. Carre, A. Lang, I. Valtingoer, J. Moll, D. Lötsch, F. Erhart, G. Widhalm, D. Surdez, O. Delattre, N. André, J. Stampfl, T. Tomasić, S. Taschner-Mandl, M. Distel, Refined high-content imaging-based phenotypic drug screening in zebrafish xenografts, *Npj Precis. Oncol.* 7 (2023) 1–16, <https://doi.org/10.1038/s41698-023-00386-9>.
- [61] S. Grissenberger, C. Sturtzel, A. Wenninger-Weinzierl, B. Radic-Sarikas, E. Scheuringer, L. Bierbaumer, V. Etienne, F. Némati, S. Pascoal, M. Tötzl, E. M. Tomazou, M. Metzelder, E.M. Putz, D. Decaudin, O. Delattre, D. Surdez, H. Kovar, F. Halbritter, M. Distel, High-content drug screening in zebrafish xenografts reveals high efficacy of dual MCL-1/BCL-XL inhibition against Ewing sarcoma, *Cancer Lett.* 554 (2023) 216028, <https://doi.org/10.1016/j.canlet.2022.216028>.
- [62] S. Ulenberg, K. Ciura, P. Georgiev, M. Pastewska, G. Ślifirski, M. Król, F. Herold, T. Bączek, Use of biomimetic chromatography and in vitro assay to develop predictive GA-MLR model for use in drug-property prediction among anti-depressant drug candidates, *Microchem. J.* 175 (2022) 107183, <https://doi.org/10.1016/j.microc.2022.107183>.
- [63] D. Szulczyk, M. Wozniński, M. Koliński, S. Kmiecik, A. Głogowska, E. Augustynowicz-Kopec, M.A. Dobrowolski, P. Roszkowski, M. Struga, K. Ciura, Menthol- and thymol-based ciprofloxacin derivatives against *Mycobacterium tuberculosis*: in vitro activity, lipophilicity, and computational studies, *Sci. Rep.* 13 (2023) 16328, <https://doi.org/10.1038/s41598-023-43708-4>.
- [64] K. Ciura, S. Kovačević, M. Pastewska, H. Kapica, M. Kornela, W. Sawicki, Prediction of the chromatographic hydrophobicity index with immobilized artificial membrane chromatography using simple molecular descriptors and artificial neural networks, *J. Chromatogr. A* 1660 (2021) 462666, <https://doi.org/10.1016/j.chroma.2021.462666>.
- [65] T. Tomasić, M. Durcik, B.M. Keegan, D.G. Skledar, Ž. Zajec, B.S.J. Blagg, S. D. Bryant, Discovery of Novel Hsp90 C-Terminal Inhibitors Using 3D-Pharmacophores Derived from Molecular Dynamics Simulations, *Int. J. Mol. Sci.* 21 (2020) 6898, <https://doi.org/10.3390/ijms21186898>.
- [66] P.C.D. Hawkins, A.G. Skillman, G.L. Warren, B.A. Ellingson, M.T. Stahl, Conformer Generation with OMEGA: Algorithm and Validation Using High Quality Structures from the Protein Databank and Cambridge Structural Database, *J. Chem. Inf. Model.* 50 (2010) 572–584, <https://doi.org/10.1021/ci100031x>.
- [67] M. McGann, FRED pose prediction and virtual screening accuracy, *J. Chem. Inf. Model.* 51 (2011) 578–596, <https://doi.org/10.1021/ci100436p>.
- [68] M. McGann, FRED and HYBRID docking performance on standardized datasets, *J. Comput. Aided Mol. Des.* 26 (2012) 897–906, <https://doi.org/10.1007/s10822-012-9584-8>.
- [69] J.C. Phillips, R. Braun, W. Wang, J. Gumbart, E. Tajkhorshid, E. Villa, C. Chipot, R. D. Skeel, L. Kalé, K. Schulten, Scalable molecular dynamics with NAMD, *J. Comput. Chem.* 26 (2005) 1781–1802, <https://doi.org/10.1002/jcc.20289>.
- [70] J. Huang, S. Rauscher, G. Nawrocki, T. Ran, M. Feig, B.L. de Groot, H. Grubmüller, A.D. MacKerell, CHARMM36m: an improved force field for folded and intrinsically disordered proteins, *Nat. Methods* 14 (2017) 71–73, <https://doi.org/10.1038/nmeth.4067>.
- [71] K. Vanommeslaeghe, E. Hatcher, C. Acharya, S. Kundu, S. Zhong, J. Shim, E. Darian, O. Guvench, P. Lopes, I. Vorobyov, A.D. Mackerell, CHARMM general force field: A force field for drug-like molecules compatible with the CHARMM all-atom additive biological force fields, *J. Comput. Chem.* 31 (2010) 671–690, <https://doi.org/10.1002/jcc.21367>.
- [72] K. Vanommeslaeghe, E.P. Raman, A.D. MacKerell, Automation of the CHARMM General Force Field (CGenFF) II: Assignment of Bonded Parameters and Partial Atomic Charges, *J. Chem. Inf. Model.* 52 (2012) 3155–3168, <https://doi.org/10.1021/ci3003649>.
- [73] K. Vanommeslaeghe, A.D. MacKerell, Automation of the CHARMM General Force Field (CGenFF) I: Bond Perception and Atom Typing, *J. Chem. Inf. Model.* 52 (2012) 3144–3154, <https://doi.org/10.1021/ci300363c>.
- [74] W. Humphrey, A. Dalke, K. Schulten, VMD: Visual molecular dynamics, *J. Mol. Graph.* 14 (1996) 33–38, [https://doi.org/10.1016/0263-7855\(96\)00018-5](https://doi.org/10.1016/0263-7855(96)00018-5).
- [75] U. Essmann, L. Perera, M.L. Berkowitz, T. Darden, H. Lee, L.G. Pedersen, A smooth particle mesh Ewald method, *J. Chem. Phys.* 103 (1995) 8577–8593, <https://doi.org/10.1063/1.470117>.
- [76] J.-P. Ryckaert, G. Ciccotti, H.J.C. Berendsen, Numerical integration of the cartesian equations of motion of a system with constraints: molecular dynamics of n-alkanes, *J. Comput. Phys.* 23 (1977) 327–341, [https://doi.org/10.1016/0021-9991\(77\)90098-5](https://doi.org/10.1016/0021-9991(77)90098-5).
- [77] G. Wolber, T. Langer, LigandScout: 3-D Pharmacophores Derived from Protein-Bound Ligands and Their Use as Virtual Screening Filters, *J. Chem. Inf. Model.* 45 (2005) 160–169, <https://doi.org/10.1021/ci049885e>.
- [78] T.L. Hwang, A.J. Shaka, Water Suppression That Works. Excitation Sculpting Using Arbitrary Wave-Forms and Pulsed-Field Gradients, *J. Magn. Reson. A* 112 (1995) 275–279, <https://doi.org/10.1006/jmra.1995.1047>.
- [79] M. Mayer, B. Meyer, Group Epitope Mapping by Saturation Transfer Difference NMR To Identify Segments of a Ligand in Direct Contact with a Protein Receptor, *J. Am. Chem. Soc.* 123 (2001) 6108–6117, <https://doi.org/10.1021/ja0100120>.
- [80] J. Yan, A.D. Kline, H. Mo, M.J. Shapiro, E.R. Zartler, The effect of relaxation on the epitope mapping by saturation transfer difference NMR, *J. Magn. Reson.* 163 (2003) 270–276, [https://doi.org/10.1016/S1090-7807\(03\)00106-X](https://doi.org/10.1016/S1090-7807(03)00106-X).
- [81] C. McCullough, M. Wang, L. Rong, M. Caffrey, Characterization of Influenza Hemagglutinin Interactions with Receptor by NMR, *PLOS ONE* 7 (2012) e33958, <https://doi.org/10.1371/journal.pone.0033958>.
- [82] M. Gedgaudas, D. Baronas, E. Kazlauskas, V. Petrauskas, D. Matulis, Thermott: A comprehensive online tool for protein-ligand binding constant determination, *Drug Discov. Today* 27 (2022) 2076–2079, <https://doi.org/10.1016/j.drudis.2022.05.008>.
- [83] G. Poje, M. Marinović, K. Pavić, M. Mioč, M. Kralj, L.P. de Carvalho, J. Held, I. Perković, Z. Rajić, Harmicins, Novel Harmine and Ferrocene Hybrids: Design, Synthesis and Biological Activity, *Int. J. Mol. Sci.* 23 (2022) 9315, <https://doi.org/10.3390/ijms23169315>.
- [84] S. Pascoal, S. Grissenberger, E. Scheuringer, R. Fior, M.G. Ferreira, M. Distel, Using Zebrafish Larvae as a Xenotransplantation Model to Study Ewing Sarcoma, in: F. Cidre-Aranaz, T. G. P. Grünwald (Eds.), *Ewing Sarcoma Methods Protoc.*, Springer US, New York, NY, 2021: pp. 243–255. [https://doi.org/10.1007/978-1-0716-1020-6\\_19](https://doi.org/10.1007/978-1-0716-1020-6_19).